EFFECT OF MAJOR TRITERPENOIDS OF *CENTELLA ASIATICA* ON NEURITE OUTGROWTH

IN NEURO-2A CELLS

Mr. Nonthaneth Nalinratana

จุฬาลงกรณ์มหาวิทยาลัย
CHULALONGKORN UNIVERSITY

A Dissertation Submitted in Partial Fulfillment of the Requirements

for the Degree of Doctor of Philosophy in Biomedicinal Chemistry

Department of Biochemistry and Microbiology

Faculty of Pharmaceutical Sciences

Chulalongkorn University

Academic Year 2018

ผลของไตรเทอร์พีนอยด์หลักในบัวบกต่อการงอกของแขนงประสาทในเซลล์ชนิด Neuro-2a

นายนนท์ธเนศ นลินรัตน์

วิทยานิพนธ์นี้เป็นส่วนหนึ่งของการศึกษาตามหลักสูตรปริญญาวิทยาศาสตรดุษฎีบัณฑิต
สาขาวิชาชีวเวชเคมี ภาควิชาชีวเคมีและจุลชีววิทยา
คณะเภสัชศาสตร์ จุฬาลงกรณ์มหาวิทยาลัย
ปีการศึกษา 2561
ลิขสิทธิ์ของจุฬาลงกรณ์มหาวิทยาลัย

Thesis Title	EFFECT OF MAJOR TRITERPENOIDS OF *CENTELLA ASIATICA* ON NEURITE OUTGROWTH IN NEURO-2A CELLS
By	Mr. Nonthaneth Nalinratana
Field of Study	Biomedicinal Chemistry
Thesis Advisor	Assistant Professor Boonsri Ongpipattanakul, Ph.D.
Thesis Co Advisor	Associate Professor Duangdeun Meksuriyen, Ph.D.

Accepted by the Faculty of Pharmaceutical Sciences, Chulalongkorn University in Partial Fulfillment of the Requirement for the Doctor of Philosophy

⋯⋯⋯⋯⋯⋯⋯⋯⋯⋯⋯⋯ Dean of the Faculty of Pharmaceutical Sciences

(Assistant Professor Rungpetch Sakulbumrungsil, Ph.D.)

DISSERTATION COMMITTEE

⋯⋯⋯⋯⋯⋯⋯⋯⋯⋯⋯⋯ Chairman

(Associate Professor Maneewan Suksomtip, Ph.D.)

⋯⋯⋯⋯⋯⋯⋯⋯⋯⋯⋯⋯ Thesis Advisor

(Assistant Professor Boonsri Ongpipattanakul, Ph.D.)

⋯⋯⋯⋯⋯⋯⋯⋯⋯⋯⋯⋯ Thesis Co-Advisor

(Associate Professor Duangdeun Meksuriyen, Ph.D.)

⋯⋯⋯⋯⋯⋯⋯⋯⋯⋯⋯⋯ Examiner

(Weerapong Prasongchean, Ph.D.)

⋯⋯⋯⋯⋯⋯⋯⋯⋯⋯⋯⋯ Examiner

(Assistant Professor Chatchai Chaotham, Ph.D.)

⋯⋯⋯⋯⋯⋯⋯⋯⋯⋯⋯⋯ External Examiner

(Assistant Professor Boonrat Chantong, Ph.D.)

นนท์ธเนศ นลินรัตน์ : ผลของไตรเทอร์พีนอยด์หลักในบัวบกต่อการงอกของแขนงประสาทในเซลล์ชนิด Neuro-2a. (

EFFECT OF MAJOR TRITERPENOIDS OF *CENTELLA ASIATICA* ON NEURITE OUTGROWTH IN NEURO-2A CELLS) อ.ที่ปรึกษาหลัก : ผศ. ภญ. ดร.บุญศรี องค์พิพัฒนกุล, อ.ที่ปรึกษาร่วม : รศ. ภญ. ดร.ดวงเดือน เมฆสุริเยนทร์

บัวบก หรือ *Centella asiatica* เป็นสมุนไพรที่มีรายงานถึงฤทธิ์ฟื้นฟูความทรงจำ และปกป้องเซลล์ประสาทในสัตว์ทดลอง โดยสารสำคัญที่เป็นตัวออกฤทธิ์คือสารกลุ่มไตรเทอร์ปีนอยด์ไกลโคไซด์ ได้แก่ มาเดคาสโซไซด์ (MS) และเอเชียติโคไซด์ (AS) รวมถึงสารในรูปอะไกลโคนได้แก่ กรดมาเดคาสสิก (MA) และกรดเอเชียติก (AA) โดยการศึกษาครั้งนี้ได้ทำการศึกษาเปรียบเทียบฤทธิ์ของสารทั้ง 4 ชนิดต่อฤทธิ์เพิ่มการงอกแขนงประสาทในหลอดทดลอง รวมถึงกลไกที่เกี่ยวข้องในเซลล์ประสาทเพาะเลี้ยงชนิด Neuro-2a การวิเคราะห์ด้วยเทคนิคอิมมูโนฟลูออเรสเซนต์ต่อโปรตีนโครงสร้าง βIII-tubulin พบว่าสารสำคัญทั้ง 4 ชนิดสามารถเพิ่มการงอกแขนงประสาทได้ และเพิ่มความยาวของแขนงประสาทได้อย่างมีนัยสำคัญทางสถิติ เมื่อศึกษาถึงกลไกที่เกี่ยวข้องพบว่า สารในรูปไกลโคไซด์มีการออกฤทธิ์ผ่านกลไกที่แตกต่างจากสารในรูปอะไกลโคน โดยฤทธิ์เพิ่มการงอกแขนงประสาทของ MS และ AS นั้นผ่านทางการนำส่งสัญญาณของตัวรับชนิด TrkA ส่งผลให้เกิดการกระตุ้นอย่างต่อเนื่องของโปรตีน ERK1/2 นำไปสู่การกระตุ้นโปรตีน CREB ที่เกี่ยวข้องกับกระบวนการเปลี่ยนแปลงของเซลล์ประสาท นอกจากนี้ยังส่งผลกระตุ้นการทำงานของโปรตีน Akt ทำให้เกิดการกระตุ้นของโปรตีน Nrf2 รวมถึงยับยั้งการทำงานของโปรตีน GSK3β และ RhoA ที่ควบคุมการจัดเรียงตัวของโปรตีนโครงสร้าง ส่งผลให้เกิดกระบวนการเพิ่มความยาวของแขนงประสาท ขณะที่อะไกลโคน MA และ AA นั้นพบว่ากลไกแตกต่างจากสารในรูปไกลโคไซด์คือ สามารถกระตุ้นการทำงานของโปรตีน CREB ได้โดยไม่ผ่านวิถี ERK1/2 และการยับยั้งโปรตีน RhoA นั้นไม่ต้องอาศัยวิถี Akt ในขณะที่การกระตุ้นโปรตีน Nrf2 และการยับยั้งโปรตีน GSK3β นั้นยังต้องผ่านทางวิถี Akt เช่นกัน แต่อย่างไรก็ตาม พบว่าการกระตุ้นสัญญาณต่าง ๆ ภายในเซลล์ รวมถึงฤทธิ์กระตุ้นการงอกแขนงประสาทของ MA และ AA นั้นไม่ได้เกิดจากการนำส่งสัญญาณผ่านตัวรับ TrkA ดั่งเช่น MS และ AS ซึ่งความแตกต่างนี้ อาจจะสามารถนำมาอธิบายถึงฤทธิ์ในการเพิ่มการงอกแขนงประสาทที่มากกว่าของ MS และ AS เมื่อเทียบกับ MA และ AA ได้ จากการศึกษานี้ ทำให้ได้ข้อมูลสนับสนุนฤทธิ์ของสารสำคัญแต่ละชนิดในบัวบก รวมถึงผลของความแตกต่างทางโครงสร้างของสารออกฤทธิ์แต่ละตัวนั้นอาจจะนำไปใช้เป็นแนวทางในการออกแบบสารที่ออกฤทธิ์ฟื้นฟูความทรงจำและปกป้องเซลล์ประสาทต่อไปในอนาคต

สาขาวิชา	ชีวเวชเคมี	ลายมือชื่อนิสิต ....
ปีการศึกษา	2561	ลายมือชื่อ อ.ที่ปรึกษาหลัก ....
		ลายมือชื่อ อ.ที่ปรึกษาร่วม ....

5676458333 : MAJOR BIOMEDICINAL CHEMISTRY

KEYWORD: Centella asiatica, madecassoside, asiaticoside, madecassic acid, asiatic acid, neurite outgrowth

Nonthaneth Nalinratana :
EFFECT OF MAJOR TRITERPENOIDS OF *CENTELLA ASIATICA* ON NEURITE OUTGROWTH IN NEURO-2A CELLS. Advisor: Asst. Prof. Boonsri Ongpipattanakul, Ph.D. Co-advisor: Assoc. Prof. Duangdeun Meksuriyen, Ph.D.

Centella asiatica has been reported to demonstrate neuroprotection and memory improvement in various animal models. Triterpenoid glycosides, madecassoside (MS), asiaticoside (AS), and their aglycones, madecassic acid (MA) and asiatic acid (AA) are considered as major neuroactive constituents in *C. asiatica*. In this study we aimed to compared MS, AS, MA and AA for their neurite outgrowth activities and mechanisms in Neuro-2a cells. Immunofluorescent staining against βIII-tubulin showed that MS and AS significantly increased the percentage of neurite-bearing cells and neurite length with higher potency than MA and AA. Our mechanistic studies revealed the differences in signal activation between glycosides and aglycones. Neurite outgrowth activities of MS and AS were found to be regulated by activation of TrkA receptor signaling, resulting in sustained ERK1/2 activation coupled with cAMP response element binding (CREB) phosphorylation which involved with neuronal differentiation. Activation on TrkA receptor also triggered Akt phosphorylation, resulting in inhibitory effects on glycogen synthase kinase (GSK) 3β and RhoA, which controlled cytoskeleton dynamic, resulting in allowing neurite extension. Translocation of nuclear factor erythroid 2–related factor 2 (Nrf2) was also regulated by Akt signaling, which might be associated with neurite outgrowth. On the contrary, MA and AA induced neurite outgrowth with different mechanisms by ERK1/2-independent activation of CREB and Akt-independent inhibition on GSK3β, while Nrf2 translocation and RhoA inhibition were also mediated by Akt signaling. These differences between glycosides and aglycones might be associated with neurite outgrowth potency that glycosides exhibited higher potency than aglycones. Taken together, our findings have provided the evidence to support the neuroprotection and memory improvement activity of active constituents in *C. asiatica* and might be useful for drug design.

Field of Study:	Biomedicinal Chemistry	Student's Signature	....
Academic Year:	2018	Advisor's Signature	....
		Co-advisor's Signature	....

ACKNOWLEDGEMENTS

TABLE OF CONTENTS

LIST OF TABLES

LIST OF FIGURES

CHAPTER I INTRODUCTION

Neurodegenerative diseases such as Alzheimer's disease, Parkinson's disease and dementia are characterized by the progressive deterioration of brain function, resulting in motor and cognitive disability (Sun *et al.*, 2015b). The fundamental structural change in patients with neurodegenerative diseases is the damage of nerve cells, leading to subsequent destruction and dysfunction of the neural networks. Prevention of the nerve cell damage as well as promotion of neurite formation and synapse plasticity would be the essential strategies for suppressing the deterioration and enhancing the recovery of brain function. The increasing in dendritic complexity such as dendrite length and dendritic spine density in cortex and hippocampus was observed in animal which exhibited improvement of performance in memory-related behavioral tests (Leggio *et al.*, 2005; Yang *et al.*, 2009; Wartman *et al.*, 2014). These suggested the association between neurite formation and memory improvement.

In search of treatment for neuronal degeneration including memory impairment, the measurement of neuronal morphological changes thus is a possible primary tool for evaluating potential drugs or compounds (Ramm *et al.*, 2003; Radio *et al.*, 2008; Al-Ali *et al.*, 2015). One of such neuronal morphological assays is in vitro neurite outgrowth assessment which not only can provide a rapid phenotypic screening for effective compounds but also can be useful to examine their molecular mechanisms on neurogenesis, neuritogenesis and synaptic plasticity in relevance to improvement of memory impairment (Tohda *et al.*, 2009; Harrill *et al.*, 2011; Lee *et al.*, 2011).

Neurotrophin-mediated signaling pathways are the major mechanisms in nervous system development (Hallbook, 1999; Huang *et al.*, 2001). Neurotrophins bind to their receptors, Trk receptors, and activate many signaling pathways such as Ras/Rho G protein families, MAP kinase, PI-3 kinase and Jun kinase (Kaplan *et al.*, 1997), which regulate the neural cell fate decisions, neurite outgrowth, synapse plasticity and expression of proteins crucial for neuronal functions including memory formation (De Luca *et al.*, 1997; Yamashita *et al.*, 1999; Skaper, 2008). Therefore, neurotrophin-

mediated signaling pathways are currently considered as part of key targets for drug development to treatment neurological diseases (Longo *et al.*, 2013; Roloff *et al.*, 2015).

Many chemicals were reported to exhibit in vitro neuritogenic effect. These included several drugs which are available in the current market such as donepezil (Oda *et al.*, 2007), statins (Evangelopoulos *et al.*, 2009; Jin *et al.*, 2012; Raina *et al.*, 2013) and rosiglitazone (Chiang *et al.*, 2014). The neuritogenic effect of plant extracts and several classes of natural compounds such as flavonoids (Chen *et al.*, 2009; Nakajima *et al.*, 2011), saponins (Zou *et al.*, 2002; Xu *et al.*, 2009b; Liffert *et al.*, 2013) were also reported. Moreover, many of these compounds revealed the improvement of cognitive impairment in animal models (Liu *et al.*, 2011; Aguiar *et al.*, 2013), supporting the association between neuritogenicity and in vivo memory improvement.

From the traditional medicine perspective, there are herbs which had been traditionally used as brain tonics such as ginseng (*Panax spp.*), brahmi (*Bacopa monnieri*), centella (*Centella asiatica*), and Indian ginseng (*Withania somnifera*). Interestingly, the constituents in these herbs mostly are saponins (Sun *et al.*, 2015a). Saponins belong to a class of naturally occurring glycosides which contain a non-polar steroid or triterpenoid aglycone with one or more sugar chains. Structure-activity relationship studies revealed that the number, position and length of sugar chains of saponins had the important roles to their bioactivities such as anti-fungal activity (Takechi *et al.*, 1996), anti-proliferation (Mu *et al.*, 2013), glucose uptake enhancing (Hu *et al.*, 2014), hemolytic activity (Vo *et al.*, 2016) and neuritogenicity (Liffert *et al.*, 2013). However, these studies were mostly conducted in the *in vitro* cell culture setting, where cells were directly exposed to test materials; while these herbs were often orally given in the *in vivo* studies as well as in the traditional uses. Therefore, the overlooked point is drug disposition processes of saponin including absorption, transformation and distribution.

However, the information on the pharmacokinetic profiles of most natural products are still adequate. The present knowledge suggests that saponins are poorly absorbed in the gastrointestinal tract, leading to low bioavailability (Yu *et al.*, 2012).

Moreover, orally administered saponins often were partially metabolized by intestinal microflora through stepwise cleavage of sugar moieties to generate the deglycosylated metabolites (Wan *et al.*, 2013), resulting in subsequent decrease of parent compound. These often impede the drug development efforts targeted at saponins as oral therapeutic agents. However, recent pharmacokinetic studies showed that the amount of orally given saponin was found in several tissues such as liver, kidney, heart and lung, although the amount was generally low (Chao *et al.*, 2006; Yu *et al.*, 2012; Kandhare *et al.*, 2013). Several reports also showed that the distribution of saponins to the brain was very low, which might be due to the inefficient penetrating of blood-brain barrier (Zhang *et al.*, 2006; Leng *et al.*, 2013; Jeong *et al.*, 2014). Therefore, the effects of saponins on neuronal activities in physiological condition were still controversial.

Centella asiatica is one of the herbs that have been traditionally used as a brain tonic (Orhan, 2012). Numerous preparations of *C. asiatica* are available in the market as dietary supplements. The major saponins found in this plant are pentacyclic triterpenoid type, which mainly are madecassoside (**MS**) and asiaticoside (**AS**), and their aglycone derivatives i.e. madecassic acid (**MA**) and asiatic acid (**AA**) (James *et al.*, 2009). Although the amount of each constituent is not always the same due to different growing environment, **MS** and **AS** were mostly reported as major constituents and regarded as the primary bioactive constituents (Gohil *et al.*, 2010; Hashim *et al.*, 2011). Oral administration of **MS** and **AS** including *C. asiatica* extracts containing high amounts of **MS** and **AS** were reported to exhibit positive results in various animal models of neurodegenerative diseases such as memory impairment, anxiolytic effect and Parkinson's disease (Tantisira *et al.*, 2010; Wanasuntronwong *et al.*, 2012; Xu *et al.*, 2013; Lin *et al.*, 2014). Pharmacokinetic studies of orally administered **MS** and **AS** revealed the low bioavailability of both compounds, while the brain distribution was also low (Han *et al.*, 2012; Kandhare *et al.*, 2013; Leng *et al.*, 2013; Jeong *et al.*, 2014). These bring into question whether their neuronal activities come from their glycoside forms or other species. Because orally administered **MS** and **AS** were reported to be hydrolyzed by hydrolase enzymes of intestinal microflora in stepwise hydrolysis

manner to become **MA** and **AA** (Jun *et al.*, 2006; Leng *et al.*, 2013), which produced higher bioavailability when compared to their parent glycoside forms (Nair *et al.*, 2012; Yuan *et al.*, 2015). Therefore, the question was raised that whether glycoside or aglycone forms were exactly responsible for neurological bioactivities.

To clarify this question, the present research aims to examine the effects of individual constituents in *C. asiatica*, which are **MS**, **AS**, **MA** and **AA**, on neuritogenicity by using *in vitro* neurite outgrowth assay. The result will provide the information that whether glysoside or aglycone forms exhibit the neuritogenic effect. The target of action and intracellular mechanism will also be identified by investigation of neurotrophin-mediated signaling pathway. This comprehensive investigation would not only provide the information of action of individual triterpenoids in *C. asiatica* to support the traditional use, but also provide the possible mechanisms and drug target, which might be applied to the study of other triterpenoids and glycoside compounds.
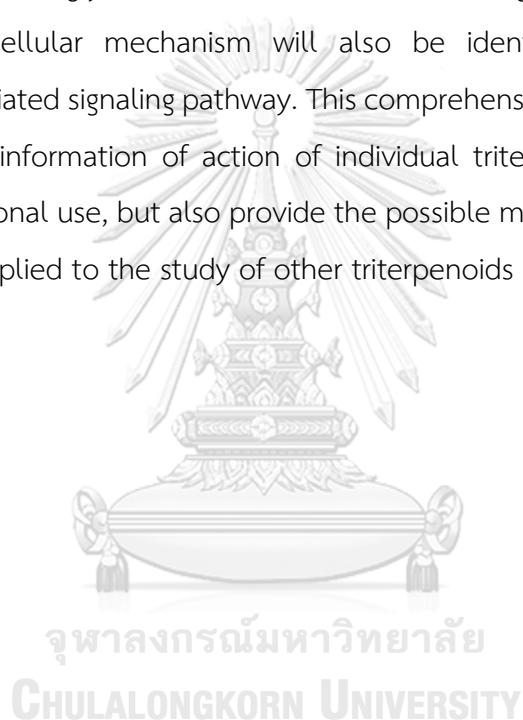
Research questions and objectives

Research questions

1. Which glycoside or aglycone forms of constituents in *C. asiatica* are responsible for neurite outgrowth activity?

2. What is the possible target and subsequent intracellular mechanism of each constituent that is responsible for neurite outgrowth activity?

Objectives

1. To evaluate the effect of major triterpenoids in *C. asiatica,* which are madecassoside, asiaticoside, madecassic acid and asiatic acid on neurite outgrowth in Neuro-2a cells.

2. To investigate the intracellular mechanism and putative target responsible for neurite outgrowth in Neuro-2a cells.

Hypothesis

Madecassoside and asiaticoside, which are the major triterpenoids in *C. asiatica* exhibited the neuritogenic effect in Neuro-2a cells by modulation of neurotrophin-regulated signaling pathways such as ERK/CREB, PI3K/Akt and RhoA/ROCK pathways.

Experimental design
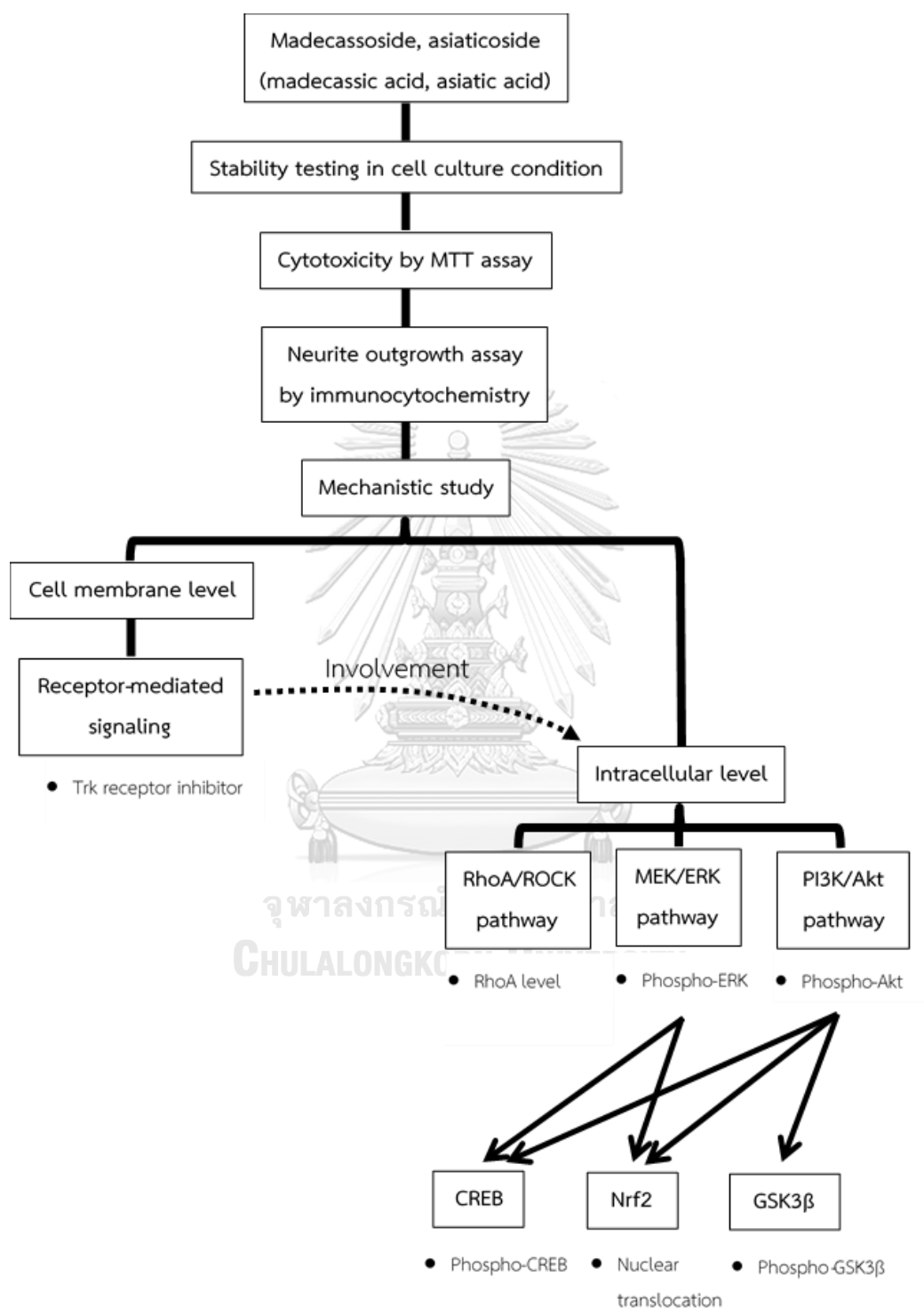
Benefits of this study

1. This study would provide the scientific evidence for the effect of major triterpenoids in *C. asiatica* which are madecassoside, asiaticoside, madecassic acid and asiatic acid on neurite outgrowth in Neuro-2a cells.

2. This study would also provide the information of the intracellular mechanism and putative target responsible for neurite outgrowth in Neuro-2a cells.

3. This study would provide the detail of different action of triterpenoid glycosides and aglycones in *C. asiatica* on neurite outgrowth activity.

CHAPTER II LITERATURE REVIEW

Involvement of neurite formation and memory improvement

The functions of nervous system are determined by the connections which formed between neurons during development. Typically, a neuron consists of a cell body, dendrites and an axon, which collectively called neurites. Axons and dendrites are formed to the pattern of synaptic connections, which regulates the distribution of signaling within the nervous system. Nowadays, several evidences suggest that neurons can continue to proliferate and neurites can also extend in the adult brain. The structural remodeling of neurite is necessary for adaptive brain functions such as learning and memory. However, in the aged brain, the progressive deterioration of neural network such as neurite degeneration, neuronal atrophy, and loss of synapses usually occurs, leading to neurodegenerative conditions, such as Alzheimer's disease, Parkinson's diseases and memory impairment in elderly.

Memory is defined as a capacity to encode, store and retrieve the information to guide the behavioral responses (Stuchlik, 2014). In memory formation, there are several types of memory including sensory memory, short-term memory and long-term memory. Each type of memory occurs in different regions of the brain such as short-term memory is processed and occurs in prefrontal lobe of cerebral cortex (Jonides *et al.*, 2008). Short-term memory can become long-term memory through the memory consolidation process, which mainly occurs in hippocampus (Poldrack *et al.*, 1997). Long-term memory consolidation consists of 2 steps: (1) synaptic consolidation which rapidly happens within hours after learning and occurs at each single synapse of neurons in hippocampus. The repeating stimuli (e.g. repeating learning or practice) induce the structural changes of the synapses in term of synapse strength, which calls synaptic plasticity. In this step, the proteins involving in synapse formation are synthesized and expressed at the synapses. (2) System consolidation is the process for changing the hippocampus-dependent memory to hippocampus-independent. The memory retrieved from hippocampus gradually transfers to the neocortical circuits in

cerebral cortex for long-term storage (Takashima *et al.,* 2009). In both steps of memory consolidation, several evidences suggested the neurite and synapse formation might play important roles in hippocampus and neocortex structural re-organization (Restivo *et al.,* 2009; Lesburgueres *et al.,* 2011; Wartman *et al.,* 2014).

Several behavioral studies reported the association between neurite formation and memory improvement. In Morris water maze trained rats, those rats could learn to escape from water onto the hidden platform, the increasing in dendritic complexity such as dendrite length and dendritic spine density in cortex and hippocampus more than un-trained rats was observed (Moser *et al.,* 1994; Yang *et al.,* 2009). From behavioral testing models, spatial learning of adult rats in also induced neurogenesis, dendrite length and synapse density in dendrate gyrus region of hippocampus (Tronel *et al.,* 2010). Moreover, rats trained on 2 tasks displayed the increased dendritic complexity in anterior cingulate cortex and hippocampus more than rats trained only one task (Wartman *et al.,* 2014). In the newborn rats which housed in the enrichment condition for 3 months showed the better performance in Morris water maze training with more quickly acquired tuned navigational strategies than rats grew up in normal condition (Leggio *et al.,* 2005). Furthermore, dendritic length and branching in cortical region also significantly enhanced in environmental enrichment-housed rats. These suggested the involvement of dendritic complexity including length, branching and synaptic formation on learning and memory (Martin *et al.,* 2000; Silva, 2003).

Several drugs and herbs, which have been reported to improve memory impairment in animal models, also exhibited the neuritogenic effects. Ginsenoside Rb1, which is an active compound isolated from *Panax ginseng* showed improvement of learning and memory impairment in several rodent models (Wang *et al.,* 2010; Liu *et al.,* 2011). Various studies suggested that effects on memory of ginsenoside Rb1 might come from effects on neurons. It also increased neurogenesis in rat brain (Gao *et al.,* 2010) and neurite outgrowth in mesencephalic dopaminergic cell cultures (Radad *et al.,* 2004), rat primary hippocampal neurons (Liu *et al.,* 2014). Ginsenoside Rb1 also increased the expression of several proteins involving in memory consolidation process such as synaptophysin and microtubule-associated protein 2 (MAP2) (Nam *et al.,* 2013).

Donepezil is a drug used for treatment of dementia condition in Alzheimer's disease and other dementia (Malouf *et al.*, 2004; Marder, 2008). Besides donepezil acts as an acetylcholinesterase inhibitor, the precise mechanism is not fully understood. Several evidence claimed that the nootropic effect of donepezil might come from the neuritogenic effect (Oda *et al.*, 2007; Ishima *et al.*, 2008; Page *et al.*, 2015). These clues suggested that neurite formation might at least partly be responsible for memory improvement activities of drugs or herbs. Therefore, assessment of neurite outgrowth was widely used as a test for neurogenesis, neuritogenesis and synaptic plasticity in relevance to improvement of memory impairment (Conti *et al.*, 1997).

Neurotrophin-mediated signaling in neurite outgrowth

Neurite outgrowth is a complex process which involves multiple interactions between neurons and the extracellular stimuli such as growth factors, neurotransmitters, hormones, extracellular matrix, cytokines and other chemicals. These factors triggered intracellular signals to induce morphological changes such as sprouting and elongation of axons and dendrites. Among various endogenous factors, neurotrophic factors are one of the most important factors in induction of neuronal differentiation.

Neurotrophic factors or neurotrophins are a family of secreted proteins that regulate the survival, development, function and plasticity of the nervous system (Huang *et al.*, 2001). Nowadays, there are four neurotrophic factors characterized in mammals consist of nerve growth factor (NGF), brain-derived neurotrophic factor (BDNF), neurotrophin-3 (NT-3) and neurotrophin-4 (NT-4). Each type of neurotrophic factors has its specific functions and targets, but still regulates overall to maintain survival, differentiation and plasticity of the neurons.

NGF is considered as the prototypic neurotrophic factor and the best characterized member of the neurotrophin family. NGF is important for the development and maintenance of both central and peripheral neurons. At time of synthesis, pro-NGF protein was synthesized, and underwent further post-translational

modification at both amino- and carboxyl-terminus to become the mature NGF (Fahnestock *et al.*, 2004). The regulation of NGF maturation is also one of important steps in control the specificity and activity of mature NGF (Skaper, 2008). While, BDNF is also a protein in neurotrophin family, which acts mainly in central nervous system. Similar to NGF, BDNF is also synthesized as a pro-BDNF and further processed to generate mature BDNF. This post-translational process also occurs for other neurotrophin, NT-3 and NT-4.

The target proteins of these neurotrophins are neurotrophic receptors which are classified as tyrosine kinase receptors. The neurotrophic receptors can be classified into two types which are the tropomyosin receptor kinase (Trk) receptor and Low-affinity nerve growth factor receptor (LNGFR) or p75 neurotrophic receptor (p75NTR). The Trk receptor family mainly consists of TrkA, TrkB and TrkC receptors which bind to the specific neurotrophins with high affinity. NGF binds specifically to TrkA receptor, while BDNF and NT-4 bind to TrkB receptor. However, some reports reveal that NT-3 also binds to TrkA and TrkB receptors, and NT-4 also binds to TrkC receptor but their affinity are relatively low (Hallbook, 1999). All neurotrophins can also bind to p75NTR with the lower affinity than their specific Trk receptors (Skaper, 2008). But if neurotrophins are in the pro-neurotrophin or un-processed forms, they can bind to p75NTR with much higher affinity (Chen *et al.*, 2008). After the neurotrophins or pro-neurotrophins bind to either Trk or p75NTR receptors, the specific signaling pathways are triggered, resulting in different effects on target neurons (Huang *et al.*, 2003).

Trk receptors consist of an extracellular ligand-binding domain, a trans-membrane domain and a cytoplasmic section that have tyrosine kinase activity for activation of downstream signaling (Huang *et al.*, 2003). Activation of Trk receptors by NGF or BDNF lead to phosphorylation of tyrosine at the cytoplasmic domain, resulting in formation of the cores of binding sites for scaffolds and enzymes which are intermediates in the signaling cascades. The major pathways activated by the Trk receptors are Grb2, Src, phosphatidyl inositol-3 kinase (PI3K), phospholipase C gamma 1 (PLCg1) and their downstream effectors (Huang *et al.*, 2003).

The activated signal through Grb2 further stimulates mitogen-activated protein (MAP) kinase cascades which are Ras-Raf-MEK-ERK pathway (Meakin *et al.*, 1999), resulting in activation of 90 kDa ribosomal s6 kinase (p90RSK) and mitogen- and stress-activated kinases (MSK) to translocate into nucleus and further activate cAMP response element-binding protein (CREB). The activated CREB would binds to the specific DNA sequences called cAMP response elements (CRE) and regulate the gene transcription of various proteins such as BDNF, tyrosine hydroxylase, neuropeptides and other proteins involving in neuronal function including neurite outgrowth. Moreover, Trk activation by neurotrophins also induces phosphorylation of PLCg1, leading to the breakdown of diacylglycerol and inositol (1,4,5) triphosphate (IP_3). Activation of IP_3 triggers the intracellular level of Ca^{2+}, resulting in activation of calmodulin and further calmodulin kinase II (CaMKII). CREB has also been reported to be activated by CaMKII in the process of long-term memory formation (De Luca *et al.*, 1997; Silva *et al.*, 1998). Therefore, activation of Trk receptor through either Ras-Raf-MEK-ERK-CREB or PLCg1-IP_3-CaMKII-CREB pathways plays the important roles in neuronal plasticity and long-term memory formation in the brain (Barco *et al.*, 2003).

Another major pathway stimulated by Trk activation is the PI3K signaling pathway. After Trk activation, PI3K is recruited to intracellular domain by the adaptor proteins such as Shc and Gab-1. Moreover, PI3K is also activated by Grb2, the upstream signaling of MAPK pathway. Activation of PI3K would further stimulate the protein kinase B or Akt which further activates several downstream signaling proteins. PI3K-Akt activity is important for Trk receptor-mediated survival signaling via the regulation of signaling proteins such as Bad, Caspase-9 and IkB. Moreover, PI3K-Akt cascade activation also regulate the activity of glycogen synthase kinase 3 beta (GSK3β) which plays several roles in regulation of cell morphogenesis requires reorganization of the cytoskeleton, especially microtubules (Zhou *et al.*, 2005).

While p75NTR is considered as a member of the tumor necrosis factor receptor superfamily (Gschwendtner *et al.*, 2003). Activation of p75NTR leads to the stimulation of several signaling to mediate cell apoptosis. This effect is counteracted by the signaling from activation of Trk receptor (Bibel *et al.*, 1999). However, several recent

studies revealed the role of p75NTR in regulation of neurite length (Brann *et al.*, 1999; Gentry *et al.*, 2004) by the involvement of RhoA activity (Yamashita *et al.*, 1999). RhoA is a small GTPase protein in Rho family that primarily associated with cytoskeleton regulation especially actin (Wheeler *et al.*, 2004). RhoA is involved in regulating axonal growth and growth cone morphology (Bito *et al.*, 2000; Kuhn *et al.*, 2000). RhoA has been reported that it can be regulated by the cytoplasmic domain of p75NTR (Yamashita *et al.*, 1999). RhoA is activated by conversion to GTP-bound state from GDP-bound state by guanine nucleotide exchange factor (GEF) and inactivated by hydrolysis of bound GTP to GDP by GTPase activating protein (GAP). The GTP-bound form of RhoA can stimulate Rho-Associated Coiled-Coil-Containing Protein Kinase (ROCK) activation (Lehmann *et al.*, 1999) and further activates downstream signaling molecules which regulate cytoskeleton reorganization such as growth cone collapse and inhibition of neurite outgrowth (Lehmann *et al.*, 1999). Several reports indicated that activation of p75BTR by pro-BDNF could inhibit neurites outgrowth and filopodia growth cones by activating RhoA through the p75NTR signaling pathway (Gehler *et al.*, 2004; Sun *et al.*, 2012). Therefore, the RhoA/ROCK inhibition is believed to a promising strategy to overcome CNS disorders such as spinal cord injuries and memory deficit (Kubo *et al.*, 2008).
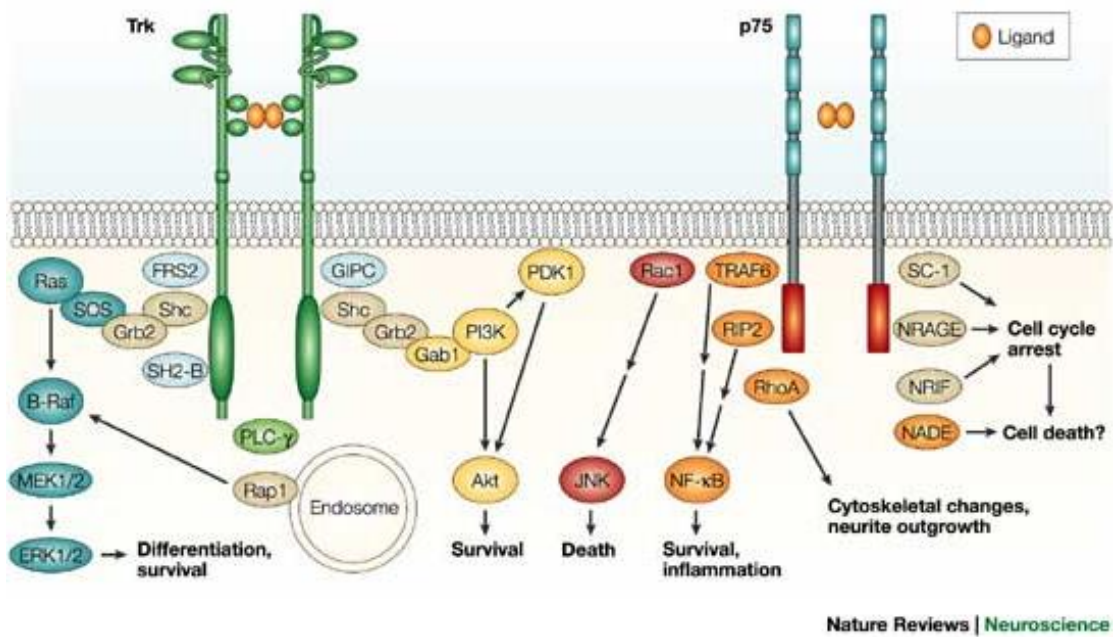
Figure 1 Neurotrophin signaling pathways mediated by Trk receptor and p75NTR
receptor
(Chao, 2003).

Cellular model for studying neurite outgrowth

Several experimental systems have been used to investigate the neuritogenic effects. Various models such as *Drosophila melanogaster* (fruit fly) and *Caenorhabditis elegans*, which are non-vertebrate organisms, were previously used to investigate the regulation of transcriptional control due to these models were convenient for genetic modification and handling. Nowadays, chick embryos, mammalian cell lines and primary cultures were widely used for studying neuritogenic effects. Dorsal root ganglia neurons from chick embryos were mostly used in investigation of recovery effect from spinal cord injury model (Fang *et al.*, 2012).

For learning and memory aspects, primary neurons isolated from cerebral cortex (Yoshikawa *et al.*, 2009; Zhang *et al.*, 2015) and hippocampus (Hirata *et al.*, 2005; Hannan *et al.*, 2014), which are the regions of the brain involved with learning and memory processes, are widely used. These primary cultures are considered to be more morphologically and physiologically similar to *in vivo*. However, the major limitation of these primary cell cultures is the period that the cultures can survive *in vitro*, and need to be prepared from the fresh tissues each time of study, resulting to batch-to-batch variation of the quality of the primary cell culture. Moreover, all primary cell culture experiments using animals need animal ethics approval.

Therefore, the immortal cell lines are often used in research in place of primary cells. They offer several advantages, such as they are cost-effective, easy to use, and provide a pure population of cells, which is valuable since it provides a consistent sample and reproducible results. Although there was no perfect cellular system available as the cell lines for studying the neuronal signaling due to the complexity of the neuronal cells, but there were several cell lines which were acceptable to be models for studying neurite outgrowth. According to literature review in the topic about neuritogenic effects of compounds, the most popular cell line seems to be rat pheochromocytoma PC-12 cell line and its commercial subclones, followed by mouse neuroblastoma Neuro-2a cell line, human neuroblastoma SH-SY5Y cell line, and other cell lines such as P19-derived neurons, NG108-15 cells and IMR-32 cells were also used.

PC12 is a cell line derived from pheochromocytoma cells of the rat adrenal medulla. Because of their embryonic origin from the neural crest, the important feature of PC12 cells is that they can be differentiated into neuron-like cells when induced by various substances including NGF (Greene *et al.*, 1976) and retinoic acid (Cosgaya *et al.*, 1996). PC12 cells are also reported to express TrkA receptor on the cell surface (Nusser *et al.*, 2002). Differentiated PC12 cells exhibit the significant change in phenotypes such as ceasing proliferation, neurite extension, and becoming electrically excitable (Greene *et al.*, 1976). This makes PC12 cells are widely used as a model for neuronal differentiation. However, the significant difference between phenotypes of undifferentiated and differentiated PC12 cells has to be concerned. Study on protective effect of huprine derivative, an acetylcholinesterase inhibitor, showed the cholinergic receptor-mediated cytoprotective effect only occurred in differentiated PC12 cells (Pera *et al.*, 2013). These also happened in several studies of difference between undifferentiated and differentiated PC12 cells (Oberdoerster *et al.*, 1999; Vyas *et al.*, 2004; Hayakawa *et al.*, 2013). These suggested the lacking of some neuronal characteristics of undifferentiated PC12 cells. Therefore, several studies on neurite outgrowth needed induction of PC12 cells by NGF treatment prior or together with testing compounds (Ishima *et al.*, 2008; Kano *et al.*, 2008).

Neuro-2a or N2a cell line is the one of most popular cell lines used in neurobiochemical investigation including neurotoxicity, Alzheimer's disease and neurite outgrowth (Dikshit *et al.*, 2006; Evangelopoulos *et al.*, 2009; Wang *et al.*, 2011b). Neuro-2a is a fast-growing mouse neuroblastoma cell line which derived from a spontaneous brain tumor in an albino strain A mouse (LePage *et al.*, 2005). Neuro-2a cells can differentiate into neuron-like cells, in respond to NGF and other stimuli, and can produce large quantities of microtubular protein (Mao *et al.*, 2000) such as neurofilament and βIII-tubulin which are involved in contractile system and axonal transport, suggesting this cell line was also suitable for study of neural differentiation. Neuro-2a cells also express acetylcholinesterase enzyme. This cell line was also used for routine diagnosis of rabies according to World Organization for Animal Health (OIE)'s guideline (Wang *et al.*, 2011b). Therefore, this cell line was also widely used in studies

involving central nervous system-targeting virus infection. Therefore, Neuro-2a cells, which exhibited good neuronal phenotypes and did not need special culture vessels and growth factors, seem to be a suitable model for studying the effect of testing compounds on neurite outgrowth.

Effects of drugs and natural compounds on neurite outgrowth

Several drugs that are available in the current market were reported to exhibit neurite outgrowth activity by various mechanisms. Among the drugs, several drugs in the class of statin, which are HMG-CoA reductase inhibitors used as cholesterol-lowering drugs, exhibited the neurite outgrowth activity. Simvastatin increased neurite outgrowth and expression of neurofilament, βIII-tubulin and growth associated protein 43 (GAP43) in human SY-SH5Y cells (Raina *et al.*, 2013). While Atorvastatin increased neurite outgrowth in primary cortical neurons via PI3K/Akt/mTOR and PI3K/Akt/GSK3β pathways (Jin *et al.*, 2012). Mevastatin was also reported the neurite outgrowth induction in Neuro-2a cells via activation of EGFR/ERK and Akt (Evangelopoulos *et al.*, 2009). Several anti-diabetic drugs such as a glucagon-like peptide analog Liraglutide and an insulin sensitizer Rosiglitasone increased neurite outgrowth via ERK/CREB (Li *et al.*, 2015) and CaMKII/CREB (Chiang *et al.*, 2014) pathways, respectively. Donepezil, a drug used for treatment of dementia condition in Alzheimer's disease and other dementia, had been reported to increase neurite outgrowth in PC12 cells via activation of ERK (Oda *et al.*, 2007) and sigma-1 receptor pathway (Ishima *et al.*, 2008). An immunosuppressant drug Tacrolimus also increased neurite outgrowth in NGF-treated PC12 cells by modulation of CaM and Raf/Ras/MAPK/ERK pathway (Price *et al.*, 2003). Fasudil, a drug for treatment of cerebral vasospasm which was approved in Japan and China, revealed a possibility as a drug for treatment for age related or neurodegenerative memory loss. Fasudil increased neurite outgrowth in human NT2/D1 precursor cells by inhibition of RhoA/ROCK signaling (Roloff *et al.*, 2015). Vitamin B12 and vitamin K1 (phylloquinone) were also reported to increase neurite extension by activation of MAPK/ERK pathway (Tsang *et al.*, 2002; Ina *et al.*, 2006).

Several studies reported the effects of natural compounds on neurite outgrowth by various mechanisms of action such as MAPK/ERK/CREB and PI3K/Akt pathways. Natural compounds such as ginsenoside Rb1 (Liu *et al.*, 2014), luteolin (Lin *et al.*, 2012; Nishina *et al.*, 2013), artemisinin (Sarina *et al.*, 2013), curcuminoid (Liao *et al.*, 2012), Þ-lipoic acid (Wang *et al.*, 2011a), spicatoside A (Hur *et al.*, 2009) and ß-eudesmol (Obara *et al.*, 2002) were reported to increase neurite outgrowth through activation of MAPK/ERK/CREB. While, natural compounds such as emodin (Park *et al.*, 2015) and methyl-dihydroxybenzoate (Zhang *et al.*, 2015) increased neurite outgrowth by PI3K/Akt/GSK3ß activation.

Centella asiatica and its effects on nervous system

Several studies suggested the memory enhancement effect of *C. asiatica* extract in various rodent models. *C. asiatica* has large amounts of pentacyclic triterpenoids, which mainly are **MS**, **AS**, **MA** and **AA** (James *et al.*, 2009) (**Figure 2**). Other constituents include tannins, phytosterols and flavonoids such as quercetin and kempferol are also found in little amounts (Rumalla *et al.*, 2010). Among these compounds, **MS** and **AS** are considered as the primary active constituents (Thomas *et al.*, 2010). These compounds are classified as triterpenoid glycosides or triterpenoid saponins, in which a sugar moiety (glucose-glucose-rhamnose) is linked to each of their aglycone form. The different extraction methods of *C. asiatica* resulted in different amounts of each constituent in the extracts and exhibited the variety of activities and potencies.

For the glycoside forms, standardized *C. asiatica* extract ECa233 which mainly consists of 53% **MS** and 32% **AS** (Tantisira *et al.*, 2010) exhibited protective effects on hippocampus cell death and improved memory deficit in ß-amyloid and carotid occlusion rats when given orally (Kam-eg *et al.*, 2009; Tantisira *et al.*, 2010), and also exhibited neuritogenic effect in human IMR-32 cells (Wanakhachornkrai *et al.*, 2013). **MS** and **AS** were found to improve locomotor dysfunction and to protected dopaminergic neuron in Parkinson's disease rat model when given each compound

intragastrically (Xu *et al.*, 2012a; Xu *et al.*, 2013). Orally given **MS** also ameliorates D-galactose-induced learning and memory impairments in mice by suppressing inflammatory response and up-regulation the synapse-related genes (Lin *et al.*, 2014). **AS** also improved cognitive deficits in senescence-accelerated mice (Lin *et al.*, 2013). The anxiolytic effects were also found in the methanolic extract of *C. asiatica* containing 4.3% **AS** and 0.61% **AA** (Wijeweera *et al.*, 2006) and triterpenoid glycosides-rich ECa233 extract (Wanasuntronwong *et al.*, 2012). While the protective effect on ß-amyloid-associated behavioral abnormalities in Tg2576 mouse was also found in the water extract of *C. asiatica* which did not consist of **MA** and **AA** (Soumyanath *et al.*, 2012). Most studies suggested the potential roles of **MS** and **AS** in effects on nervous system.

However, several studies also revealed that aglycone forms, **MA** and **AA**, also exhibited the bioactivities on nervous system. Treatment of **AA** could protect ß-amyloid-induced B103 cell death, while **AS** could not protect (Jew *et al.*, 2000). Protective effects on glutamate- and ceramide-induced cell death of **AA** were also reported (Xu *et al.*, 2012b; Zhang *et al.*, 2012). **AA** also attenuated glutamate-induced cognitive deficits in mice by antioxidant activity when given orally (Xu *et al.*, 2012b). The neuritogenic effect on PC12 cells was reported in **AA** and **MA** containing fraction of *C. asiatica* extract, while the fraction contained **MS** and **AS** was inactive (Jiang *et al.*, 2016). Moreover, the standardized extract consists of **AS** and **AA** at 1.09 and 48.89 mg per g extract was reported to improve cognition and mood in the healthy elderly volunteer in clinical study (Wattanathorn *et al.*, 2008).

From the evidence, it appeared that **MS**, **AS**, **MA** and **AA** all exhibited the bioactivities with a variety of different testing systems. Therefore, the controversy was raised that whether glycoside or aglycone forms were responsible for the bioactivities on nervous system. The issue of biotransformation of triterpenoid glycosides into corresponding aglycones has also not been explored.
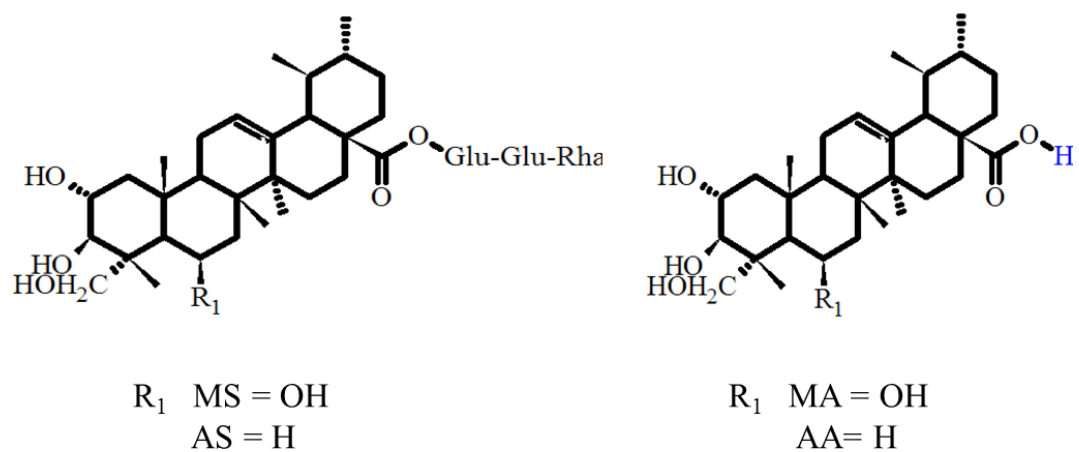
Figure 2 Structures of MS, AS, MA and AA.

CHAPTER III MATERIALS AND METHODS

Instruments

- Centrifuge (Allegra X-12R, Zentrifugen, Germany)
- CO_2 incubator (Cat. No. 3121, Forma Scientific Inc, Massachusetts, USA)
- Fluorescent inverted microscope (Eclipse Ti-U, Nikon, Tokyo, Japan)
- HPLC-photodiode array system (Shimadzu, Kyoto, Japan)
- ImageQuant LAS 4000 (GE Healthcare, Buckinghamshire, UK)
- Microplate reader (Perkin Elmer, Victor3, Massachusetts, USA)
- Mini Trans-Blot® Electrophoretic Transfer cell (Bio-Rad, USA)
- Phenomenex C_{18}column (250 × 4.6 mm, 5 μm; Phenomenex, Cheshire, UK)

Testing compounds

- Asiatic acid (purity ≥95 %, Cat No. A7332, LKT Laboratories Inc., Minnesota, USA)
- Asiaticoside (purity ≥90 %, Cat No. A7333, LKT Laboratories Inc., Minnesota, USA)
- Madecassic acid (purity ≥95 %, Cat No. M0114, LKT Laboratories Inc., Minnesota, USA)
- Madecassoside (purity ≥ 95 %, Cat No. M6949, Sigma-Aldrich, Missouri, USA)

Cellular model

- Neuro-2a mouse neuroblastoma cell line (CCL-131, American Type Culture Collection (ATCC), VA, USA)

Chemicals

- 3-(4,5-dimethylthiazol-2-yl)-2,5-diphenyltetra-zolium bromide (MTT) (Cat No. M2128, Sigma-Aldrich, Missouri, USA)
- 8-(4-chlorophenylthio)-adenosine 3',5'-cyclic monophosphate (8-cpt-cAMP) (Cat No. C0735, Sigma-Aldrich, Missouri, USA)
- Antibodies
  - Primary antibodies

- **Akt, phosphor Ser473**, Rabbit polyclonal antibody (Cat No. ab66138, Abcam, Cambridge, UK)

- **Akt**, Rabbit polyclonal antibody (Cat No. ab6076, Abcam, Cambridge, UK)

- **CREB phosphor Ser133**, Rabbit polyclonal antibody (Cat No. 06-519, EMD Millipore, California, USA)

- **CREB**, Mouse monoclonal antibody (Cat No. MAB5432, EMD Millipore, California, USA)

- **ERK1/2 (p44/42 MAPK)**, Rabbit polyclonal antibody (Cat No. 9102, Cell Signalings, Massachusetts, USA)

- **ERK1/2 phosphor Thr202/Tyr204 (p44/42 MAPK)**, Rabbit polyclonal antibody (Cat No. 9101, Cell Signalings, Massachusetts, USA)

- **Glyceraldehyde 3-phosphate dehydrogenase (GAPDH)**, Rabbit polyclonal antibody (Cat No. ab9483, Abcam, Cambridge, UK)

- **GSK3β phosphor Ser9**, Rabbit monoclonal antibody (D85E12) XP® (Cat No. 9322 Cell Signalings, Massachusetts, USA)

- **GSK3β**, Rabbit monoclonal antibody (D5C5Z) XP® (Cat No. 12456 Cell Signalings, Massachusetts, USA)

- **Histone H2A.X**, Rabbit polyclonal antibody (Cat No. ab20669, Abcam, Cambridge, UK)

- **MAP2**, Mouse polyclonal antibody (Cat No. M9942, Sigma, Missouri, USA)

- **Nrf2**, Rabbit polyclonal antibody (Cat No., Abcam, Cambridge, UK)

- **β-actin HRP-conjugated**, Mouse monoclonal antibody (Cat No. ab20272, Abcam, Cambridge, UK)

- **βIII-tubulin**, Mouse monoclonal antibody (Cat No. MAB1637, EMD Millipore, California, USA)

- Secondary antibodies

- Goat antibody against mouse IgG conjugated with AlexaFluor® 488 (Cat No. A-11029, Life Technologies-Molecular Probes, California, USA)

- Goat antibody against mouse IgG conjugated peroxidase (Cat No. AP-124P, EMD Millipore, California, USA)

- Goat antibody against rabbit IgG conjugated HRP (Cat No. ab6721, Abcam, Cambridge, UK)

- Ammonium persulfate (APS; Cat No. 1610700, Bio-Rad
- Bovine serum albumin (Cat No. 12659, Calbiochem, Massachusetts, USA)
- Calpeptin (Cat No. C8999, Sigma-Aldrich, Missouri, USA)
- Dulbecco's Modified Eagle Medium (DMEM; Cat No. 12800-58, Gibco, Auckland, New Zealand)
- ECL Prime^{Tm} Western blotting detection reagent (Cat No. RPN2232, Amersham, UK)
- Fetal bovine serum (FBS, Hyclone, Northumberland, UK)
- GNF5837 (Cat No. SML0844, Sigma-Aldrich, Missouri, USA)
- GW441756 hydrochloride (Cat No. G3420, Sigma-Aldrich, Missouri, USA)
- Hoechst33342 (bisBenzimide H 33342 trihydrochloride; Cat No. B2261, Sigma-Aldrich, Missouri, USA)
- Naphthol AS-E phosphate (Cat No. 70485, Sigma-Aldrich, Missouri, USA)
- LY294002 hydrochloride (Cat No. L9908, Sigma-Aldrich, Missouri, USA)
- LY2090314 (Cat No. SML1438, Sigma-Aldrich, Missouri, USA)
- Paraformaldehyde (Cat No. P6148, Sigma-Aldrich, Missouri, USA)
- PD098,059 (Cat No. P215, Sigma-Aldrich, Missouri, USA)
- Penicillin/streptomycin 100X solution (Cat No. 15140-122, Gibco, Auckland, New Zealand)
- Propidium iodide (Cat No. P4170, Sigma-Aldrich, Missouri, USA)
- Protease Inhibitor Cocktail (Cat No. P8340, Sigma-Aldrich, Missouri, USA)
- Retinoic acid, *all-trans* (Cat No. R2625, Sigma-Aldrich, Missouri, USA)
- RhoA activation assay kit (Cat No. ab211164, Abcam, Cambridge, UK)
- tert-butylhydroquinone (tBHQ) (Cat No. 112941, Sigma-Aldrich, Missouri, USA)

Materials

- Cell culture 24-well plate (Cat No. 3524, Corning Inc., USA)

- Cell culture 96-well plate (Cat No. 371, Corning Inc., USA)

- Cell culture dish 35 mm (Cat No. 1SPL-20035, SPL, South Korea)

- Cell culture flask 25 cm2 (Cat No. 430168, Corning Inc., USA)

- Cell culture flask 75 cm2 (Cat No. 430641, Corning Inc., USA)

- FluoroTrans® polyvinylidene fluoride (PVDF) membrane (Cat No. BSP0161, Pall Life Sciences, USA)

Methods

Stability testing in culture system

To avoid erroneous interpretation whether glycosides or aglycones affected the cells, the stability testing in culture system was performed. **MS**, **AS**, **MA** and **AA** were dissolved in DMSO at concentrations of 20 and 200 mM, and further diluted in DMEM medium supplemented with 10% FBS and 100 units/mL penicillin/streptomycin to produce the final concentration at 100 and 1000 µM. Medium was then incubated with or without Neuro-2a cells in humidified atmosphere of 5% CO_2 at 37°C. To extract the compound from the medium, each 400 µL of medium was collected at 6, 12, 24 and 36 h and mixed with 600 µL of cold-methanol (Xiao *et al.*, 2015). The mixture was kept at -20°C for 30 min to precipitate the proteins. After centrifugation at 12,000 rpm for 15 min at 4°C, an aliquot of supernatant was filtered through 0.45 µm filter and subjected to HPLC analysis. The standard curves of each compound were also produced in extracted medium to subtract the matrix effects. The condition for HPLC was as following:

HPLC system: HPLC-photodiode array system (Shimadzu, Kyoto, Japan)

Column: Phenomenex C_{18} column (250 × 4.6 mm, 5 μm; Phenomenex, UK)

Mobile phase: Solution A: water   Solution B: acetonitrile

Flow rate: 1.0 mL/min   **Detector:** 206 nm

Gradient conditions:

Time (min)	Solvent A (%)	Solvent B (%)
0	80	20
15	65	35
30	35	65
35	20	80
40	20	80
45	80	20
55	80	20

(Rafamantanana *et al.,* 2009)

Cell culture and treatment

Neuro-2a cells were cultured in DMEM medium supplemented with 10% FBS and 100 units/mL penicillin/streptomycin in humidified atmosphere of 5% CO_2 at 37°C. Neuro-2a cells were sub-cultured every 2 days. Passage numbers between 20 and 40 were used in the experiments. Madecassoside, asiaticoside, madecassic acid, asiatic acid and other testing compounds were dissolved in dimethyl sulfoxide (DMSO) and diluted with DMEM medium (0.5% final concentration of DMSO).

Cell viability assay

To determine the non-toxic concentrations for further study, cell viability was determined by MTT assay as described previously (Carmichael *et al.,* 1987). Briefly, cells (1000 cells/well) were seeded into each well of 96-well plate. After 24 h, cells

were treated with the various concentrations (0.001 to 1000 µM) of testing compounds for 6, 12, 24, 48 and 72 h. The medium was replaced by 0.4 mg/mL MTT solution and incubated for 4 h. After discarding MTT solution, DMSO was added to dissolve purple formazan crystals. The absorbance was read by microplate reader at wavelength 570 nm. Concentration which did not significantly affect the cell viability would be defined as non-toxic concentration. Cells treated with DMSO at final concentration 0.5% were used as a vehicle control group.

Neurite outgrowth assay by immunofluorescent staining

Non-toxic concentrations of each compound were used in neurite outgrowth assay. Neuro-2a cells (2500 cells/well) were seeded into each well of 24-well plate. After 24 h, cells were treated with the testing compounds at the various times and concentrations. Cells were washed twice with phosphate-buffered saline (PBS) and fixed with 4% paraformaldehyde in PBS for 20 min at room temperature. Fixed cells were permeabilized and blocked with 3% BSA/0.3% Triton-X100 in PBS for 1 h at the room temperature with gentle agitation. Cells were further incubated with mouse primary antibody against βIII-tubulin (1:500) overnight at 4°C, followed by secondary antibody against mouse IgG conjugated with AlexaFluor®488 for 1 h at room temperature. Nuclei were also stained with 1 µg/mL Hoechst33342 solution for indicating the number of total cells.

Image analysis

Cells in each well were imaged using inverted fluorescence microscope. In each well, cell images were randomly captured 6-8 fields to obtain at least 300-400 cells per well. Images were then analyzed using ImageJ software v1.50c (National Institutes of Health, MD, USA). Number of the cells was counted using Cell Counter tool in ImageJ by counting the Hoechst33342-stained nuclei, while the morphological analysis was observed by fluorescent signal against βIII-tubulin. Neurite was identified as a process equal to or longer than cell body diameter (Harrill *et al.*, 2011). The length of neurites

was measured by using Measure tools in ImageJ. The parameters which used for evaluation of neurite outgrowth were:

1. Percentage of neurite-bearing cells (%NBC): This parameter was calculated by the percentage of ratio between the numbers of cells with neurites and total cells as followed equation:

$$\%\text{NBC} = \frac{\text{Cells with neurite(s)}}{\text{Total cells}} \times 100$$

2. Number of cells with different neurite length: The neurite-bearing cells were also graded according to their lengths of the longest.

3. Average neurite length (NL): This parameter was the average value of the longest neurites from each cell which had the length of neurites equal to or longer than cell body diameter.

Investigation of intracellular signaling pathways by Western blot analysis

The effective concentrations of each compound on neurite outgrowth assay were used for treatment in Western blot analysis. Cells were lysed by lysis buffer (50 mM Tris, 150 mM NaCl, 0.1% SDS, 0.5% sodium deoxycholate, 1% Triton-X100 and 1% cocktail protease inhibitor) for 1 h and centrifuged at 12,000 rpm for 15 min at 4°C. Supernatant containing protein was collected and protein concentration was determined by Bradford assay. Proteins (20 μg) were mixed with 5X sample buffer (50 mM Tris-HCl pH 6.8, 2% SDS, 10% glycerol, 1% β-mercaptoethanol, 12.5 mM EDTA and 0.02 % bromophenol blue) and loaded into each well of 12.5% SDS-PAGE. The proteins were separated with the applied amperage of 12 mA per gel, and subsequently electrotransferred onto PVDF membranes by the applied voltage of 100 V for 90 min. The blots were blocked with 5% BSA in TBS-T buffer (10 mM Tris-HCl, pH 7.4, 150 mM NaCl with 0.1% Tween 20) and then were probed with primary antibodies against signaling proteins of interest for overnight at 4 °C. The blots were further incubated with HRP-conjugated secondary antibody for 1 h at room temperature. The protein

bands were detected by using chemiluminescent detection solution. Band images were acquired using ImageQuant LAS 4000 and quantitative analyzed by ImageQuant TL 7.0 software (GE Healthcare, Uppala, Sweden). Relative band intensity of each protein was normalized with ß-actin or GAPDH band intensity. The details of each signaling pathway were described below.

(1) ERK signaling pathway

To determine the time profile of ERK activation, cells were treated with each compound at the effective concentration for 0.5, 1, 2, 4, 6 and 12 h. Western blot analysis was performed by using primary antibodies against ERK1/2 (1:1000 dilution) and Thr202/Tyr204 phosphorylated form of ERK1/2 (p-ERK1/2; 1:1000 dilution). In concentration-dependent study, the time point, which p-ERK1/2 was maximally activated, was used as the incubation time for treatment. To confirm the activation of p-ERK1/2, the MEK inhibitor PD098,059 was used. Cells were pre-treated with PD098059 (10 µM) for 30 min before treatment and further subjected for Western blot analysis.

(2) PI3K/Akt signaling pathway

For Akt activation, the time profile study was also performed by Western blot analysis using primary antibodies against Akt (1:1000 dilution) and Ser473 phosphorylated form of Akt (p-Akt; 1:1000 dilution). To confirm the activation of p-Akt, a PI3K inhibitor LY294002 was used for inhibition of Akt phosphorylation. Cells were pre-treated with LY294002 (10 µM) for 30 min before treatment and further subjected for Western blot analysis.

(3) Investigation of downstream signaling mediated by ERK and/or Akt pathways

For investigation of downstream signaling from each ERK and Akt triggering, activation of downstream signaling molecules was determined by Western blot and immunofluorescent analysis. Due to activation of ERK and Akt often stimulate some of similar downstream signaling molecules such as CREB and Nrf2. Therefore, the specific inhibitors of ERK or Akt were also used to confirm.

(3.1) CREB signaling pathway

Time-course activation of CREB was performed by Western blot analysis using primary antibodies against CREB (1:1000 dilution) and Ser133 phosphorylated form of CREB (1:1000 dilution). To confirm the involvement of ERK or Akt signaling pathways on CREB activation, specific inhibitors of ERK or Akt were used. Cells were pre-treated with PD098059 (10 µM) or LY294002 (10 µM) for 30 min before treatment with **MS**, **AS**, **MA** and **AA** at the effective concentration, and further subjected for Western blot analysis.

(3.2) Nrf2 signaling pathway

Time-course activation of Nrf2 was performed by investigating on translocation of Nrf2 from cytosol to nucleus using subcellular fractionation followed by Western blotting analysis. Cells were pre-treated with **MS, AS, MA** or **AA** at the effective concentration for 0.5, 1, 2, 4, 6 and 12 h. Cells were then harvested in fractionation buffer (20 mM HEPES, 10 mM KCl, 2 mM $MgCl_2$, 1 mM EDTA, 1 mM EGTA) and were lysed by passing through 27G needle. Cell lysate was centrifuged at 720xg at 4°C for 5 min. Supernatant was collected to obtain cytosolic fraction. Cell pellets were dispersed in fractionation buffer and further subjected to be lysed by passing through 25G needle. Cell lysate was centrifuged at 720xg at 4°C for 10 min. Pellets were collected and dissolved in RIPA lysis buffer to obtain nuclear fraction. Both cytosolic and nuclear fractions were subjected for Western blotting analysis using primary antibody against Nfr2 (1: 400 dilution). Primary antibodies for detection of ß-actin and histone H2A.X were also used as loading control proteins for cytosolic and nuclear fractions, respectively. To confirm the involvement of ERK or Akt signaling pathways on Nrf2 activation, cells were pre-treated with PD098059 (10 µM) or LY294002 (10 µM) for 30 min before treatment with **MS, AS, MA** and **AA** at the effective concentration, and further subjected for Western blot analysis as mention above.

(3.3) GSK3β signaling pathway

Time-course activation of GSK3β was performed by Western blot analysis using primary antibodies against GSK3β (1:1000 dilution) and Ser9 phosphorylated form of GSK3β (1:1000 dilution). To confirm the involvement of ERK or Akt signaling pathways on GSK3β activation, cells were pre-treated with PD098,059 (10 μM) or LY294002 (10 μM) for 30 min before treatment with **MS, AS, MA** and **AA** at the effective concentration, and further subjected for Western blot analysis.

(4) RhoA/ROCK signaling pathway

The effect on inhibition of RhoA activity was determined by using RhoA pull-down activation assay kit (Abcam). The activated RhoA (GTP-bound RhoA) would bind to rhotekin-Rho binding domain (RBD) which is the effector of active RhoA. Therefore, we used rhotekin-RBD attached to the agarose beads for pulling down of the active RhoA. Cell lysates were subjected to pull-down assay by incubation with rhotekin-RBD beads at 4°C for 1 h. Mixture was pelleted by centrifugation at 14000xg for 10 sec at 4°C. Pellets were washed 3 times with wash buffer and resuspended with 5X sample buffer and further subjected to Western blot analysis by using anti-RhoA monoclonal antibody. In order to confirm the inhibitory effect of tested compounds, calpeptin, a RhoA activator, was used as a positive control.

Investigation of putative extracellular targets of testing compounds

To clarify the upstream regulation of intracellular signaling, the role of Trk receptor on downstream signaling activation and neurite outgrowth was also investigated. To inhibit signal transduction from TrkA receptors, a specific TrkA inhibitor, GW441756, was used for pre-treatment to the cells before treatment with tested compounds. After pretreatment with GW441756, the effects on downstream signalings, which were ERK1/2, Akt, CREB, GSK3β, Nrf2 and RhoA, as well as neurite outgrowth activity were investigated in order to determine the involvement of TrkA receptor signaling.

Statistical analysis

All data are expressed as mean ± standard error of the mean (SEM) from at least three independent experiments. The differences among the groups were evaluated by one-way analysis of variance (ANOVA), followed by LSD's test. Statistical significance was defined as $p < 0.05$ for all tests.

CHAPTER IV RESULTS

1. Stability of MS, AS, MA and AA under cell culture condition

Due to recent study reported that some glycoside compounds might be subjected to hydrolysis in cell culture system (Xiao *et al.*, 2015). Therefore, the effect of cell culture condition on stability of **MS**, **AS**, **MA** and **AA** were determined to clarify whether glycosides were hydrolyzed into aglycones during incubation period in cell culture medium by using HPLC-photodiode array system. The optimization of HPLC condition was performed and some method validation parameters were carried out (Table 1 Appendix B). The stability was tested in 2 conditions which were stability in cell culture media in the absence and presence of the Neuro-2a cells with the standard cell culture atmosphere. **Figure 3A** exhibited the HPLC chromatogram of the mixture of standard **MS**, **AS**, **MA** and **AA** in methanol with the peaks of **MS** at retention time 14.43±0.32 min, **AS** at retention time 18.21±0.23 min, **MA** at retention time 28.64±0.34 min and **AA** at retention time 31.85±0.41 min (**Table 2 Appendix B**). In cell-free culture medium, the standard **MS**, **AS**, **MA** and **AA** were diluted in culture medium and extracted with methanol prior to be subjected for HPLC analysis. HPLC chromatogram of standard **MS**, **AS**, **MA** and **AA** in extracted medium showed the peaks of each compound with similar pattern and retention times as in methanol solution. However, there were some small peaks appeared but did not interfere with the interested compounds (**Figure 3B, 3C**).

To avoid the matrix effects, the standard curves of each **MS**, **AS**, **MA** and **AA** were performed in the extracted medium at the range of 10 to 500 μg/mL (**Figure 42 Appendix B**). These standard curves in extracted medium would be used in analysis for stability testing in both cell-free medium and culture medium with the cells. The extracted medium without any tested compounds at the various incubation times (6, 12, 24 and 36 h) were also analyzed and showed the similar chromatographic profiles in each time point (**Figure 43 Appendix B**). Therefore, the extracted medium would be used as the blank for background peak subtraction in further stability study.
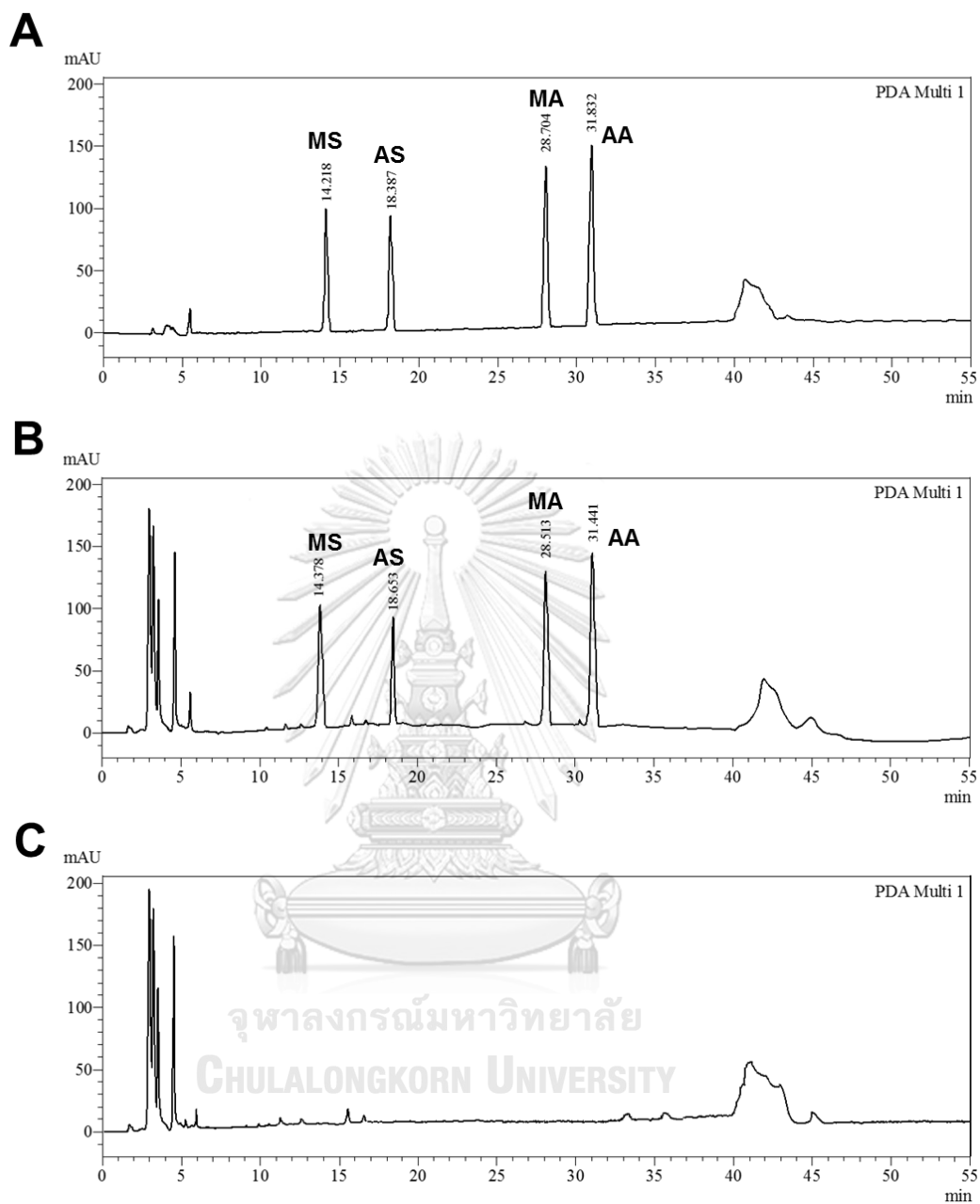
Figure 3 HPLC chromatograms of mixture of standard **MS**, **AS**, **MA** and **AA**
in (**A**) methanol and (**B**) extracted medium. (**C**) blank extracted medium. All
chromatograms were detected at 206 nm.

In cell-free condition, each **MS**, **AS**, **MA** and **AA** were diluted in DMEM at 0.1 and 1 mg/mL for 6, 12, 24 and 36 h. At each time point, medium was collected and extracted with methanol. The final concentration of each compound in extracted medium would become 40 and 400 µg/mL (100 and 1000 µM) and 10 µL of each extracted medium was subjected into HPLC system. The result showed that the concentration of all tested compounds did not significantly change at all incubation time points in cell-free condition (**Figure 4**). These suggested that there was neither hydrolysis nor decomposition occurred during the incubation time up to 36 h at the standard cell culture atmosphere detected at 206 nm (**Figure 44 Appendix B**).

In the presence of the cells, the control media were collected at each indicated time points and the additional peaks were found in HPLC chromatograms of extracted media collected from each incubation time point when compared to extracted medium at time 0 h (**Figure 45 Appendix B**). Therefore, the stability testing in the presence of the cells, the chromatogram of tested compounds would be subtracted against the blank extracted medium at the same time point. The amount of **MS** was found to be slightly decreased after 12-h incubation but the change was not significantly different (**Figure 5**). Similar to **MS**, the amount of **AS** also tended to be decreased especially at 36-h incubation for low concentration of AS (40 µg/mL) (**Figure 5**). However, we could not detect any additional peak monitored at 206 nm of decomposed compounds in this HPLC study (**Figure 46 Appendix B**).

For **MA** and **AA** in the presence of the cells, **MA** and **AA** when incubated together with the cells for long incubation time (24-36 h), they caused the cell death and the media became turbid. Therefore, the time points for high concentration of **MA** and **AA** (400 µg/mL) would be 6 and 12 h, and time point for low concentration (40 µg/mL) would be 6, 12 and 24 h. Interestingly, when **MA** or **AA** were incubated together with the cells, their concentrations were significantly decreased since first 6-h of incubation (**Figure 6**). However, there was no any new additional peak detected in the chromatograms at any wavelength detection when compared to the blank at the same time. (**Figure 47 Appendix B**).
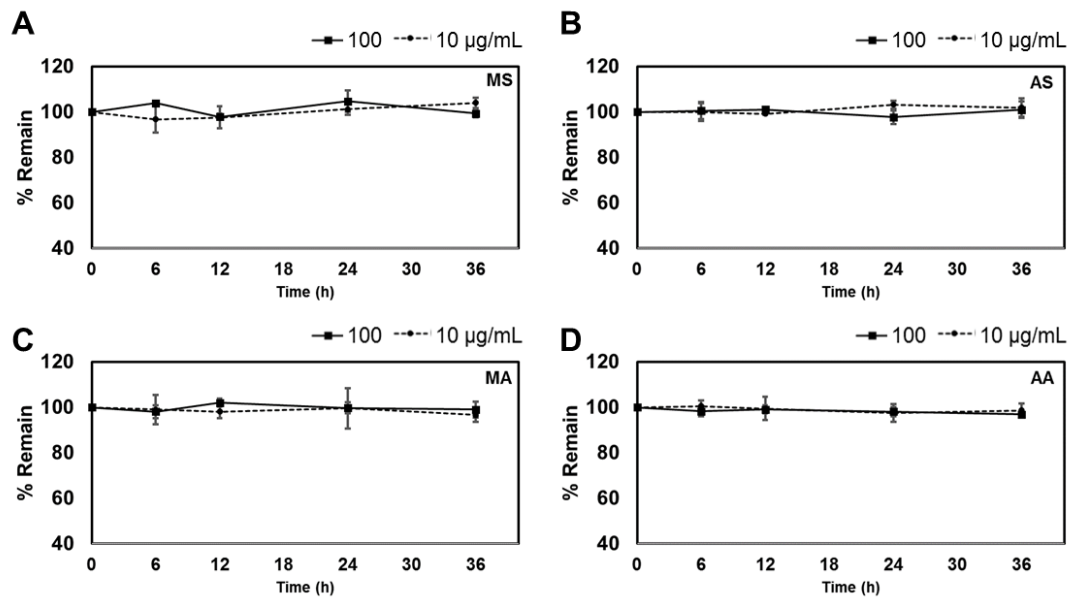
Figure 4 Percentage of concentration of (**A**) MS, (**B**) AS, (**C**) MA and (**D**) AA remaining in cell-free media at indicated time points.

Figure 5 Percentage of concentration of (**A**) **MS** and (**B**) **AS r**emaining in cell-incubated media at indicated time points.

Amounts of each analyte were calculated from their standard curves and were calculated as percentage of remaining when relative to control (t0).

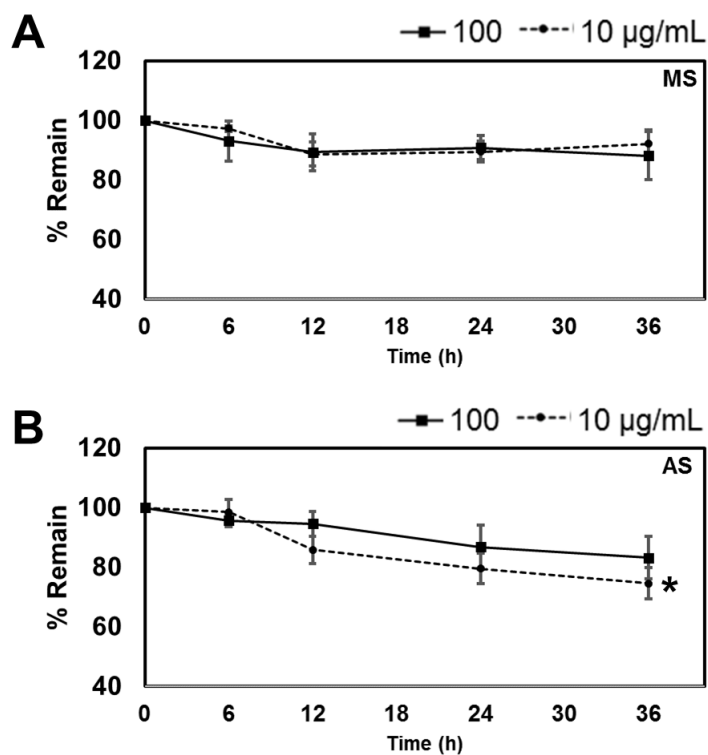**Figure 6** Percentage of concentration of (**A**) **MA** and (**B**) **AA** remaining in cell-incubated media at indicated time points.

Amounts of each analyte were calculated from their standard curves and were calculated as percentage of remaining when relative to control (t0).
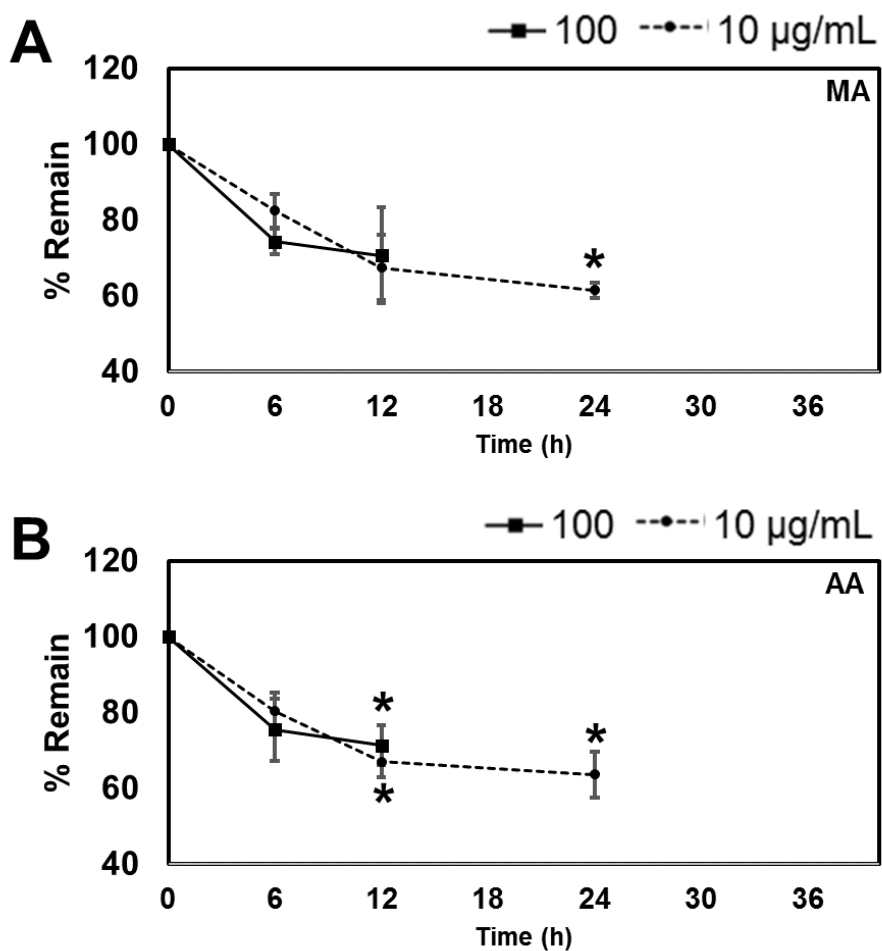
In summary, we found that the concentration of all compounds **MS, AS, MA** and **AA** were not changed in the media without cells up to 36 h. However, in the presence of the cells, the concentration of aglycones **MA** and **AA** were significantly decreased but we could not detect any new peak from the chromatogram of HPLC. Hence it was still unclear whether **MA** and **AA** were decomposed when incubated together with the cells. While more than 80% of concentrations of **MS** and **AS** were still found in the culture media in the presence of the cells.

2. Effect on Neuro-2a cell viability

To determine the nontoxic concentration, assessment of cell viability after exposure to each test compound was performed by using MTT assay. Treatment with **MS** and **AS** did not significantly affect Neuro-2a cell viability although at concentration up to 1000 µM at all incubation time points (6, 12 and 24 h), while the cytotoxicity was found in **MA** and **AA** treatment groups (**Figure 7**). After 6-h incubation, cell viability significantly decreased when the cells were treated with MA at concentration of 400 - 1000 µM or with AA at concentration of 100 - 1000 µM, while treatment with both **MA** and **AA** at concentration of 100 µM and higher caused significant decrease in cell viability after 12- and 24-h incubation. Therefore, concentrations at 50 µM and below were selected as the condition for further investigation of neurite outgrowth.

3. Effects on neurite outgrowth activity

3.1 Normal morphology of Neuro-2a cells

To investigate the effects on neurite outgrowth, the morphological change was evaluated using immunofluorescent staining against βIII-tubulin which allowed to observe the shape of cell body and neurites. Neurite was identified as a process which its length was equal or longer than cell body diameter (Harrill *et al.*, 2011). The normal Neuro-2a cells (untreated cells) mostly showed the morphology of the cells in round shape (**Figure 8; control panel**) with 10-15% of the total cells showing spontaneous neurites of average length around 40 µm.
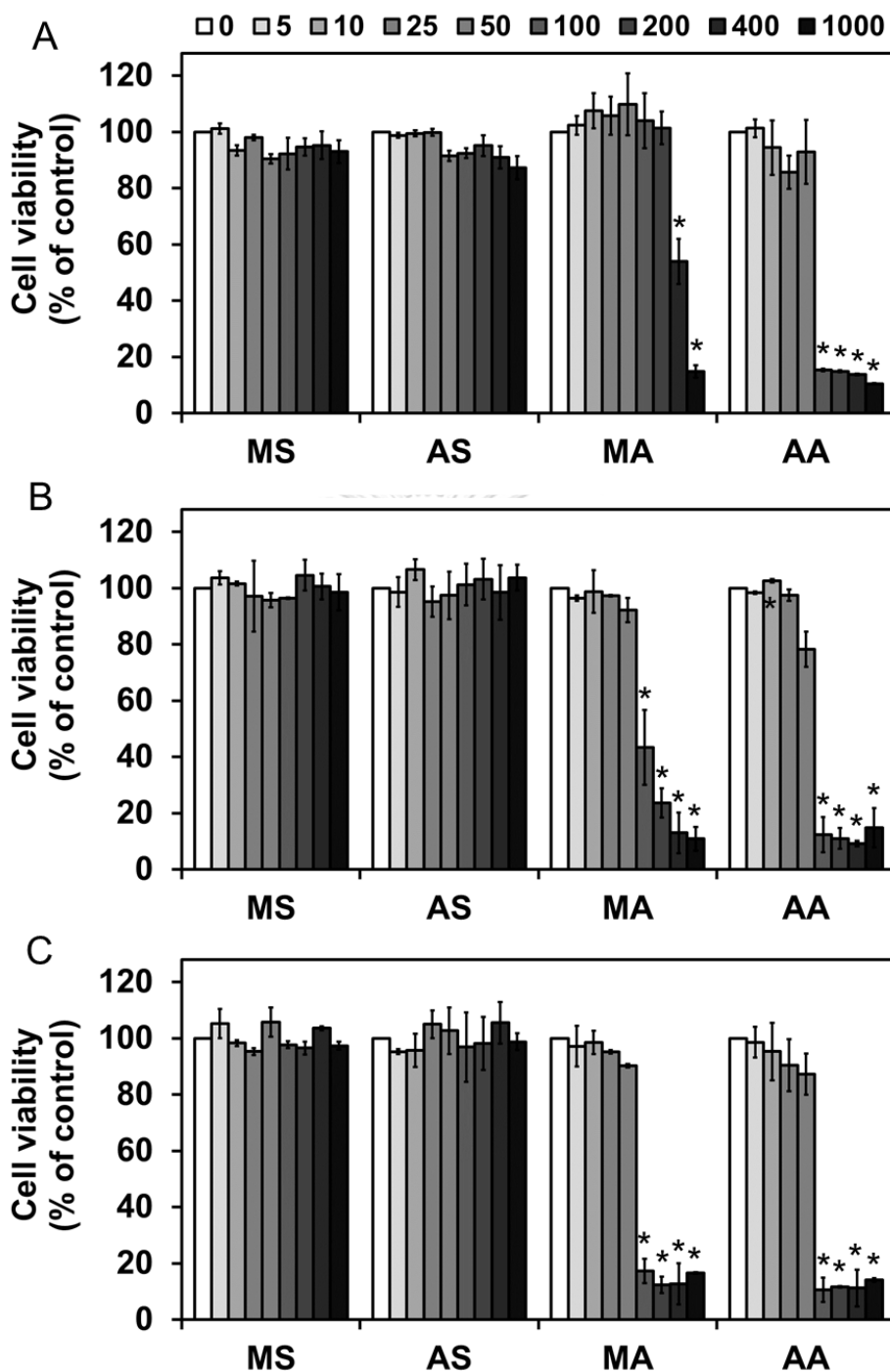
Figure 7 Effects of **MS**, **AS**, **MA** and **AA** on cell viability by MTT assay.

Cells were treated with various concentrations (5 - 1000 μM) for (**A**) 6, (**B**) 12 and (**C**) 24 h. Data are presented as mean ± SEM (n =3). * indicates the significant difference when compared to control group ($p < 0.05$).
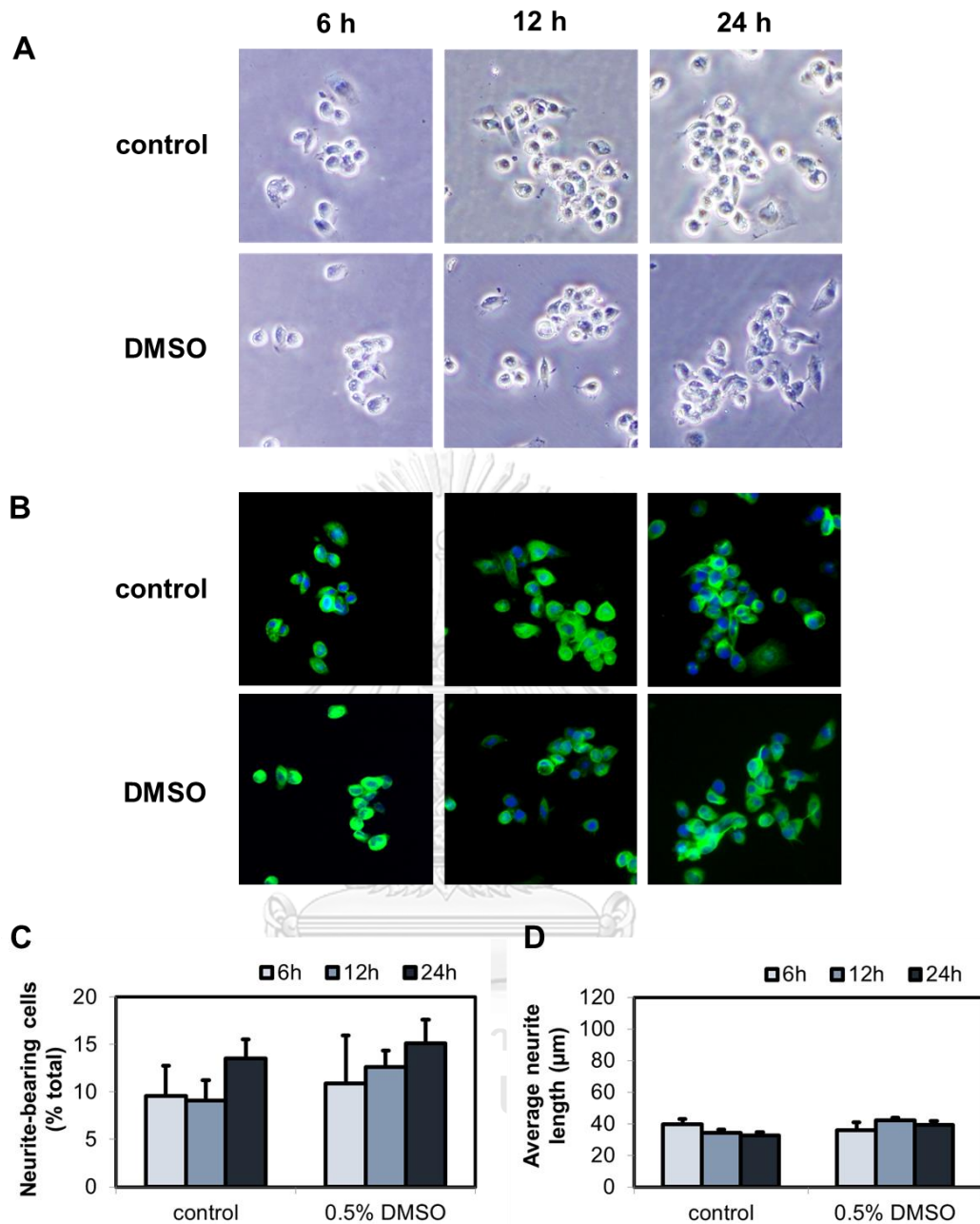
Figure 8 Effects of DMSO on neurite outgrowth in Neuro-2a cells.

Representative images of (**A**) phase-contrast images and (**B**) immunofluorescent images of cells treated with 0.5% DMSO for 6, 12, and 24 h. Cells were probes with antibody against βIII-tubulin (green fluorescence) and nuclei were stained with Hoechst33342 (blue fluorescence). Histograms show (**C**) %NBC and (**D**) neurite length of Neuro-2a cells treated with 0.5% DMSO when compared to control (untreated cells) at indicating time points. Data are presented as mean ± SEM (n=4).

3.2 Neurite outgrowth activity of well-known neuritogenic inducers

To validate the experimental settings and neuritogenic-inducible capacity of Neuro-2a cells, some well-known neuritogenic inducers were used as positive control in neurite outgrowth assay. DMSO is a one kind of solvent widely used for dissolving other compounds in the experiment. However, DMSO was also reported the ability to induce cellular differentiation in several cell types as well as neuronal cells (Kimhi *et al.*, 1976). In our study, DMSO was also used as a solvent for dissolving all tested compounds, which was further diluted with DMEM medium to become final concentration of DMSO at 0.5% *v/v*. Therefore, to avoid the interference, DMSO at this indicating concentration was evaluated for the effect on neurite outgrowth. The results showed that there was no any significant difference in both percentage of neurite-bearing cells and average length of neurite between untreated cells (control group) and cells treated with 0.5% DMSO at all incubation times (6, 12 and 24 h) (**Figure 8**). These indicated that DMSO at concentration of 0.5% did not interfere the neurite outgrowth assay and could be used throughout the experiments.

For the positive control groups, *all-trans* retinoic acid (**RA**) and analogues of cAMP are well-known neurite outgrowth inducing agents (Clagett-Dame *et al.*, 2006; Xu *et al.*, 2012c). In this study, we treated Neuro-2a cells with various concentration of **RA** for 6, 12 and 24 h. Treatment with **RA** (5, 10 and 20 µM) significantly increase %NBC in concentration-dependent manner when compared to untreated control cells (**Figure 9A, 9B**). This activity was found at 6 h of incubation, but at longer incubation time, the %NBC did not significantly increase, suggesting that neurite outgrowth was induced since 6 h after exposure of **RA** to Neuro-2a cells. For neurite extension, treatment with **RA** tended to increase average neurite length in concentration-dependent manner (5 -20 µM), but when compared to untreated control cells, only 20 µM **RA** significantly increase neurite length (**Figure 9C**).

Analogues of cAMP were also reported the neuritogenic activity. In this study, 8-cpt-cAMP, an analogue of cAMP, was used as one of positive control groups (Emery *et al.*, 2014). Neurite outgrowth activity was found in Neuro-2a cells treated with 10 and 100 µM 8-cpt-cAMP for 6, 12 and 24 h (**Figure 9A**). 8-cpt-cAMP strongly induced
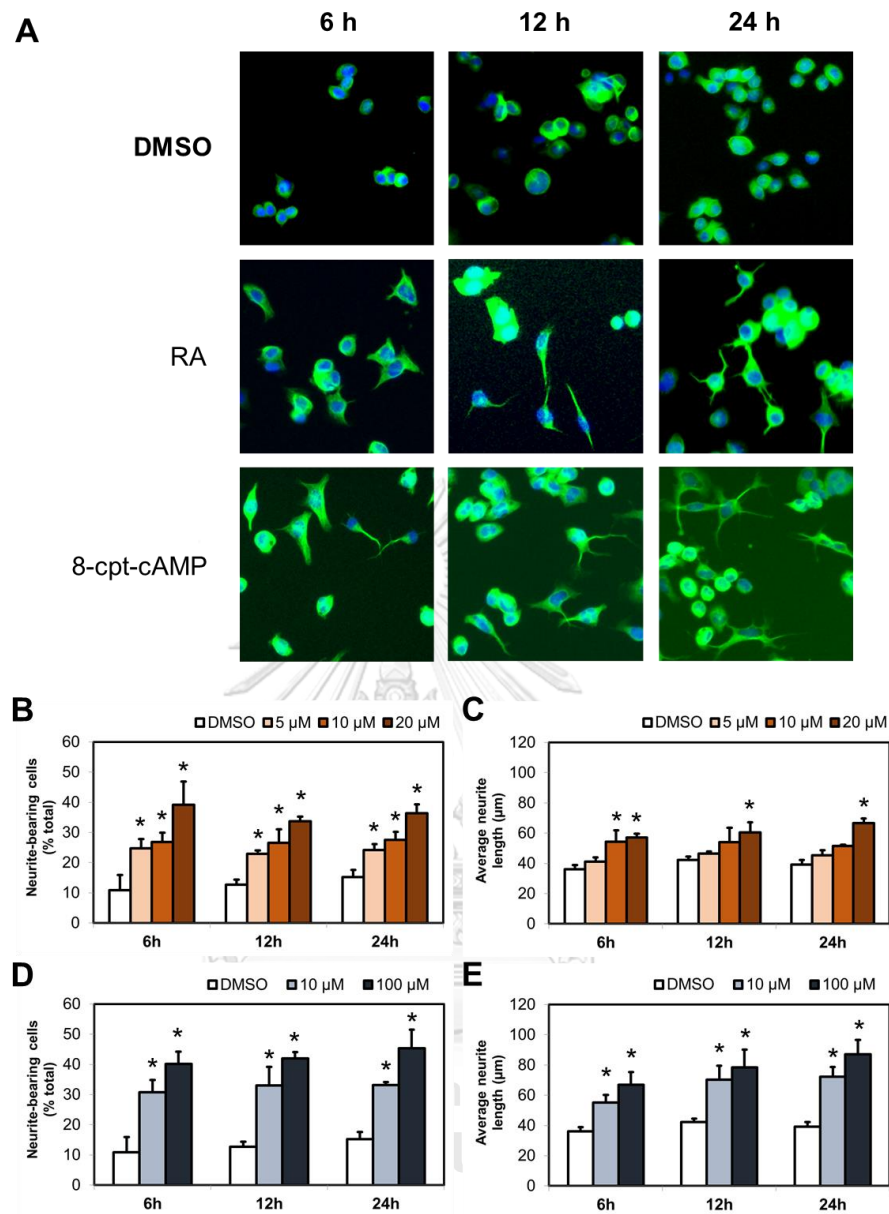
Figure 9 Effects of known inducers on neurite outgrowth in Neuro-2a cells.

(**A**) Representative immunofluorescent images of cells treated with 10 μM **RA** and 10 μM 8-cpt-cAMP. Cells were probes with antibody against βIII-tubulin (green fluorescence) and nuclei were stained with Hoechst33342 (blue fluorescence). Histograms show (**B**) %NBC and (**C**) neurite length of Neuro-2a cells treated with 5, 10 and 20 μM RA (**D**) %NBC and (**E**) neurite length of Neuro-2a cells treated with 10 and 100 μM 8-cpt-cAMP. * significant difference ($p < 0.05$) vs. control (DMSO).

neuronal differentiation by increasing in %NBC and average neurite length (**Figure 9C**). Similar to **RA**, treatment with 8-cpt-cAMP early induced neurite outgrowth since first 6 h of incubation. There was no significant difference in increasing of %NBC and neurite length among each incubation time.

From these experiments, we could conclude that DMSO, which was used as a solvent in this study at final concentration of 0.5% *v/v*, did not exhibit any neurite outgrowth activity when compared to untreated cells. Moreover, neurite outgrowth induction on Neuro-2a cells was successfully triggered by treatment with **RA** or 8-cpt-cAMP. Therefore, these inducing agents would be used as positive control groups in further experiments.

3.3 Effects of MS, AS, MA and AA on neurite outgrowth in Neuro-2a cells

Neuro-2a cells were treated with **MS**, **AS**, **MA** and **AA** at the concentration ranging from 0.01-50 μM for 6, 12 and 24 h (**Figure 10A**). Treatment with **MS** was found to increase %NBC at the concentration from 0.1-50 μM (**Figure 10B**), while the effective concentrations of **AS** varied from 1-50 μM for all incubation times (**Figure 10C**). However, the %NBC values were not significantly different when compared among each incubation time point (6, 12 and 24 h), indicating that the effects were happen since first 6-h of incubation. For aglycones, **MA** and **AA** could also induce neurite outgrowth at all time points. Treatment with **MA** at concentrations of 1-50 μM for 6 and 12 h or at concentration of 10-50 μM for 24 h significantly increased %NBC when compared untreated cells (**Figure 10D**). For treatment with **AA**, %NBC was increased in the cells treated with 1-10 μM **AA** for 6 and 12 h, while at 24-h incubation only 10 μM AA significantly increased %NBC (**Figure 10E**).

For neurite extension, treatment with **MS** and **AS** at 1-50 μM significantly increased average neurite length up to 50-80 μm at 12 and 24 h of incubation, when compared to average neurite length of untreated cells (~40 μm) (**Figure 10F, 10G**). In cells treated with **AA** at 1-50 μM for 6 h also significantly increased average neurite length (**Figure 10I**), while longer incubation with **AA** (12 and 24 h) could significantly increase average neurite length at a concentration as low as 0.01 μM. In contrast,

A
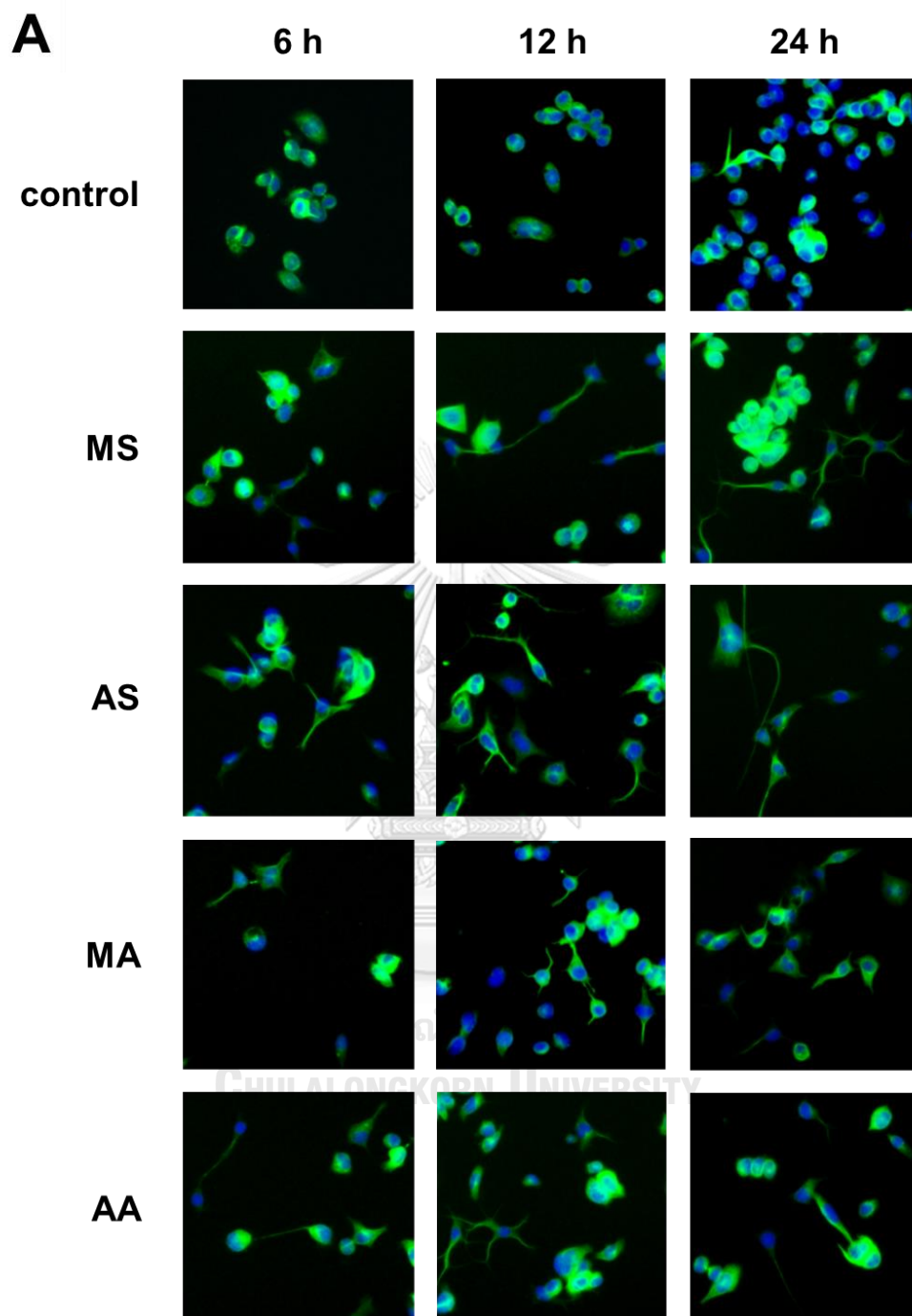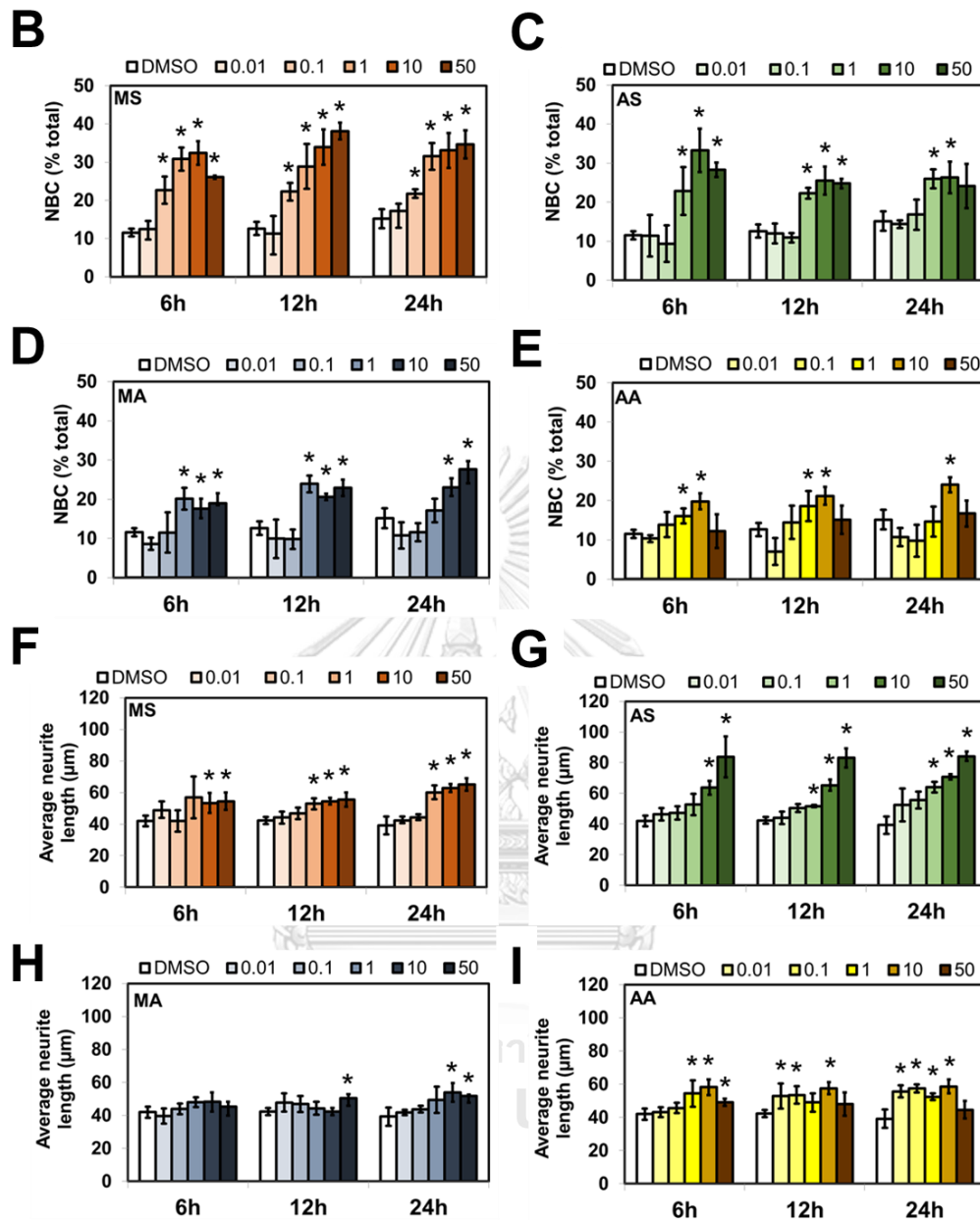
Figure 10 Representative immunofluorescent images of Neuro-2a cells treated with **MS**, **AS**, **MA** and **AA** (10 µM) at 6, 12 and 24 h.

Cells were probes with antibody against βIII-tubulin (green fluorescence) and nuclei were stained with Hoechst33342 (blue fluorescence). Histograms show the %NBC of Neuro-2a cells treated with 0.01 - 50 µM of (**B**) **MS** (**C**) **AS** (**D**) **MA** and (**E**) **AA**. Histograms show the average neurite length of Neuro-2a cells treated with 0.01 - 50 µM of (**F**) **MS** (**G**) **AS** (**H**) **MA** and (**I**) **AA**. Data are presented as mean ± SEM (n=4). * significant difference ($p < 0.05$) vs. control (DMSO).

treatment with **MA** exhibited only small effect on neurite length, because the only noticeable increase was found in cells treated with 10 μM (24 h) and 50 μM (12 or 24 h) (**Figure 10H**). For more insight, the ability of each tested compound (at 10 μM) on induction of neurite elongation was showed by classifying the number of cells with different neurite length. **AS** was found to exhibit the strongest potency on neurite elongation, followed by **MS**, **AA** and **MA**, respectively (**Figure 11**).

For neurite outgrowth assay, we could summarize that all tested compounds, **MS**, **AS**, **MA** and **AA** significantly induced neurite outgrowth in Neuro-2a cells with different potency. When the potency was compared at similar concentrations, the glycoside derivatives (**MS** and **AS**) significantly showed higher potency in enhancing both %NBC and average neurite length than their aglycones (**MS** versus **MA** and **AS** versus **AA**). Moreover, since **MS** and **MA** are 6ß-hydroxylated derivatives of **AS** and **AA**, respectively, the potency between **MS** against **AS** and **MA** against **AA** was compared. The 6ß-hydroxylated derivatives (**MS** and **MA**) appeared to possess more potency in the induction of neurite-bearing cells. However, for promoting neurite elongation, the non-hydroxylated derivatives (**AS** and **AA**) were found to be significantly better. Moreover, we found that most tested compounds in this study clearly exhibited neurite outgrowth activity at concentration of 10 μM. Therefore, this concentration would be used in further mechanistic studies.

4. Investigation on intracellular signaling pathways involving with neurite outgrowth

4.1 Time-course activation of ERK1/2 by MS, AS, MA and AA

Phosphorylation of ERK1/2 was known to be a part of the signal transduction regulating neurite outgrowth. In this study, Neuro-2a cells were treated with 10 μM of each **MS**, **AS**, **MA** or **AA** for 30 min to 12 h of incubation. From the results, all tested compounds were found to induce ERK1/2 phosphorylation (p-ERK1/2) after 30 min of incubation (**Figure 12**). Nonetheless, the different patterns of activation were observed between glycosides and aglycones. **MS** and **AS** induced sustained activation of ERK1/2 with the level of p-ERK1/2 significantly elevated from 30 min to
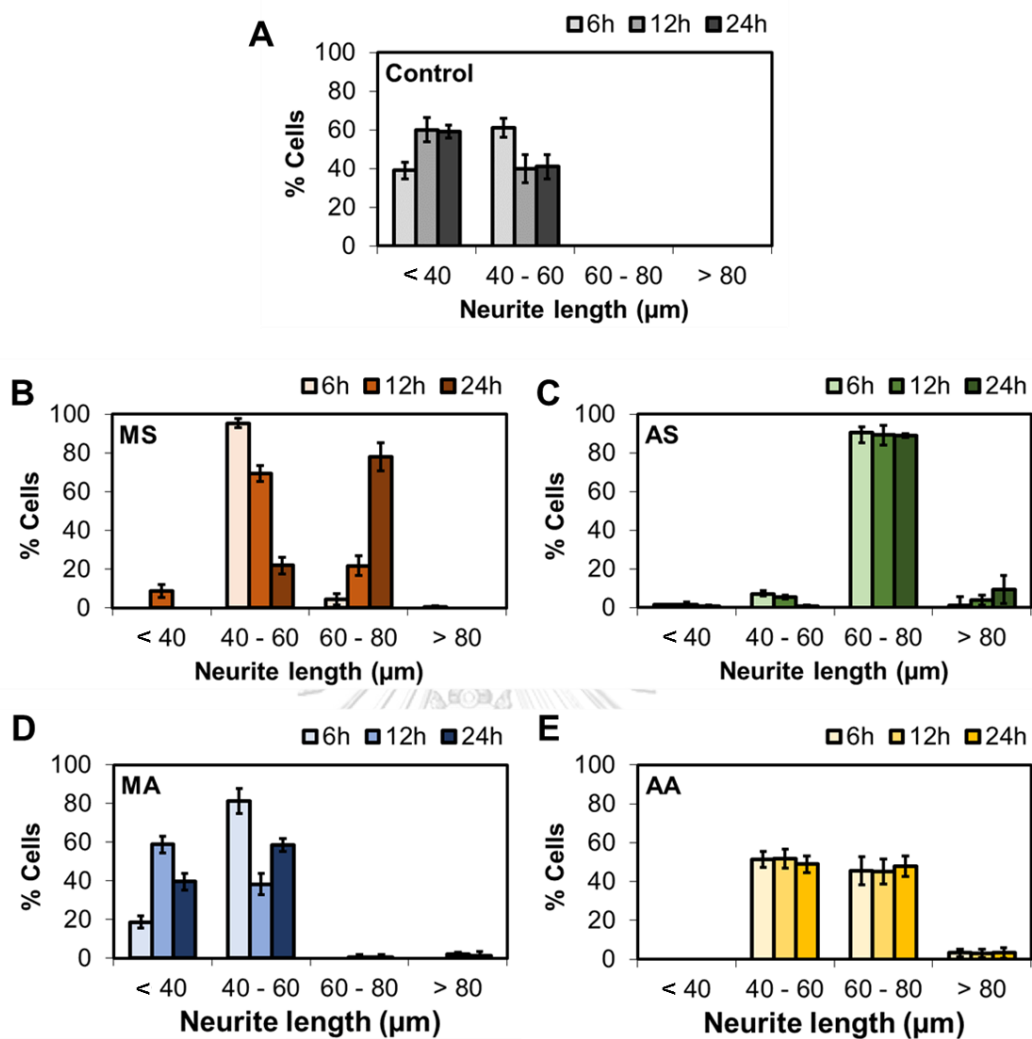
Figure 11 Ability of (**A**) control (DMSO), (**B**) **MS**, (**C**) **AS**, (**D**) **MA** and (**E**) **AA** on neurite length promotion.

Neuro-2a cells were treated with 10 µM of each compound and the length of neurites were measured and classified into 4 groups; (1) >40 (2) 40-60 (3) 60-80 and (4) >80 µm. The neurite length of control group was mostly classified in groups of shorter length. Higher %Cells in long length suggested the better ability in promoting neurite length.

Figure 12 Time profiles of ERK1/2 phosphorylation in Neuro-2a cells.
Representative immunoblots of cells treated with 10 µM of (**A**) **MS** (**B**) **AS** (**C**) **MA** and
(**D**) **AA** at 0.5 - 12 h. The intensity of GAPDH was used for normalization as a loading
control. (**E**) Histogram shows densitometric analysis of ERK1/2 phosphorylation induced
by each compound at indicated time points. Data are presented as mean ± SD (n=3).
* significant difference (*p < 0.05*) vs. control (DMSO).

12 h of incubation (**Figure 12E**), while treatment with **MA** and **AA** showed more transient activation with elevated p-ERK1/2 observed starting from approximately 30-120 min of incubation and restoring to normal level after 4 h (**Figure 12E**). When compared the magnitude of ERK1/2 activation at 30 min incubation, **AA** could increase the level of p-ERK1/2 at a greater magnitude than **MA**, while there was no significant difference between **MS** and **AS**.

4.2 Time-course activation of Akt by MS, AS, MA and AA

Since phosphorylation of Akt are also a part of the signal transduction regulating neurite outgrowth, the effects of **MS, AS, MA** and **AA** on Akt phosphorylation (p-Akt) were investigated. All tested compounds significantly increased p-Akt at the onset of 1 h after treatment and restored to the baseline level within 4 h (**Figure 13**). When compared the effect on Akt activation among the tested compounds, **MA** was found to induce p-Akt with the strongest magnitude, while similar magnitude was observed when treatment with others.

4.3 Effects of ERK1/2 and Akt inhibitors on neurite outgrowth induced by MS and AS

To further confirm that the activation of ERK1/2 and Akt was associated with morphological change, Neuro-2a cells were pretreated with either PD098059 or LY294002 followed by each tested compound. Western blotting was performed to prove the inhibitory effect, and then immunofluorescent staining was performed to monitor neurite outgrowth. Pretreatment with PD098059 or LY294002 for 30 min prior to incubated with **MS** and **AS** successfully inhibited the formation of p-ERK1/2 and p-Akt accordingly (**Figure 14A, 14B**). Moreover, inhibition on p-ERK1/2 strongly suppressed the **MS**- and **AS**-induced increment of both %NBC and average neurite length when compared to non-inhibited cells (**Figure 15**). In contrast, inhibition of p-Akt affected only the neurite length but not %NBC induced by **MS** and **AS** (**Figure 16**). Therefore, these results indicated that **MS** and **AS** could induce neurite-bearing cells and neurite length through ERK activation, while effect on neurite elongation was also involved with Akt activation.
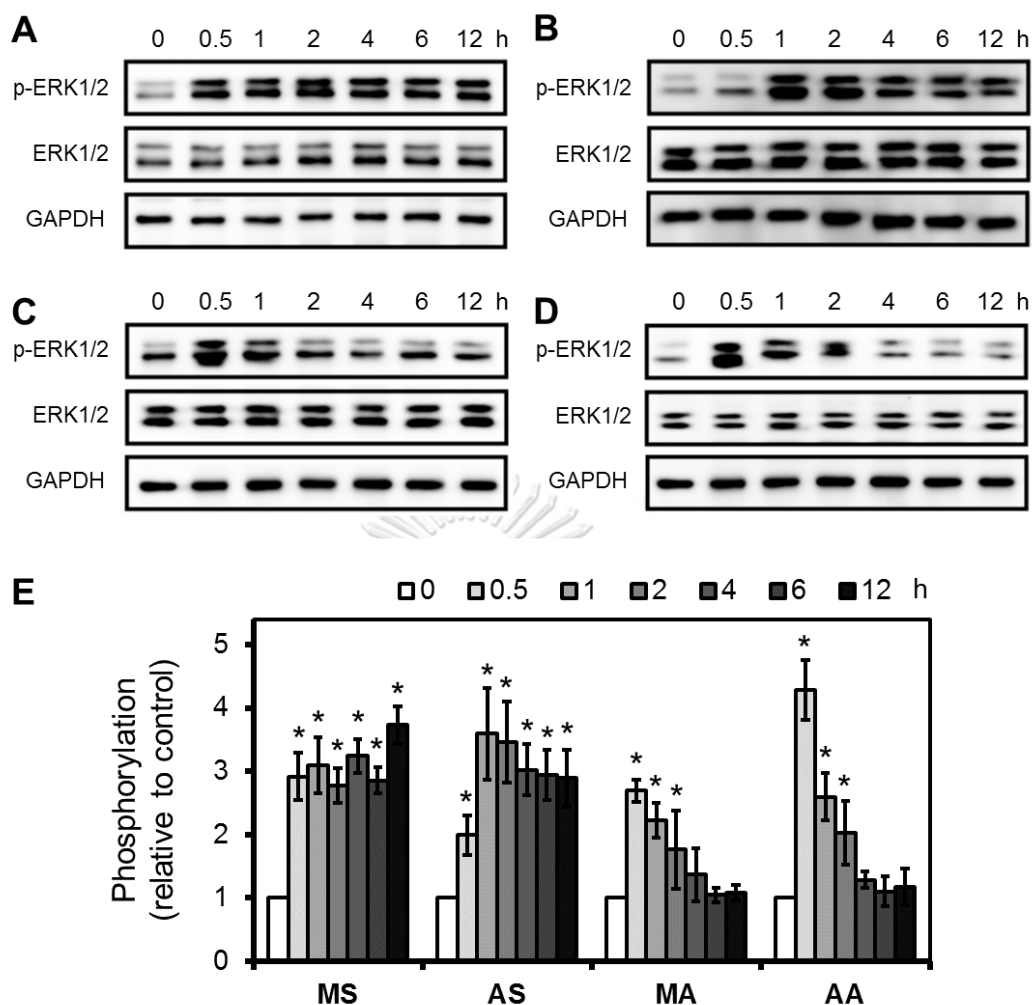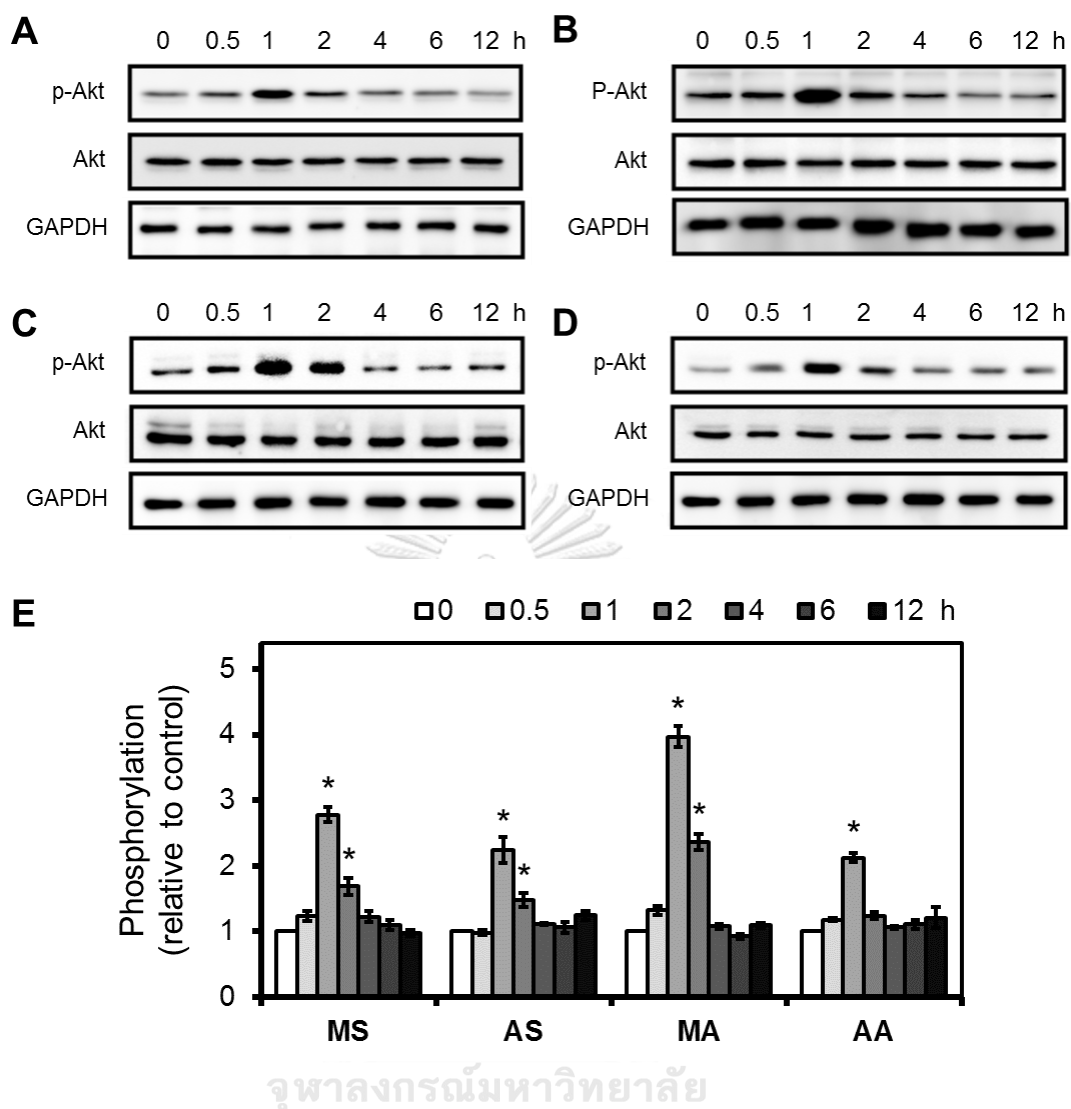
Figure 13 Time profiles of Akt phosphorylation in Neuro-2a cells.

Representative immunoblots of cells treated with 10 µM of (**A**) **MS** (**B**) **AS** (**C**) **MA** and (**D**) **AA** at 0.5 - 12 h. The intensity of GAPDH was used for normalization as a loading control. (**E**) Histogram shows densitometric analysis of Akt phosphorylation induced by each compound at indicated time points. Data are presented as mean ± SD (n=3). * significant difference ($p < 0.05$) vs. control (DMSO).

Figure 14 Effects of specific inhibitors on glycoside-induced ERK1/2 and Akt phosphorylation.

(**A**) Effects of PD098059, a MAPK inhibitor, on inhibition of p-ERK1/2 induced by **MS** and **AS**. (**B**) Effects of LY294002, a PI3K inhibitor, on inhibition of p-Akt induced by **MS** and **AS**. Data are presented as mean ± SD (n=3). * significant difference ($p < 0.05$) vs. control (DMSO). Similar letters indicate significant difference between groups with the same letters.

Figure 15 Effects of ERK1/2 inhibition on **MS**- and **AS**-induced neurite outgrowth.
(**A**) Representative immunofluorescent images (green: βIII-tubulin, blue: nuclei) and (**B**) %NBC and neurite length of Neuro-2a cells treated with **MS** or **AS** in the presence and absence of PD098059. Data are presented as mean ± SD (n=3). * significant difference ($p < 0.05$) vs. control (DMSO). # significant difference between compared groups.

Figure 16 Effects of Akt inhibition on **MS**- and **AS**-induced neurite outgrowth.
(**A**) Representative immunofluorescent images (green: βIII-tubulin, blue: nuclei) and (**B**) %NBC and neurite length of Neuro-2a cells treated with **MS** or **AS** in the presence and absence of LY294002. Data are presented as mean ± SD (n=3). * significant difference ($p < 0.05$) vs. control (DMSO). # significant difference between compared groups.

4.4 Effects of ERK1/2 and Akt inhibitors on neurite outgrowth induced by MA and AA

In Neuro-2a cells pretreated with PD098059 or LY294002 for 30 min prior to incubated with **MA** and **AA**, the successful inhibition of p-ERK1/2 or p-Akt was also observed (**Figure 17**). However, in contrast to glycosides, inhibition of ERK1/2 phosphorylation did not suppress the increment of both %NBC and average neurite length induced by **MA** and **AA** (**Figure 18**). Interestingly, although the inhibition of p-Akt could not suppress neurite-bearing cells, but the suppression of neurite length by Akt inhibition was found (**Figure 19**). Therefore, these results might rule out the involvement of ERK1/2 activation on induction of neurite-bearing cells induced by **MA** and **AA**, while Akt activation was found to involve with only neurite elongation.

5. Investigation on downstream intracellular signaling pathways involving with neurite outgrowth

5.1 Time-course activation of CREB by MS, AS, MA and AA

Activation of CREB phosphorylation at Ser133 was reported to be one of signaling responsible for neurite outgrowth and could be modulated by several signaling pathways including ERK1/2 and Akt. Investigation on time-course activation of CREB by **MS, AS, MA** and **AA** were performed. The results showed that all tested compounds significantly induced CREB phosphorylation (p-CREB) at the onset of 30-60 min of incubation, which peaked at around 1-2 h and subsided to the baseline level by 4 h (**Figure 20**). **MS** and **AS** were found to show higher magnitudes of p-CREB induction than **MA** and **AA**. However, induction of p-CREB by **MS** and **AS** showed the peak activation at 2-h incubation, while the peak activation by **MA** and **AA** was found at 1 h (**Figure 20E**).
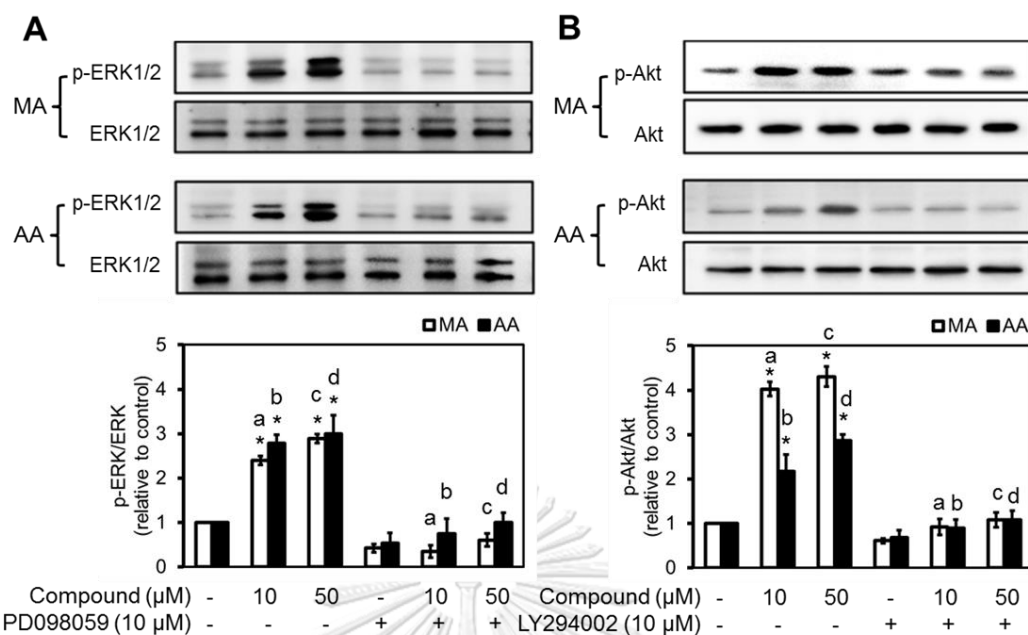
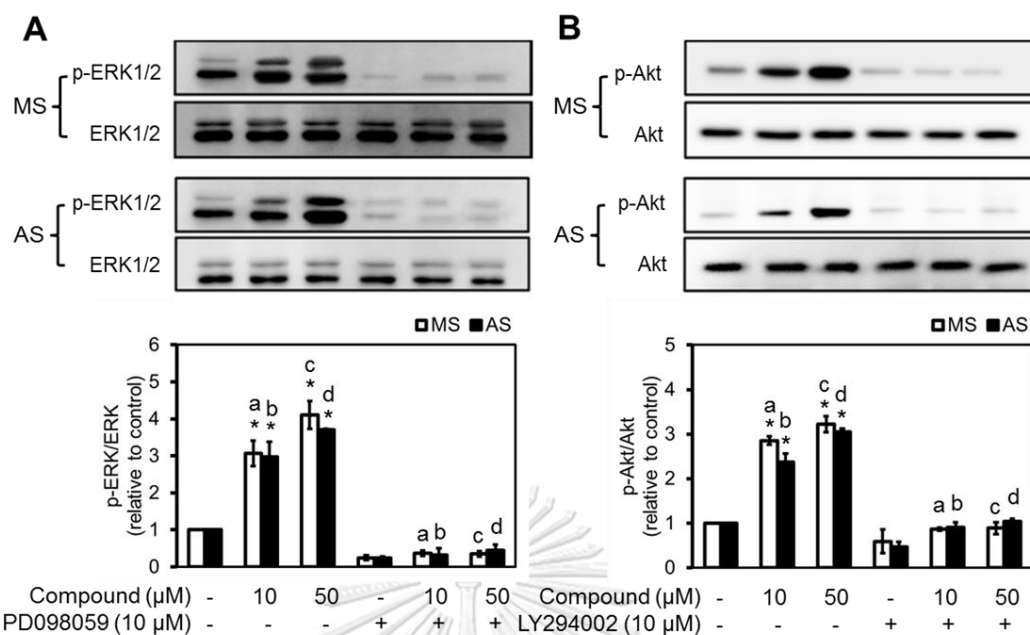**Figure 17** Effects of specific inhibitors on aglycone-induced ERK1/2 and Akt phosphorylation.

(**A**) Effects of PD098059 on inhibition of p-ERK1/2 induced by **MA** and **AA**. (**B**) Effects of LY294002 on inhibition of p-Akt induced by **MA** and **AA**. Data are presented as mean ± SD (n=3). * significant difference (*p < 0.05*) vs. control (DMSO). Similar letters indicate significant difference between groups with the same letters.
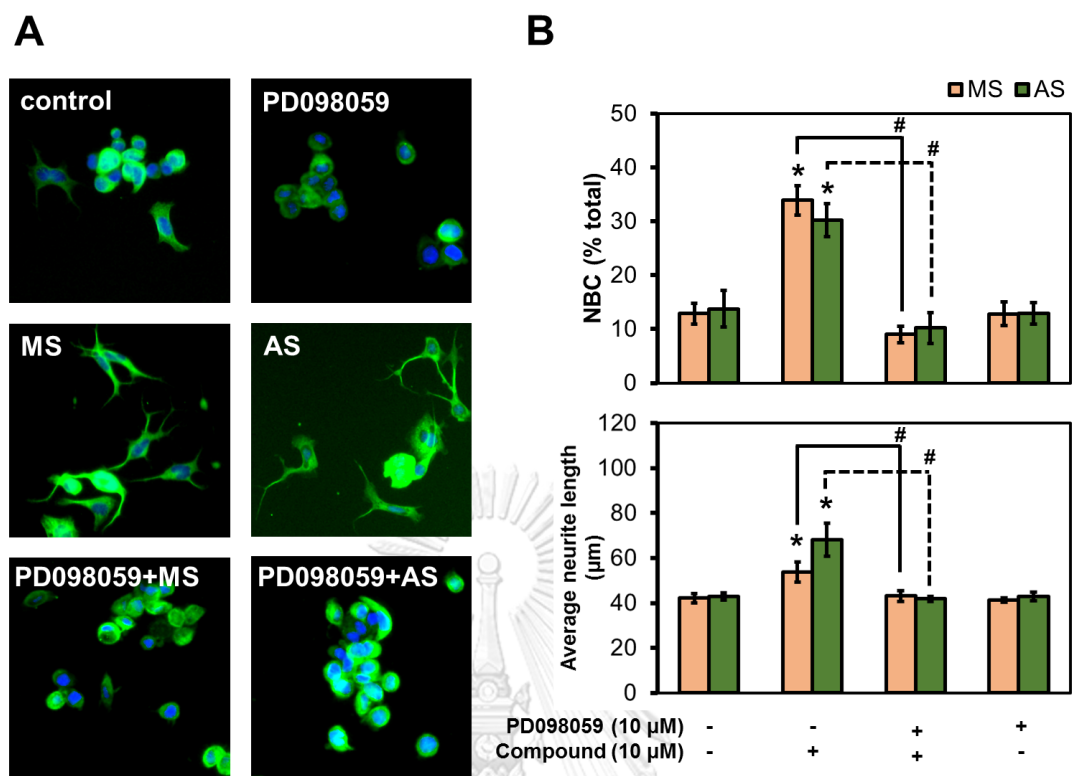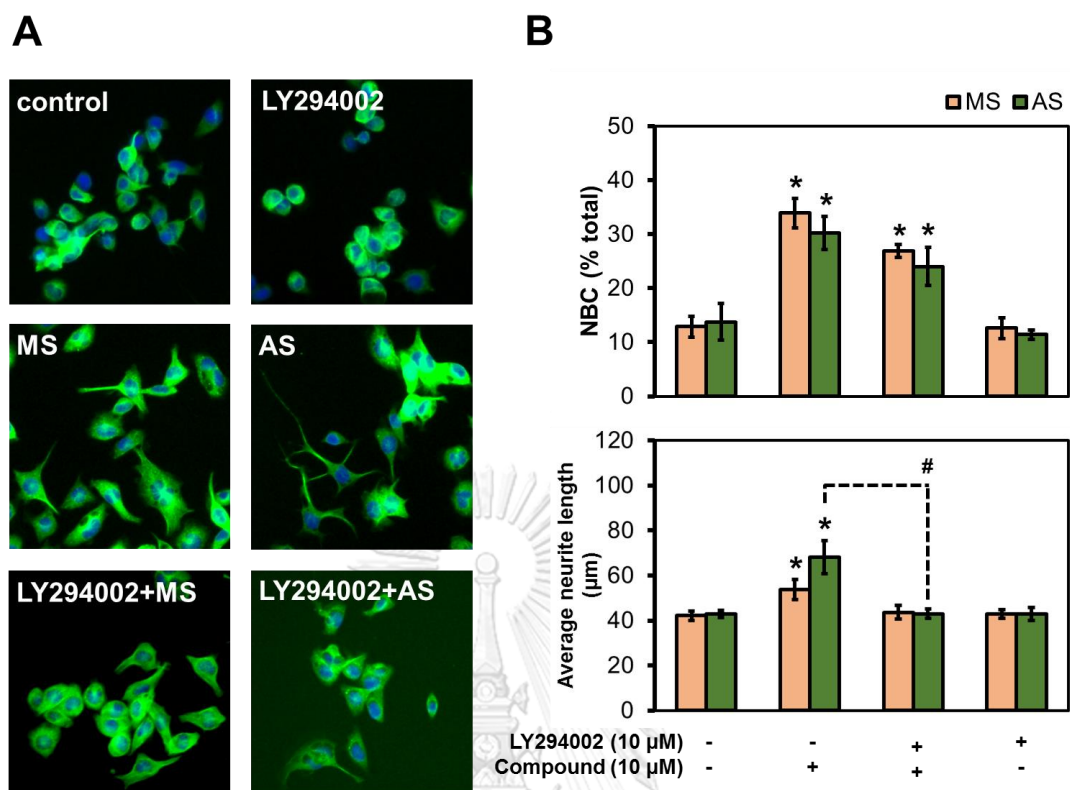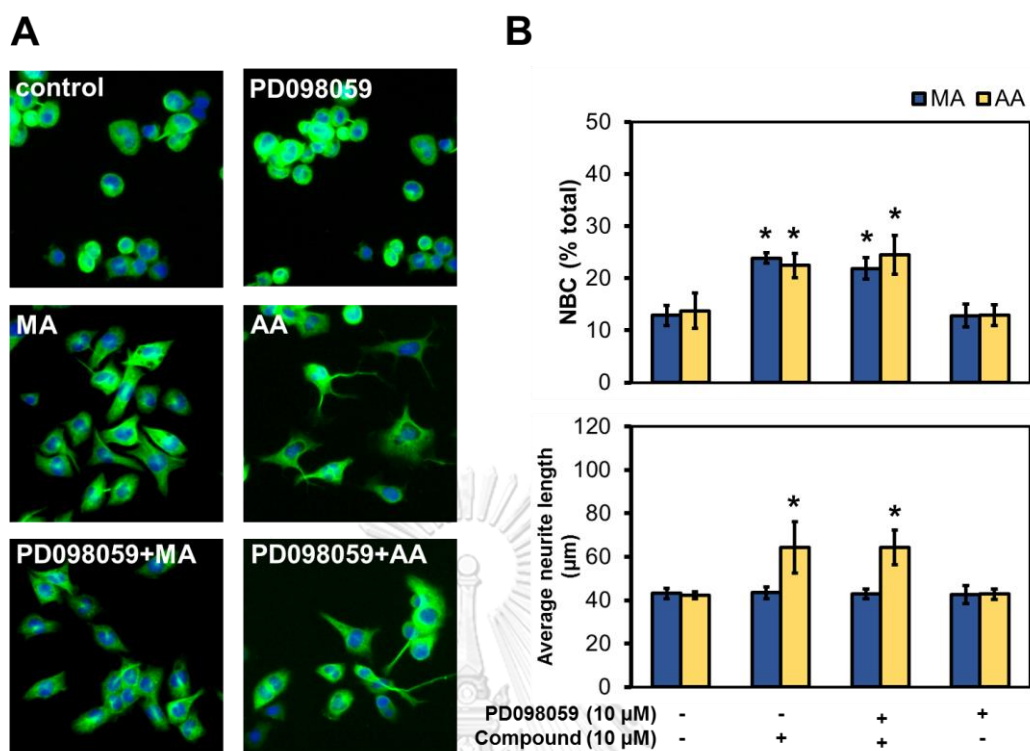
Figure 18 Effects of ERK1/2 inhibition on **MA**- and **AA**-induced neurite outgrowth.
(**A**) Representative immunofluorescent images (green: βIII-tubulin, blue: nuclei) and (**B**)
%NBC and neurite length of Neuro-2a cells treated with **MA** or **AA** in the presence and
absence of PD098059. Data are presented as mean ± SD (n=3). * significant difference
($p < 0.05$) vs. control (DMSO).
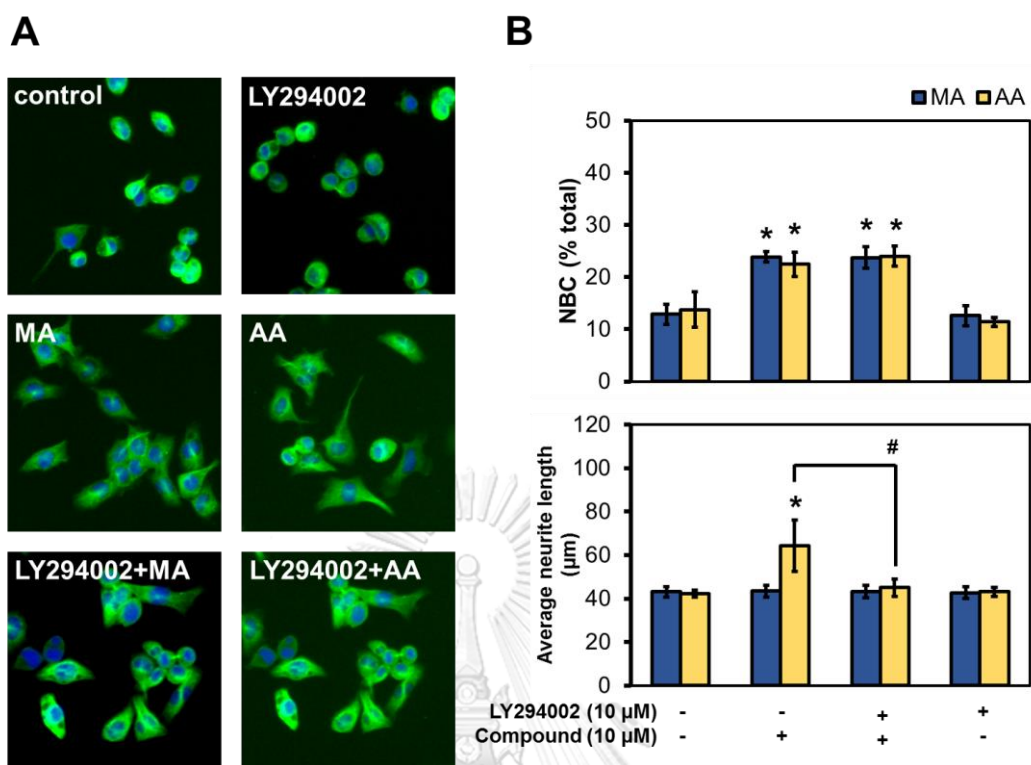
Figure 19 Effects of Akt inhibition on **MA**- and **AA**-induced neurite outgrowth.
(**A**) Representative immunofluorescent images (green: βIII-tubulin, blue: nuclei) and (**B**)
%NBC and neurite length of Neuro-2a cells treated with **MA** or **AA** in the presence and
absence of LY294002. Data are presented as mean ± SD (n=3). * significant difference
($p < 0.05$) vs. control (DMSO). # significant difference between compared groups.
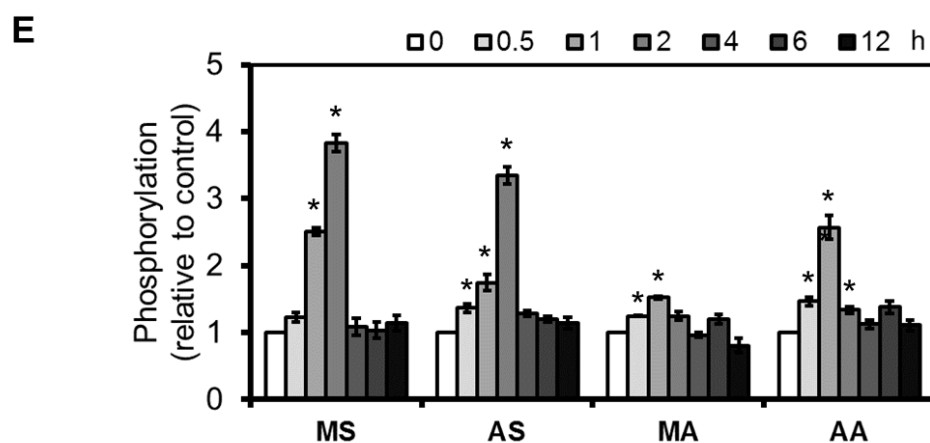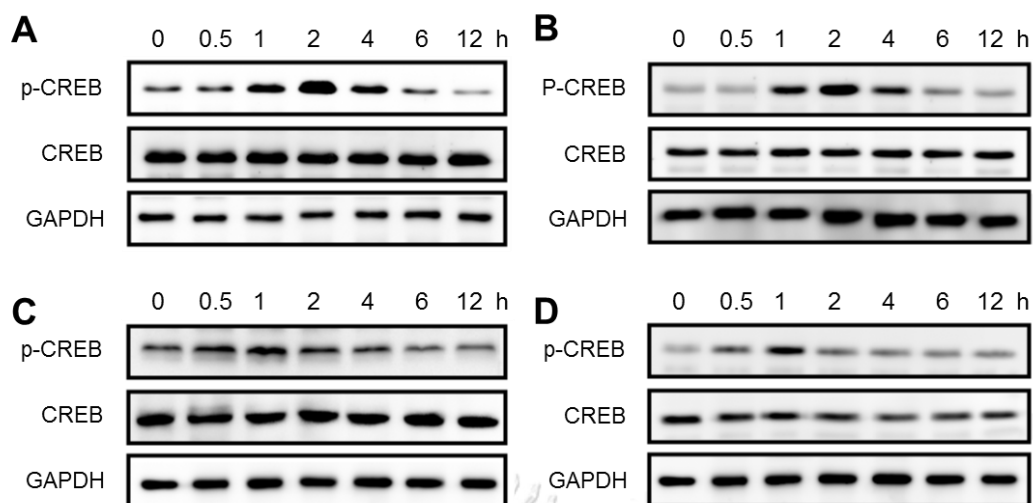
Figure 20 Time profiles of CREB phosphorylation in Neuro-2a cells.
Representative immunoblots of cells treated with 10 µM of (**A**) **MS** (**B**) **AS** (**C**) **MA** and
(**D**) **AA** at 0.5 - 12 h. The intensity of GAPDH was used for normalization as a loading
control. (**E**) Histogram shows densitometric analysis of CREB phosphorylation induced
by each compound at indicated time points. Data are presented as mean ± SD (n=3).
* significant difference ($p < 0.05$) vs. control (DMSO).

5.1.1 Involvement of ERK1/2 or Akt on CREB phosphorylation

To confirm that the activation of p-CREB was regulated by ERK1/2 or Akt, Neuro-2a cells were pretreated with either PD098059 or LY294002 followed by each tested compound. Inhibition of ERK1/2 signaling by PD098059 abolished p-CREB in **MS**- and **AS**-treated cells (**Figure 21A**), while there was no significant change of p-CREB in **MA**- and **AA**-treated cells (**Figure 21B**). For inhibition of Akt, pretreatment with LY294002 did not suppress p-CREB induced by all tested compounds, suggesting that Akt phosphorylation induced by tested compounds might not involve in the activation of CREB (**Figure 21A, 21B**).

5.1.2 Involvement of CREB activation on neurite outgrowth

To confirm the important of p-CREB induction in neurite outgrowth activity, naphthol AS-E phosphate, an inhibitor on CREB activity, was used. Naphthol AS-E phosphate (**Naph**) would suppress CREB activity by interfering in the binding between the KID domain of activated CREB and KIX domain of CREB-binding protein, resulting in blocking CREB-dependent target gene transcription (Li *et al.*, 2012). Treatment of 8-cpt-cAMP successfully induced p-CREB and βIII-tubulin expression which in accordance with promoting of neurite outgrowth activity (**Figure 48 Appendix B**). However, when the cells were pre-treated with **Naph,** although 8-cpt-cAMP-induced p-CREB was still observed (**Figure 28A**), but the βIII-tubulin expression was decreased (**Figure 48B Appendix B)** and neurite outgrowth activity was totally inhibited (**Figure 48C, 28D, 28E Appendix B**). These results indicated the important role of CREB activation in regulation of neurite outgrowth activity.

From neurite outgrowth assay, pretreatment of **Naph** prior exposure to **MS, AS, MA** and **AA** at the effective concentration (10 μM) could totally suppressed the neurite outgrowth activities in both %NBC and neurite length parameters (**Figure 22**). Moreover, we also used the determination of βIII-tubulin expression as an indicator for neurite outgrowth. Treatment of **MS, AS, MA** or **AA** significantly increased βIII-tubulin expression when compared to control. But when CREB activity was suppressed
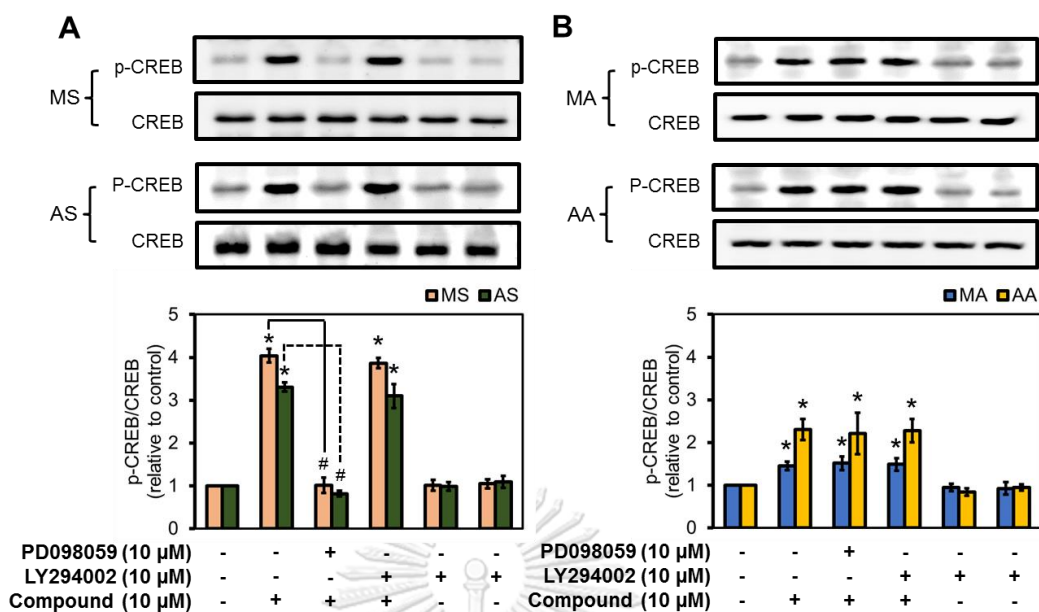
Figure 21 Effects of ERK1/2 and Akt inhibition on CREB phosphorylation induced by (**A**) **MS** and **AS** (**B**) **MA** and **AA**.

Neuro-2a cells were pre-treated with each specific inhibitor for 30 min, followed by treatment. CREB phosphorylation was detected after 2 h of incubation. Data are presented as mean ± SD (n=3). * significant difference ($p < 0.05$) vs. control (DMSO). # significant difference between compared groups.
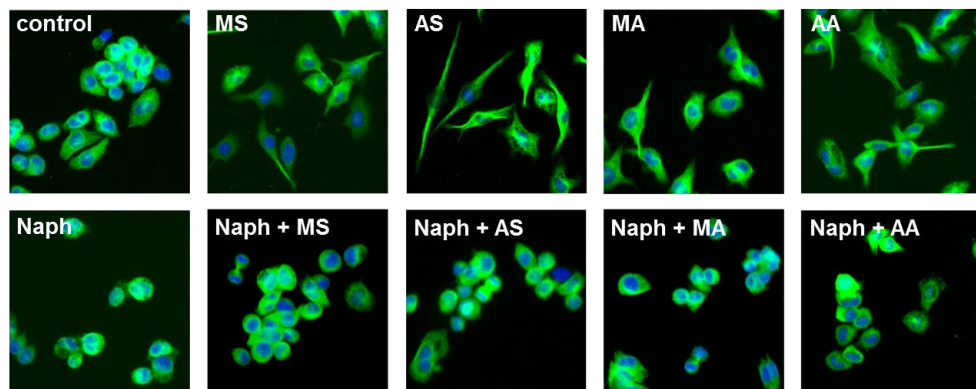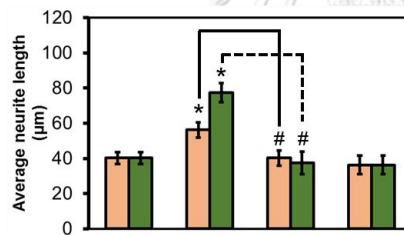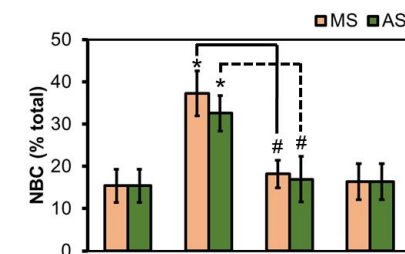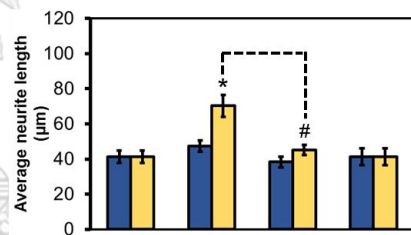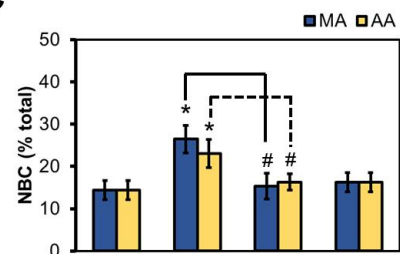
Figure 22 Effects of CREB activity inhibitor on neurite outgrowth.
(**A**) Representative images of βIII-tubulin-stained cells. Cells were treated with 10 µM of **MS, AS, MA** or **AA** for 6 h with or without 30-min pre-treatment of 20 µM Naph. Histograms showed neurite outgrowth parameters on %NBC and neurite length of (**B**) **MS** and **AS** and (**C**) **MA** and **AA** in the presence and absence of **Naph**. Data are presented as mean ± SD (n=3). * significant difference ($p < 0.05$) vs. control (DMSO). # significant difference between compared groups.

by pretreatment of **Naph**, the increasing in βIII-tubulin expression was abolished in all groups (**Figure 23**). These results suggested that the neurite outgrowth activity of all **MS, AS, MA** and **AA** might come from activation of CREB activity by induction of CREB phosphorylation.

5.2 Time-course phosphorylation of GSK3β at Ser9 by MS, AS, MA and AA

GSK3β is a serine/threonine protein kinase that negatively regulated neurite formation. Inhibition of GSK3β activity by phosphorylation at Ser9 on GSK3β resulted in promoting of neurite outgrowth (Seira *et al.*, 2014). Therefore, the inhibitory effect of each compound was investigated by determining the induction of GSK3β phosphorylation. In our study, **MS, AS, MA** and **AA** significantly induced GSK3β phosphorylation with the different degree (**Figure 24**). For glycosides, **MS** and **AS** triggered p-GSK3β after incubation for 1 h and lasting for 12 h. When compared the magnitude of phosphorylation, **AS** was found to possess the higher potency than **MS** (**Figure 24E**). While aglycones, **MA** and **AA**, showed less potency in triggering p-GSK3β than glycosides. Similar to glycoside derivatives, **AA** also exhibited higher potency than **MA**.

5.2.1 Involvement of ERK1/2 or Akt on GSK3β phosphorylation

To confirm that the phosphorylation of GSK3β was regulated by either ERK1/2 or Akt, Neuro-2a cells were pretreated with either PD098059 or LY294002 followed by each tested compound. In glycoside-treated groups, our results showed that inhibition on ERK signaling did not significantly affect p-GSK3β induced by **MS** and **AS** (**Figure 25A, 25B**), while the neurite outgrowth activity was suppressed (**Figure 15**). When using inhibitor on Akt signaling, **MS**- and **AS**-induced p-GSK3β was found to be totally abolished (**Figure 25C, 25D**), which might relate to suppression on neurite elongation (**Figure 16B**). In aglycone-treated groups, there was also no effect on **MA**- and **AA**-induced p-GSK3β when ERK signaling was inhibited by pre-treatment of PD098059 (**Figure 26A, 26B**). However, **MA**- and **AA**-induced p-GSK3β was also significantly suppressed by inhibition on Akt signaling (**Figure 26C, 26D**). These results clearly
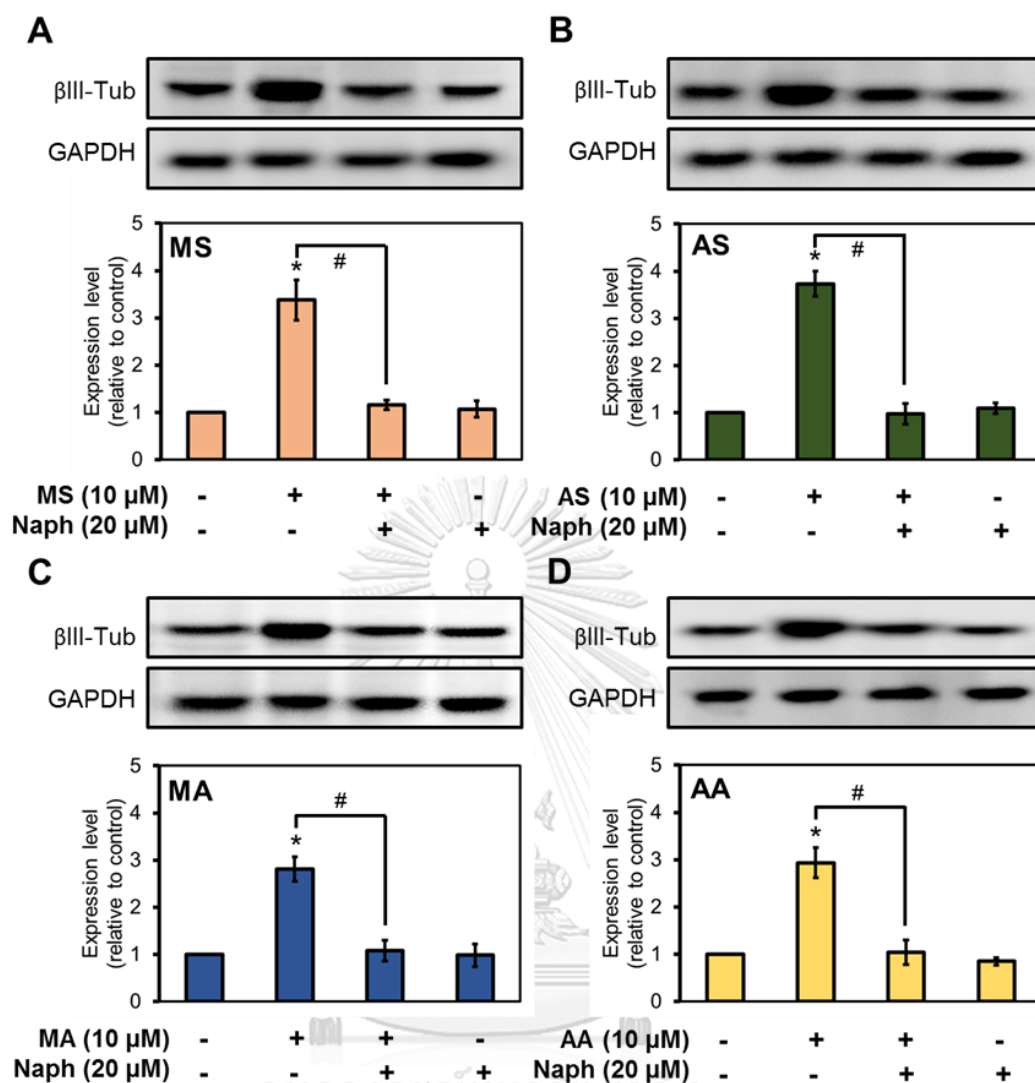
Figure 23 Effects of CREB activity inhibitor on βIII-tubulin expression.

Cells were treated with 10 μM of (**A**) **MS,** (**B**) **AS,** (**C**) **MA** or (**D**) **AA** for 6 h with or without 30-min pre-treatment of 20 μM Naph. Expression of βIII-tubulin was detected by Western blot analysis. Data are presented as mean ± SD (n=3). * significant difference ($p < 0.05$) vs. control (DMSO). # significant difference between compared groups.
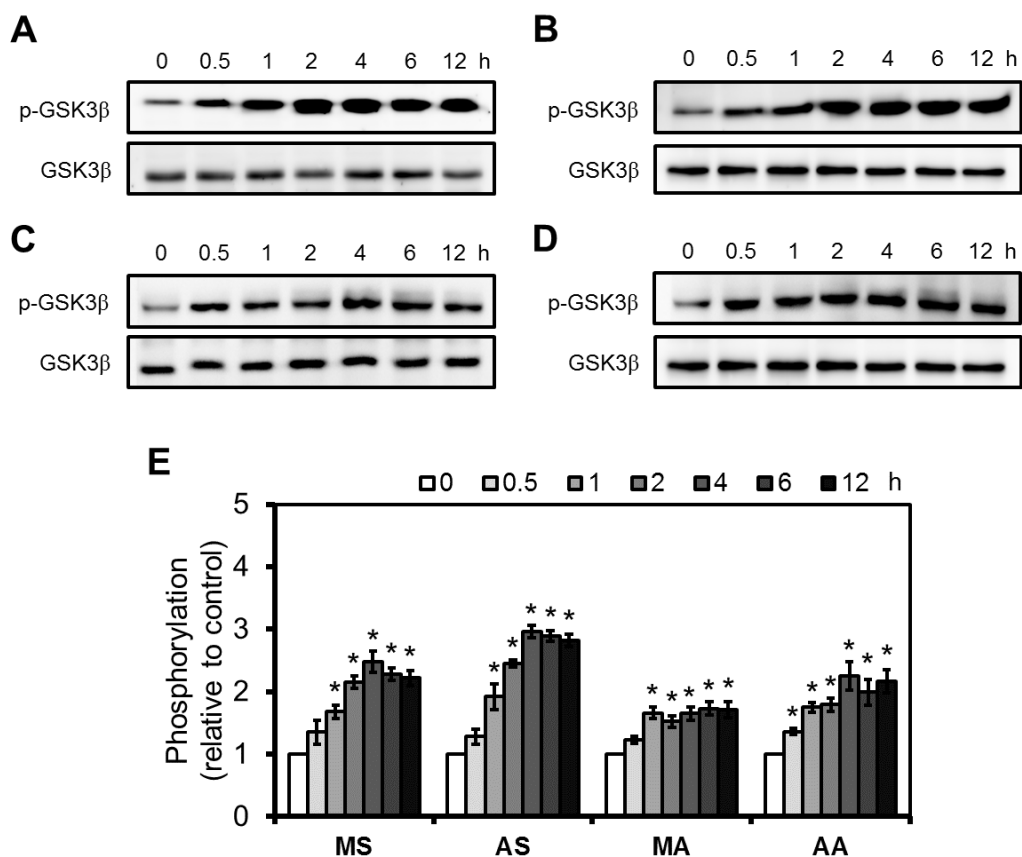
Figure 24 Time profiles of GSK3β phosphorylation in Neuro-2a cells.

Representative immunoblots of cells treated with 10 μM of (**A**) **MS** (**B**) **AS** (**C**) **MA** and (**D**) **AA** at 0.5 - 12 h. The intensity of GAPDH was used for normalization as a loading control. (**E**) Histogram shows densitometric analysis of GSK3β phosphorylation induced by each compound at indicated time points. Data are presented as mean ± SD (n=3). * significant difference ($p < 0.05$) vs. control (DMSO).
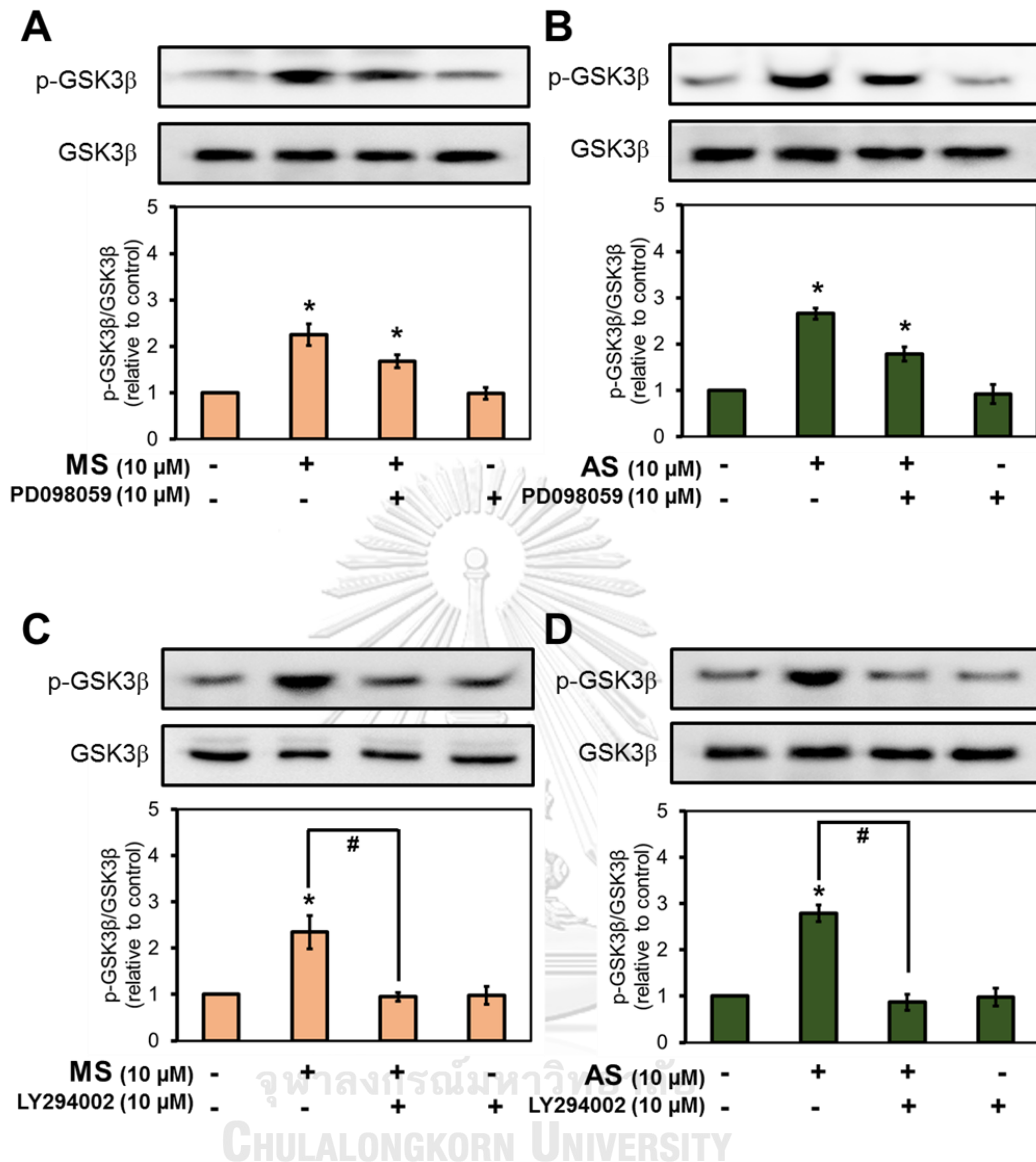
Figure 25 Effects of ERK1/2 and Akt inhibition on GSK3β phosphorylation.

Neuro-2a cells were pre-treated with each specific inhibitor for 30 min, followed by treatment. GSK3β phosphorylation was detected after 4 h of incubation. Effects of ERK1/2 inhibition on (**A**) **MS**- and (**B**) **AS**-treated cells. Effects of Akt inhibition on (**C**) **MS**- and (**D**) **AS**-treated cells. Data are presented as mean ± SD (n=3). * significant difference ($p < 0.05$) vs. control (DMSO). # significant difference between compared groups.
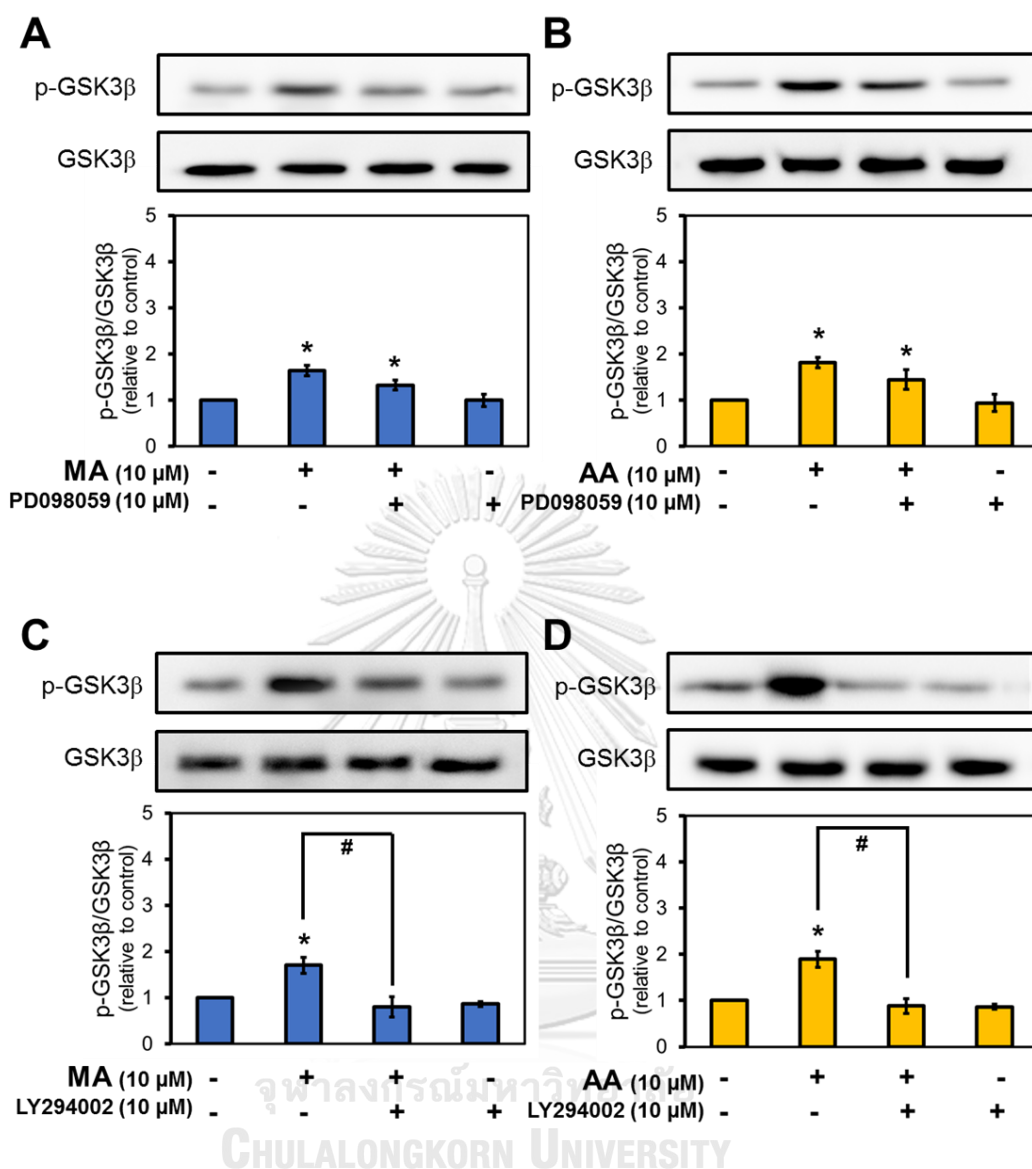
Figure 26 Effects of ERK1/2 and Akt inhibition on GSK3β phosphorylation.

Neuro-2a cells were pre-treated with each specific inhibitor for 30 min, followed by treatment. GSK3β phosphorylation was detected after 4 h of incubation. Effects of ERK1/2 inhibition on (**A**) **MA**- and (**B**) **AA**-treated cells. Effects of Akt inhibition on (**C**) **MA**- and (**D**) **AA**-treated cells. Data are presented as mean ± SD (n=3). * significant difference ($p < 0.05$) vs. control (DMSO). # significant difference between compared groups.

indicated that Akt phosphorylation induced by **MS, AS, MA** or **AA** was essential for GSK3ß phosphorylation at Ser9 to inhibit its activity.

5.3 Inhibitory effects on RhoA/ROCK signaling pathway

Activation of RhoA activity was known to inhibit the neurite formation (Kozma *et al.*, 1997). Inhibition of RhoA activity by several neurite outgrowth inducing agents such as cAMP derivatives or **RA** was found to be one mechanism for neurite outgrowth promoting activity (Puttagunta *et al.*, 2011; Jeon *et al.*, 2012). In our study, we used RhoA activation assay to evaluate the ability of **MS, AS, MA** and **AA** on inhibition of RhoA by measuring the level of GTP-RhoA, an active form of RhoA. In Neuro-2a cells treated by **MS, AS, MA** or **AA** for 2 h, the levels of GTP-RhoA were significantly decreased when compared to control group (**Figure 27**). Calpeptin, a RhoA activator as a positive control, was found to significantly increase GTP-RhoA level. In comparison, MS and AS exhibited the percentage of inhibition about 74.3% and 73.7%, respectively (**Figure 27C**), while lower inhibitory activities were found in MA (35.0%) and AA (36.7%).

5.3.1 Involvement of PI3K on RhoA inactivation induced by MS, AS, MA and AA

Inactivation of RhoA activity has been reported to be regulated by PI3K signaling pathway (Nusser *et al.*, 2002). In this study, we used LY294002, a PI3K inhibitor, to inhibit the regulation of RhoA activity in order to confirm the role of PI3K signaling in inhibitory effect of **MS, AS, MA** and **AA.** Pre-treatment by the inhibitor was found to reverse the inhibitory effect of **MS** and **AS** observed by the significant increasing level of GTP-RhoA (**Figure 28**), while the level of GTP-RhoA in **MA**- and **AA**-treated groups was slightly increased. However, there was no change in GTP-RhoA level of between non-inhibited and inhibited PI3K signaling in calpeptin-treated group (**Figure 28C**), suggesting the promoting activity of calpeptin might not come from PI3K signaling pathway. In summary, we found that **MS,** and **AS** possessed the inhibitory activity on RhoA which might be regulated by PI3K signaling, while **MA** and **AA** also inhibited RhoA activity with the independent of PI3K activity.
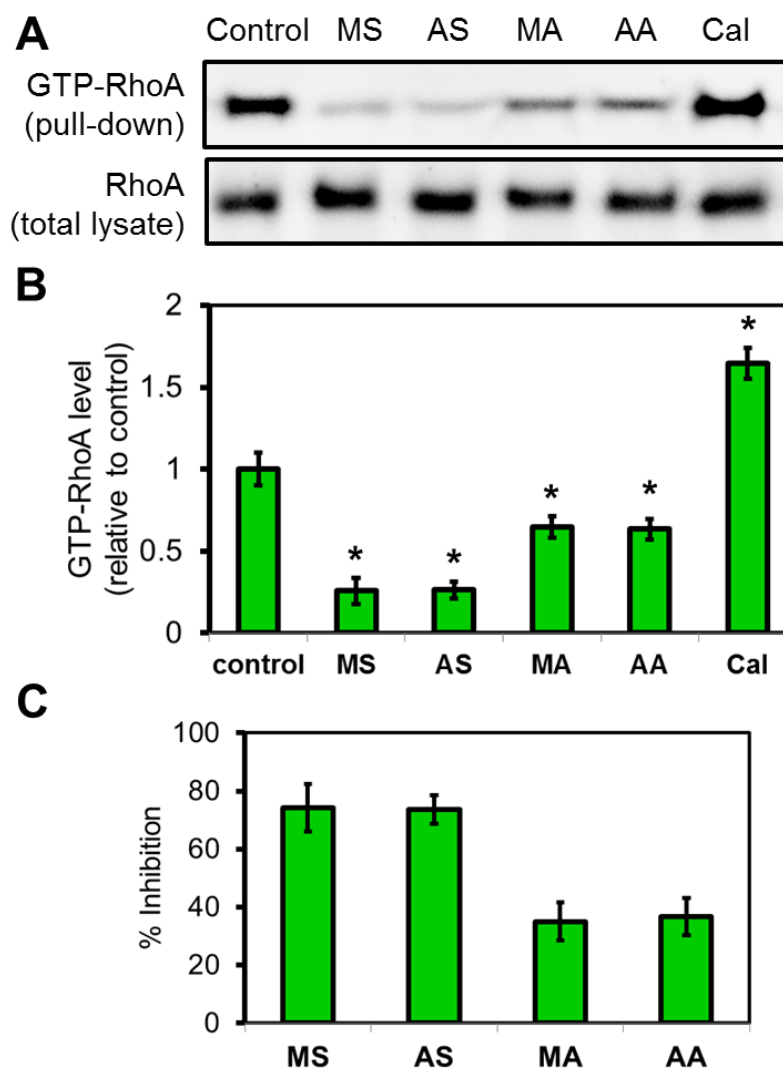
Figure 27 Effects of **MS**, **AS**, **MA** and **AA** on RhoA inhibition.

Neuro-2a cells were treated with each compound for 2 h. (**A**) Representative immunoblot of GTP-RhoA level detected by pull-down assay. (**B**) Histogram showed the decreasing levels of active GTP-RhoA in treatment groups when compared to untreated cells. Calpeptin (**Cal**), a RhoA activator used as a positive control showed the induction activity of active RhoA by increasing on GTP-RhoA level. (**C**) Histogram showed percentage of inhibition of **MS**, **AS**, **MA** and **AA** when normalized with untreated group (0% inhibition). Data are presented as mean ± SD (n=3). * significant difference ($p < 0.05$) vs. control (DMSO).
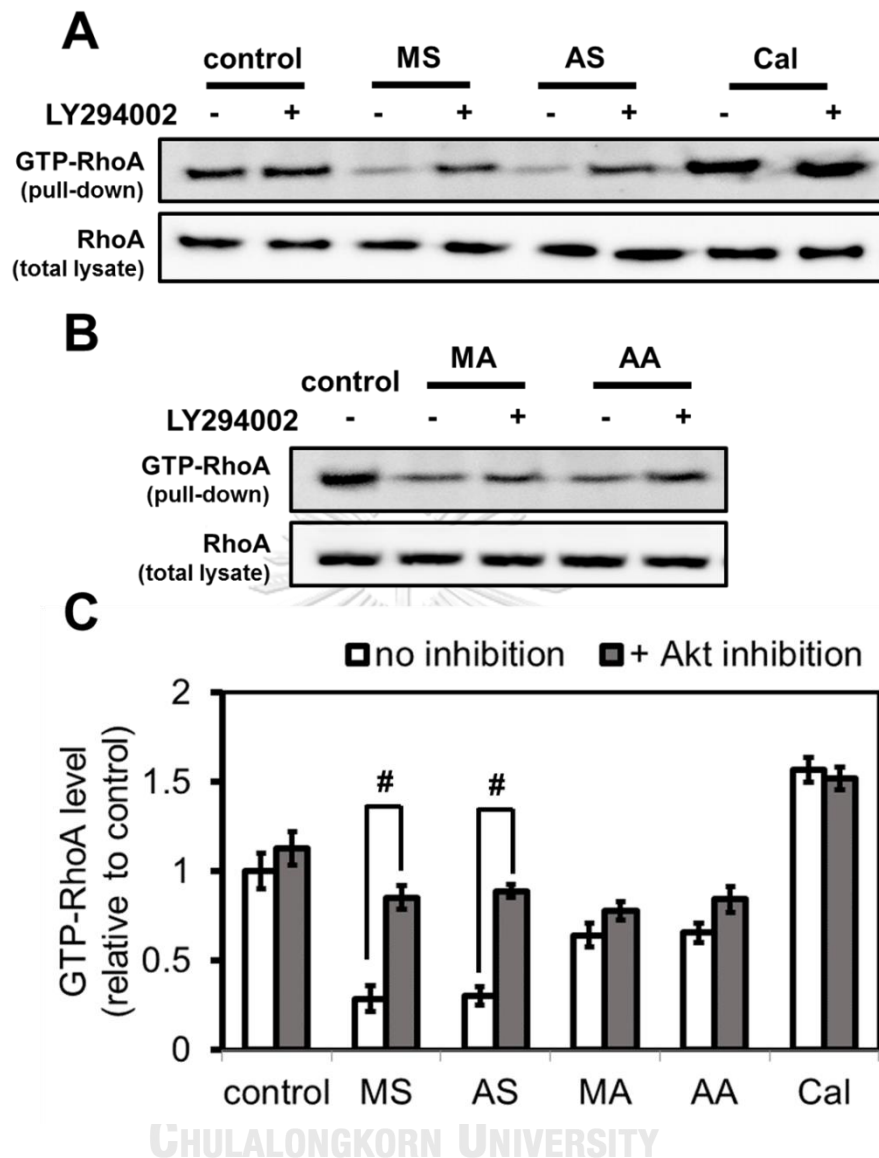
Figure 28 Effect of Akt inhibition on RhoA inhibition.

Neuro-2a cells were pre-treated with 10 µM of LY294002 for 30 min prior to treatment. Level of active GTP-RhoA in each treatment group was determined by pull-down assay. Representative immunoblot of (**A**) **MS**- and **AS**- and (**B**) **MA**- and **AA**-treated cells in the presence or absence of inhibitor. (**C**) Histograms shows the effect on level of active GTP-RhoA which compared between the presence or absence of inhibitor. Data are presented as mean ± SD (n=3). # significant difference between compared groups.

5.4 Effect on Nrf2 translocation

Translocation of Nrf2 from cytosol into nucleus in neuronal cells was also report to be one of the mechanisms related to neuronal cell differentiation and neurite extension process (Zhao *et al.*, 2009). In this study, we used subcellular fractionation technic followed by determination of Nrf2 level in cytosolic and nuclear fraction using Western blotting. The results showed that **MS**, **AS**, **MA** and **AA** could trigger Nrf2 translocation from cytosol into nucleus by increasing in Nrf2 levels in nuclear fraction, while cytosolic Nrf2 level was decreased (**Figure 29, 30**). However, the onset of each compound was found to be different. Glycosides (**MS** and **AS**) significantly increased nuclear Nrf2 level after 2-h of incubation (**Figure 29B, 29D**), while nuclear Nrf2 level was significantly increased after incubation of aglycones (**MA** and **AA**) for 30 min, suggesting the faster onset of aglycones (**Figure 30B, 30D**).

5.4.1 Involvement of ERK1/2 or Akt on Nrf2 translocation

Nrf2 translocation was reported to be regulated by either ERK1/2 and Akt signalings. Therefore, we pre-treated the cells with the inhibitors, PD098059 or LY294002 to inhibit ERK1/2 or Akt signalings, respectively, prior to incubate with tested compounds for 2 h. In **MS**-treated cells, inhibition on Akt but not ERK1/2 signaling resulted in significant decreasing in Nrf2 translocation observed by nuclear Nrf2 level (**Figure 31**). Similar result was found in **AS**-treated cells that only Akt inhibition affected the Nrf2 translocation when compared to non-inhibited cells (**Figure 32**). In aglycone-treated cells (**MA** and **AA**), the similar effects were also found that inhibition on ERK1/2 did not affect Nrf2 translocation. However, inhibition on Akt signaling was found to dramatically decrease level of Nrf2 translocation (**Figure 33, 34**). These results informed that only Akt but not ERK1/2 signaling involved in promoting of Nrf2 translocation activity of our tested compounds. Moreover, Akt signaling might be the main mechanism in **MA**- and **AA**-induced Nrf2 translocation because of degree of Nrf2 translocation was almost totally inhibited when using Akt signaling inhibitor, while inhibition on Akt only decreased the level of Nrf2 translocation in **MS**- and **AS**-treated groups.
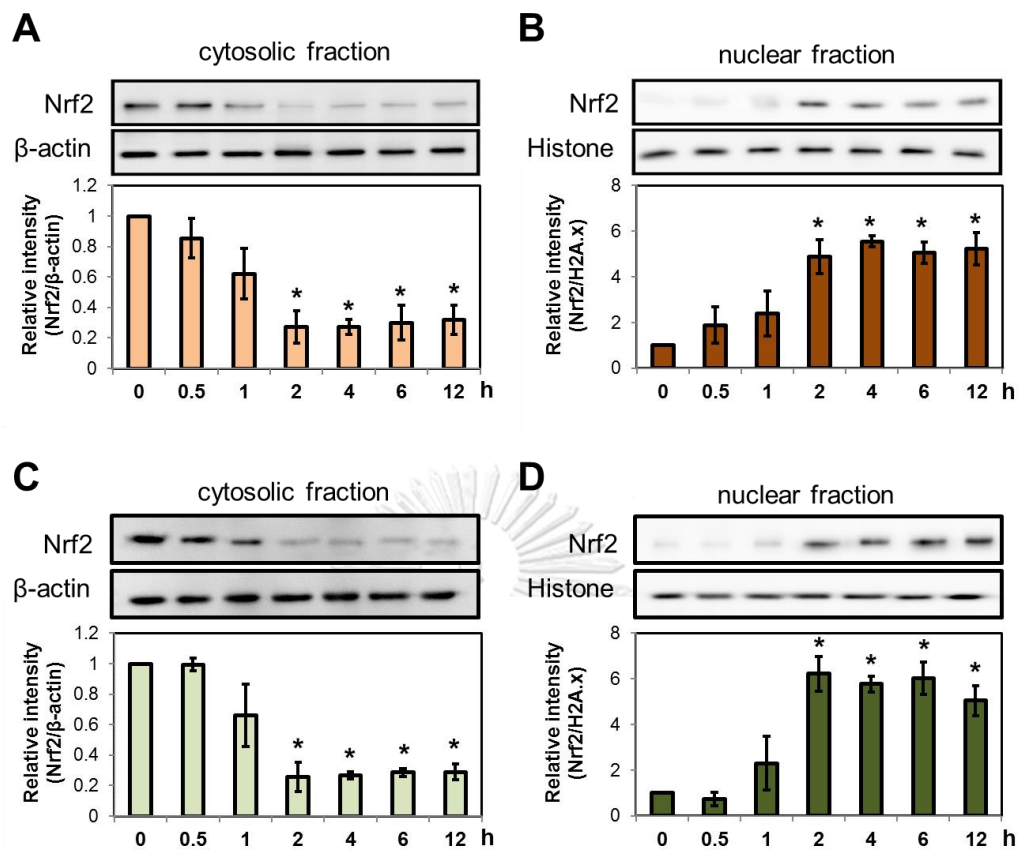
Figure 29 Effects of **MS** and **AS** on Nrf2 translocation.

Neuro-2a cells were treated with **MS** or **AS** (10 µM) for 0.5 - 12 h. Levels of Nrf2 in cytosol and nuclear were determined by using subcellular fractionation and Western blot analysis. Decreasing in cytosolic fraction and increasing in nuclear fraction of Nrf2 level indicates the translocation from cytosol into nucleus. Histograms show Nrf2 level in (**A**) cytosolic and (**B**) nuclear fractions of **MS**-treated cells and (**C**) cytosolic and (**D**) nuclear fractions of **AS**-treated cells. Data are presented as mean ± SD (n=3). * significant difference ($p < 0.05$) vs. control (DMSO).
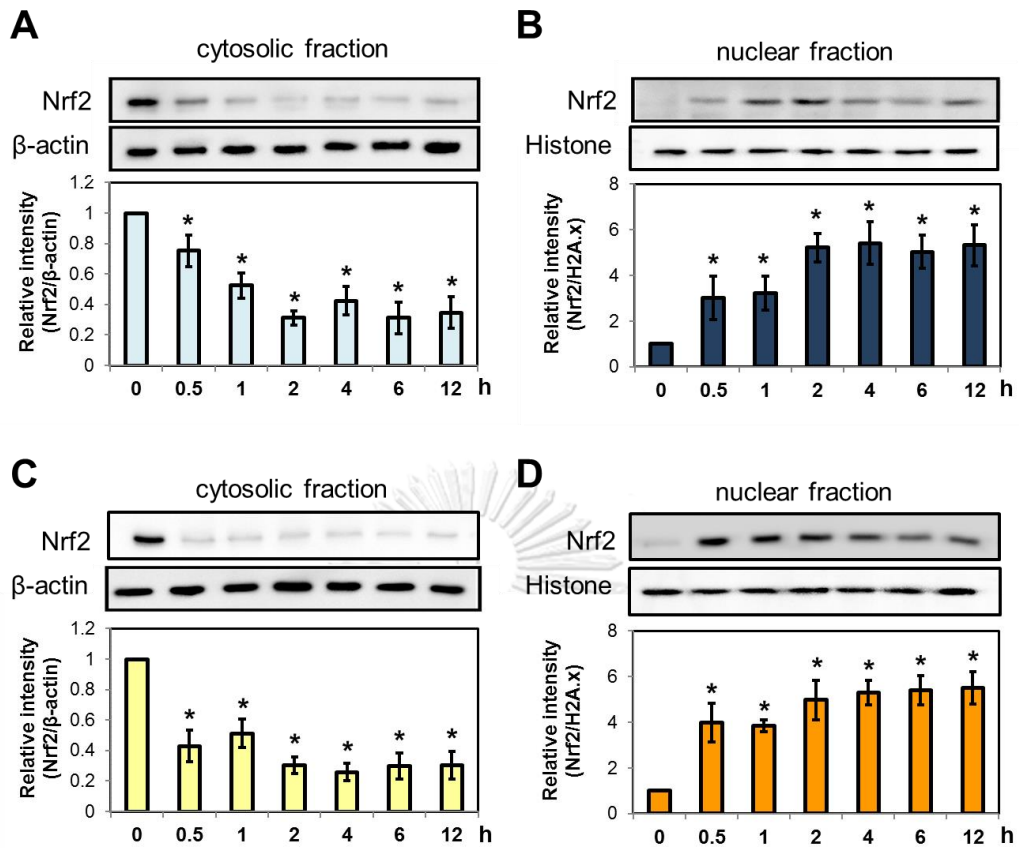
Figure 30 Effects of **MA** and **AA** on Nrf2 translocation.

Neuro-2a cells were treated with **MA** or **AA** (10 μM) for 0.5 - 12 h. Levels of Nrf2 in cytosol and nuclear were determined by using subcellular fractionation and Western blot analysis. Decreasing in cytosolic fraction and increasing in nuclear fraction of Nrf2 level indicates the translocation from cytosol into nucleus. Histograms show Nrf2 level in (**A**) cytosolic and (**B**) nuclear fractions of **MA**-treated cells and (**C**) cytosolic and (**D**) nuclear fractions of **AA**-treated cells. Data are presented as mean ± SD (n=3). * significant difference (*p < 0.05*) vs. control (DMSO).
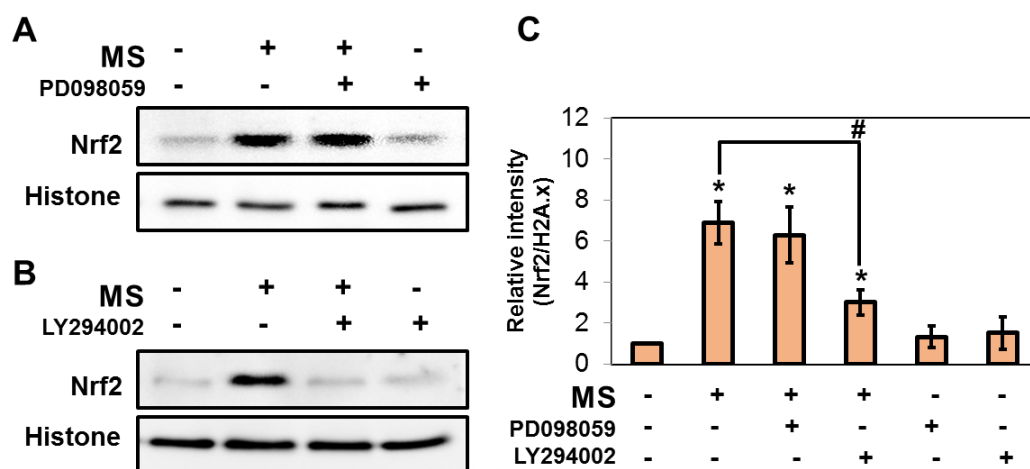
Figure 31 Effects of ERK and Akt inhibition on **MS**-induced Nrf2 translocation. Neuro-2 cells were pre-treated with PD098059 or LY294002 for 30 min prior to **MS** treatment. Representative immunoblots of nuclear Nrf2 levels in cells with (**A**) ERK or (**B**) Akt inhibition. (**C**) Histogram shows the levels of nuclear Nrf2 of **MS**-treated cells in the presence and absence of each inhibitor. Data are presented as mean ± SD (n=3). * significant difference ($p < 0.05$) vs. control (DMSO). # significant difference between compared groups.
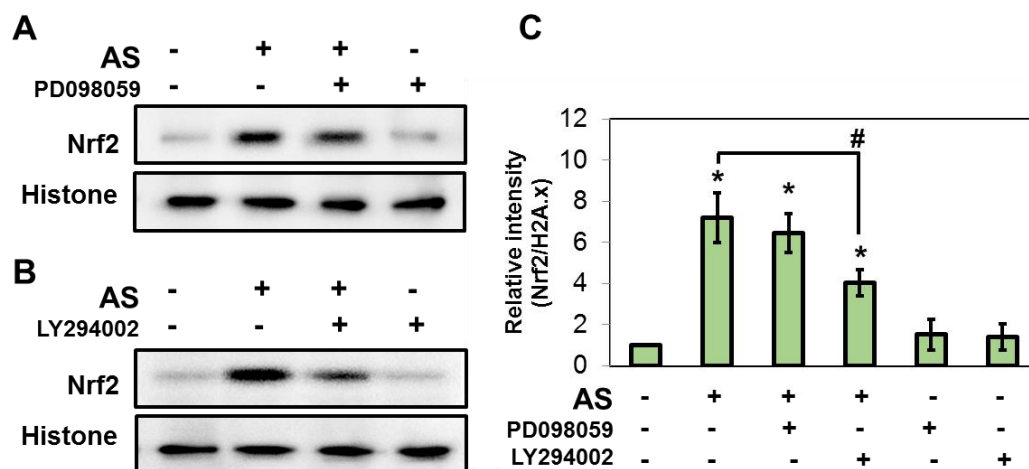
Figure 32 Effects of ERK and Akt inhibition on **AS**-induced Nrf2 translocation.
Neuro-2 cells were pre-treated with PD098059 or LY294002 for 30 min prior to **AS**
treatment. Representative immunoblots of nuclear Nrf2 levels in cells with (**A**) ERK or
(**B**) Akt inhibition. (**C**) Histogram shows the levels of nuclear Nrf2 of **AS**-treated cells in
the presence and absence of each inhibitor. Data are presented as mean ± SD (n=3).
* significant difference (*p < 0.05*) vs. control (DMSO). # significant difference between
compared groups.
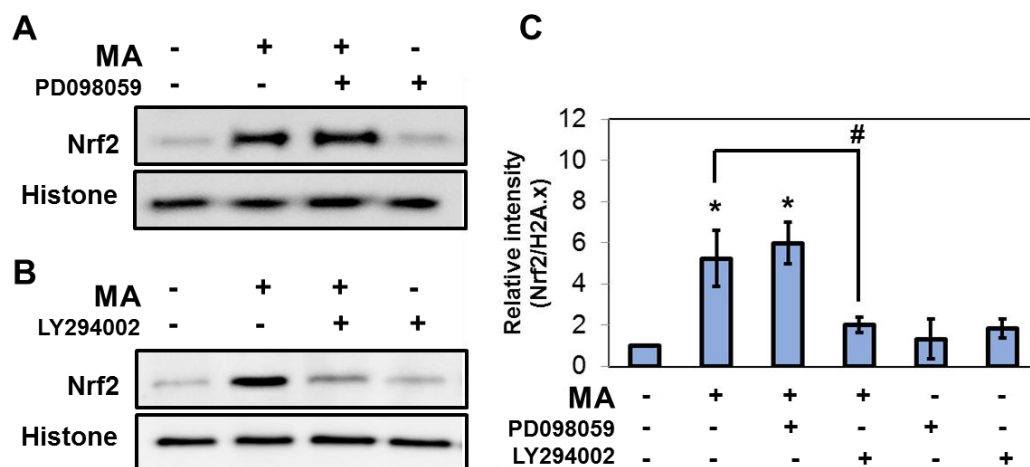
Figure 33 Effects of ERK and Akt inhibition on **MA**-induced Nrf2 translocation. Neuro-2 cells were pre-treated with PD098059 or LY294002 for 30 min prior to **MA** treatment. Representative immunoblots of nuclear Nrf2 levels in cells with (**A**) ERK or (**B**) Akt inhibition. (**C**) Histogram shows the levels of nuclear Nrf2 of **MA**-treated cells in the presence and absence of each inhibitor. Data are presented as mean ± SD (n=3). * significant difference ($p < 0.05$) vs. control (DMSO). # significant difference between compared groups.
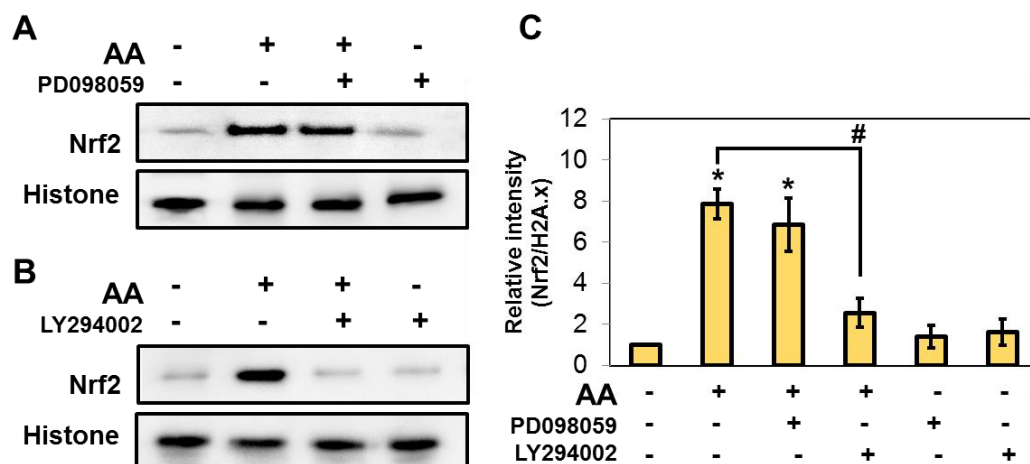
Figure 34 Effects of ERK and Akt inhibition on **AA**-induced Nrf2 translocation. Neuro-2 cells were pre-treated with PD098059 or LY294002 for 30 min prior to **AA** treatment. Representative immunoblots of nuclear Nrf2 levels in cells with (**A**) ERK or (**B**) Akt inhibition. (**C**) Histogram shows the levels of nuclear Nrf2 of **AA**-treated cells in the presence and absence of each inhibitor. Data are presented as mean ± SD (n=3). * significant difference (*p < 0.05*) vs. control (DMSO). # significant difference between compared groups.

However, when Nrf2 translocation was induced by using a Nrf2 activator, tBHQ, which directly bound and modified the stability of Nrf2-KEAP1 complex to promote translocation into nucleus (Abiko *et al.,* 2011) (**Figure 49A Appendix B**), the ERK1/2- or Akt-independent regulation of Nrf2 translocation were found. When using ERK1/2 and Akt inhibitors, there was no significant effect on tBHQ-induced Nrf2 translocation when detected at 2 h (**Figure 49B Appendix B**). This result indicated that Nrf2 activating activity of tBHQ was ERK1/2 and Akt independent. We also confirmed the ability of neurite outgrowth induction of tBHQ and the result showed that although tBHQ strongly promoted Nrf2 translocation but it could not induce neurite outgrowth when compared to positive groups which were **MS**- and **RA**-treated cells (**Figure 50 Appendix B**). These suggested that only Nrf2 activation might be not the main mechanism for neurite outgrowth promoting activity.

6. Effect on Trk signaling pathway and regulation of downstream signaling proteins

Activation of Trk receptor, leading to regulate several downstream signaling is a main mechanism in neurite outgrowth induction. In this study, we used a specific TrkA signaling inhibitor, GW441756, to inhibit signal transduction mediated by TrkA receptor. Neuro-2a cells were pre-treated with 20 µM GW441756 for 30 min prior treatment with **MS, AS, MA** or **AA**. After that effects on phosphorylation of ERK1/2, Akt, CREB and GS3β as well as Nrf2 translocation and inhibition of RhoA activity were determined at their specific time points (**Figure 35**). For ERK1/2 signaling, inhibition on TrkA signaling resulted in suppression on p-ERK1/2 in both glycosides and aglycones (**Figure 36A**), suggesting that regulation of p-ERK1/2 by tested compounds might come from TrkA receptor signaling.

For the effects on p-Akt, inhibition on TrkA receptor was found to decrease p-Akt induced by only **MS** and **AS**, but there was no effect on **MA**- and **AA**-induced p-Akt (**Figure 36B**). These results indicated that activation of Akt by aglycones might
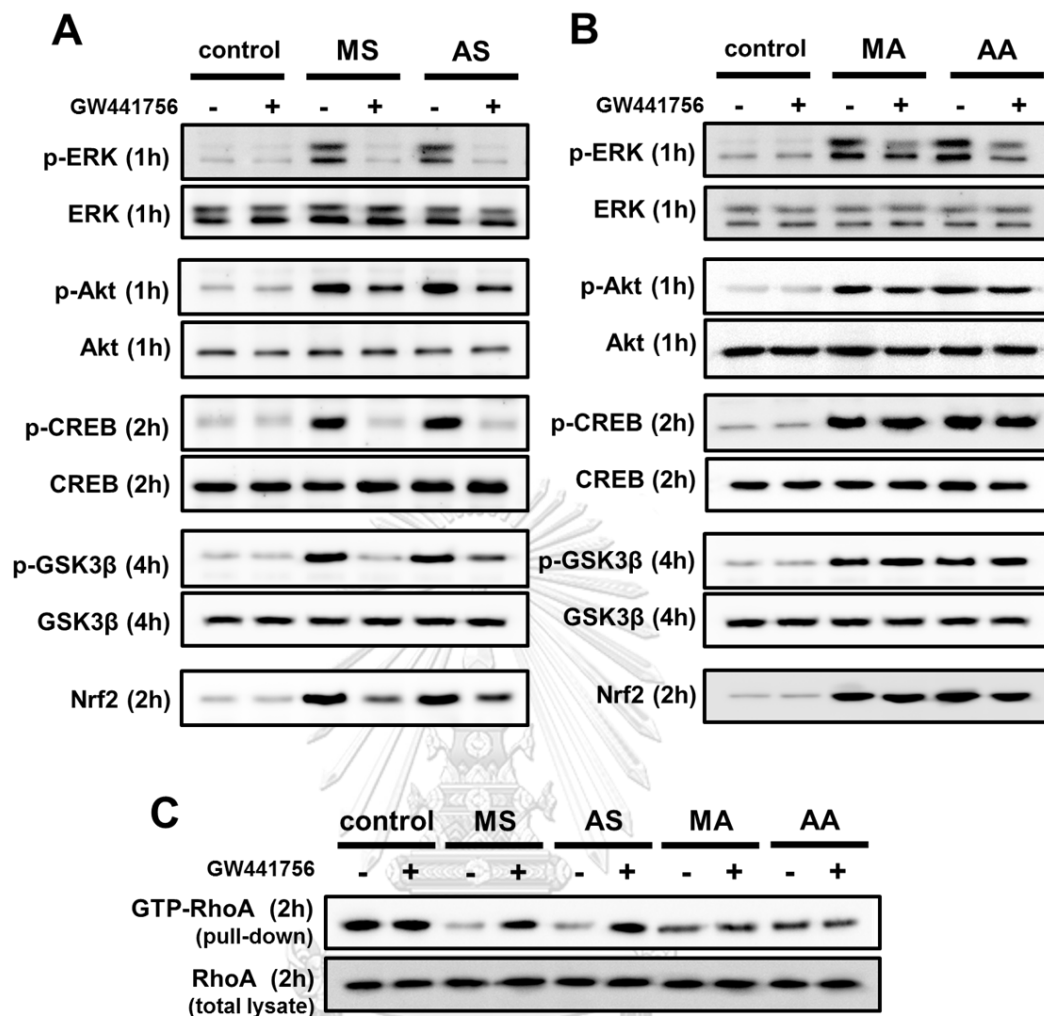
Figure 35 Effects of TrkA inhibitor on activation of neurite outgrowth-involving signaling molecules.

Neuro-2a cells were pre-treated with GW 441756, a TrkA signaling inhibitor, and the effects on downstream signalings were investigated at their specific time points: p-ERK (1 h), p-Akt (1 h), p-CREB (2 h), p-GSK3β (4 h) and Nrf2 translocation (2 h). Representative immunoblots of (**A**) **MS**- and **AS**-treated cells, (**B**) **MA**- and **AA**-treated cells. (**C**) Representative immunoblot of GTP-RhoA by pull-down assay detected at 2 h of treatment. Each immunoblot represents the results which come from three-independent experiments.
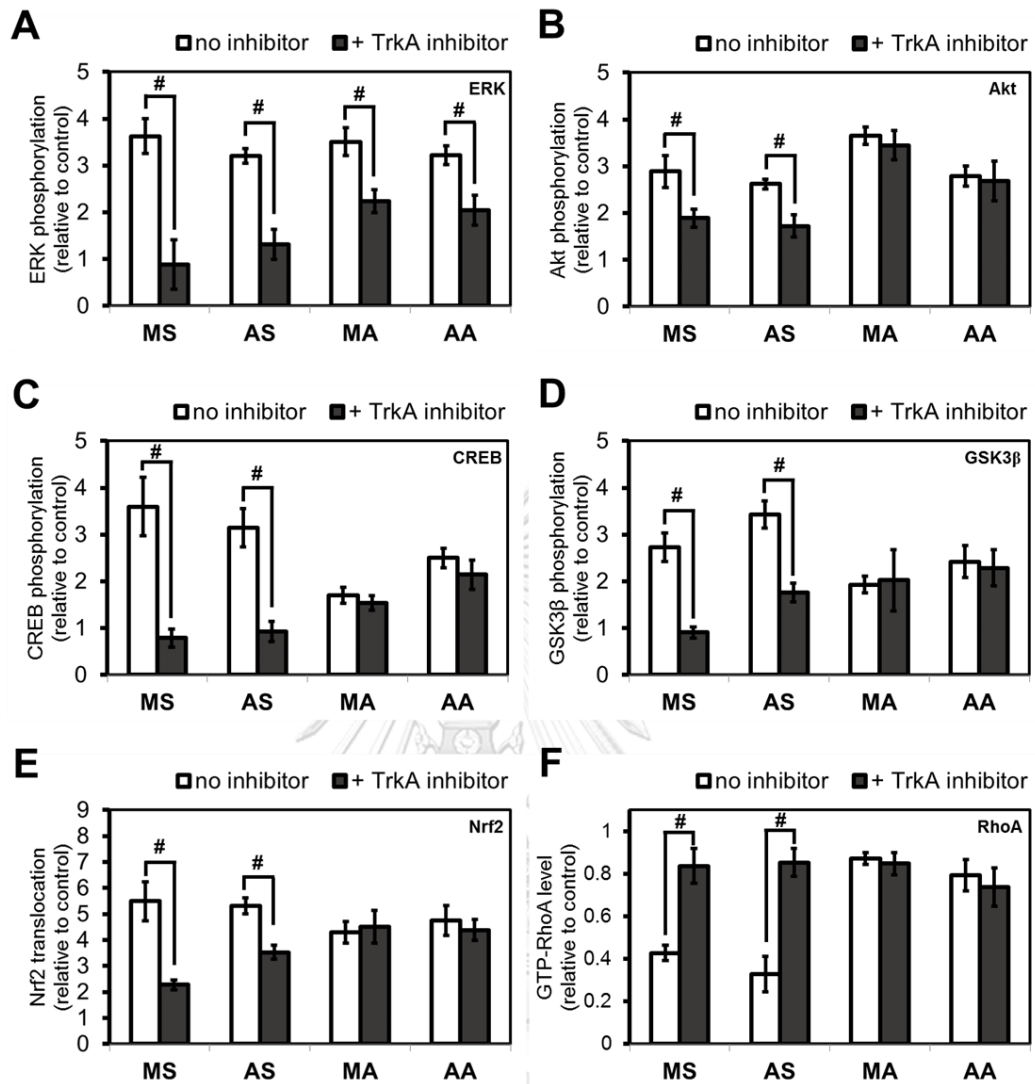
Figure 36 Histograms shows the effects of TrkA inhibitor on activation of neurite outgrowth-involving signaling molecules.

Effects on (**A**) ERK1/2, (**B**) Akt, (**C**) CREB, (**D**) GSK3β, (**E**) Nrf2 translocation and (**F**) GTP-RhoA. Data are presented as mean ± SD (n=3). * significant difference ($p < 0.05$) vs. control (DMSO). # significant difference between compared groups.

come from other signaling mediation, while p-Akt induced by **MS** and **AS** might be partly regulated by TrkA signaling. For CREB phosphorylation, inhibition on TrkA signaling clearly abolished p-CREB induced by **MS** and **AS** (**Figure 36C**), while p-CREB induced by **MA** and **AA** was not affected. These characteristics were also found in GSK3β phosphorylation that inhibition on TrkA signaling affected only in glycoside-treated cells (**Figure 36D**).

For the effects on induction of Nrf2 translocation, inhibition on TrkA signaling also did not affect aglycone-treated cells (**Figure 36E**), and translocation of Nrf2 induced by **MS** and **AS** was inhibited when inhibited TrkA signaling. Similar to Nrf2 translocation, inhibition of RhoA activity detected by GTP-RhoA level was also restored by inhibition on TrkA signaling in glycoside-treated cells. The decreasing in GTP-RhoA level induced by **MS** and **AS** was restored in GW441756-pretreated cells (**Figure 36F**), while this reverse effect was not observed in **MA**- and **AA**-treated groups.

6.1 Inhibition on TrkA signaling resulted in neurite outgrowth suppression in only glycoside-treated cells

To confirm the role of TrkA mediated signaling on neurite outgrowth, Neuro-2a cells were pre-treated with GW441756 for 30 min prior to be incubated with **MS, AS, MA** and **AA** for 6 h. The result showed that pre-treatment with TrkA inhibitor totally suppressed neurite outgrowth activity which induced by **MS** and **AS** in both %NBC and neurite length parameters (**Figure 37A, 37B**). However, there was no suppressive effect on **MA**- and **AA**-treated cells (**Figure 37A, 37C**). These results clearly suggested that the mechanism of **MS** and **AS** in induction of neurite outgrowth might be mainly come from activation of TrkA receptor signaling, while neurite outgrowth activity of **MA** and **AA** might be TrkA-signaling independent.
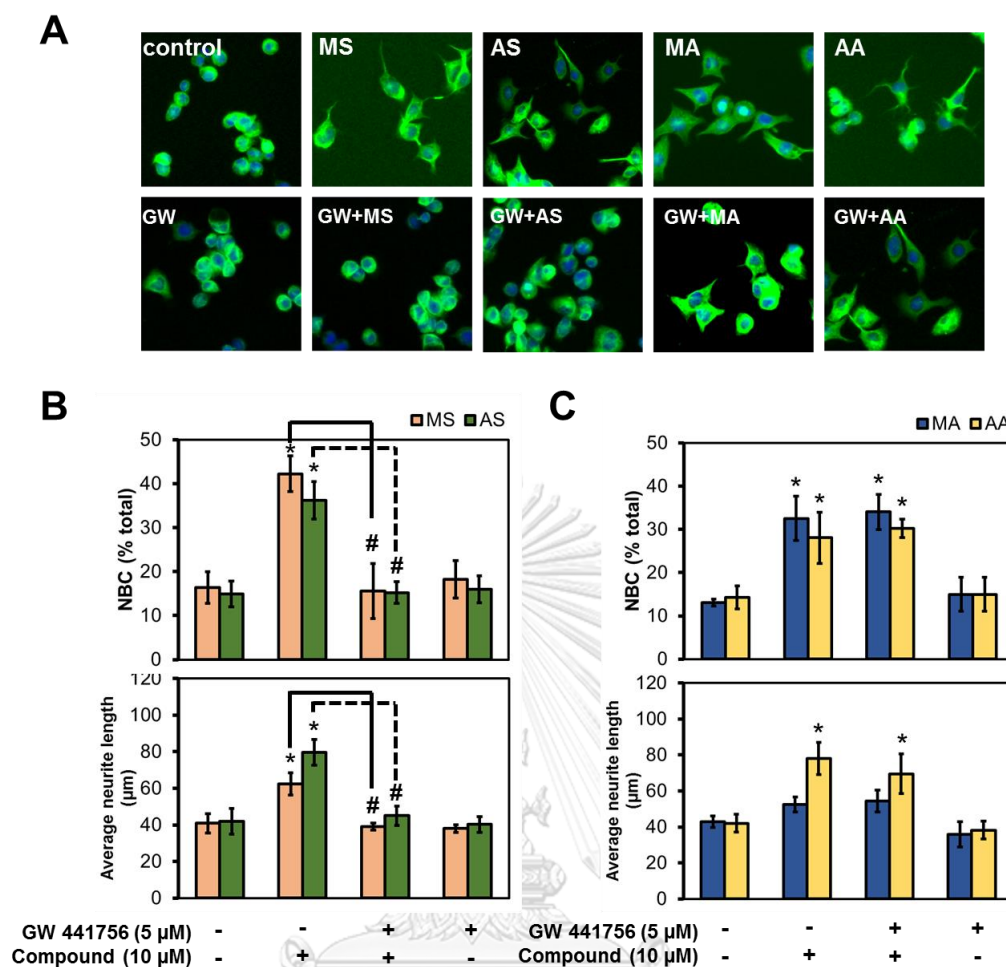
Figure 37 Effects of TrkA inhibitor on neurite outgrowth induced by **MS, AS, MA** and **AA**.

(**A**) Representative fluorescent images of βIII-tubulin-stained Neuro-2a cells. Cells were pre-treated with GW 441756 for 30 min prior treatment by 10 μM of each compound. (**B - C**) Histograms shows %NBC and neurite length of treated cells in the presence and absence of Trk inhibitor. Data are presented as mean ± SD (n=3). * significant difference ($p < 0.05$) vs. control (DMSO). # significant difference between compared groups.

7. Summary of signaling activation/inhibition by MS, AS, MA and AA

According to time-course studies on activation/inhibition of signaling proteins involving with neurite outgrowth, we could summarize that the overall characteristics of signaling activation between glycosides (**MS** and **AS**) and aglycones (**MA** and **AA**) were different (**Figure 38**). Especially in ERK phosphorylation, glycosides were found to activate p-ERK in more sustained manner when compared to aglycones. Moreover, aglycones tended to show faster onset in activation of most signaling proteins than glycosides especially in induction of Nrf2 translocation.

When using the specific inhibitors to inhibit ERK1/2 and Akt signalings, which are the upstream signalings, we also found the different results from inhibition between glycosides and aglycones (**Figure 39**). In glycosides, inhibition on ERK1/2 signaling caused the suppression of CREB phosphorylation and abolishment in neurite outgrowth activity which might come from the loss of p-CREB activation as previously described (**Figure 22**). Inhibition on Akt was found to cause the suppression of p-GSK3β, inactivation of RhoA and Nrf2 translocation. However, the only neurite length promotion was also suppressed, while the number of neurite-bearing cells was not affected when Akt signaling was inhibited.

In aglycones, inhibition on ERK1/2 and Akt was found to less affect the downstream signalings. Inhibition on ERK1/2 did not suppress any investigated signalings. However, inhibition on Akt could cause the negative effects by abolishment of p-GSK3β and Nrf2 translocation. Neurite length promotion was also found to be suppressed when Akt signaling was inhibited in **AA**-treated cells.

When TrkA receptor signaling was inhibited by using a specific inhibitor, we found that almost investigated intracellular signalings induced by glycosides were inhibited especially p-ERK1/2 and p-Akt and their downstream signalings such as p-CREB, p-GSK3β, Nrf2 translocation and RhoA inactivation (**Figure 40**). The neurite outgrowth induction activity was also totally abolished. On the contrary, inhibition on TrkA signaling in aglycone-treated cells did not affect the neurite outgrowth activity and downstream signalings except p-ERK1/2 which was only significantly decreased.
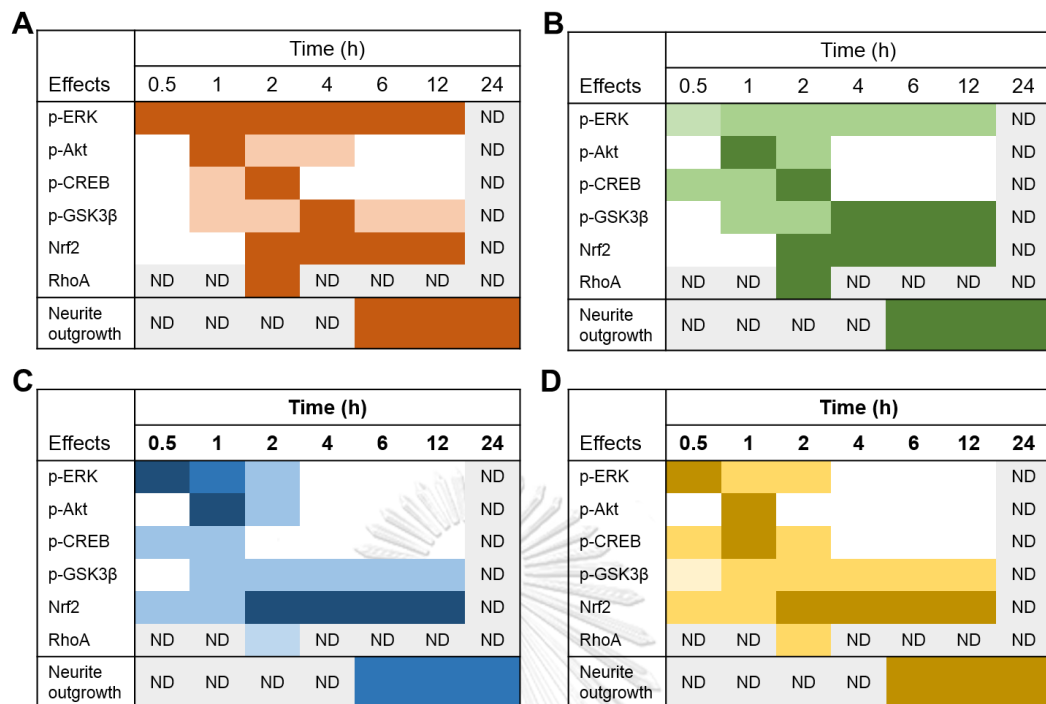
Figure 38 Graphical maps of time profiles of signaling activation induced by (**A**) **MS**, (**B**) **AS**, (**C**) **MA** and (**D**) **AA**.

Intensity of color indicates the degree of activation/inhibition. **ND**: not determined.

Effect \ Inhibition	MS		AS		MA		AA	
	ERK	Akt	ERK	Akt	ERK	Akt	ERK	Akt
p-CREB	🟥	🟨	🟥	🟨	🟨		🟨	
p-GSK3β	🟧	🟥	🟧	🟥	🟨	🟥	🟨	🟥
Nrf2	🟨	🟧	🟨	🟧		🟥		🟥
RhoA	ND	🟥	ND	🟥	ND	🟨	ND	🟨
NBC	🟥	🟨	🟥	🟨	🟨		🟨	
Neurite length	🟥	🟥	🟥	🟥	🟨	ND	🟨	🟥

🟥 totally abolished ▓ slightly decreased

🟧 significantly decreased 🟨 not changed

ND not determined
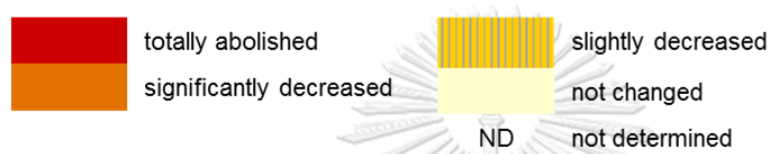
Figure 39 Summary of effects of ERK and Akt inhibition on downstream signaling activation.

Inhibition on TrkA	MS	AS	MA	AA
p-ERK				
p-Akt				
p-CREB				
p-GSK3β				
Nrf2				
RhoA				
NBC				
Neurite length				

totally abolished | slightly decreased
significantly decreased | not changed

Figure 40 Summary of effects of TrkA inhibition on downstream signaling activation.

CHAPTER V DISCUSSION AND CONCLUSION

Several pharmacological studies have suggested the beneficial effect of *C. asiatica* extract and its constituents on mitigation of various neurodegenerative diseases such as memory impairment, anxiety and locomotor dysfunction (Xu *et al.*, 2008; Tantisira *et al.*, 2010; Wanasuntronwong *et al.*, 2012; Lin *et al.*, 2013). The pentacyclic triterpenoids, **MA** and **AA** and their glycoside derivatives, **MS** and **AS**, found in *C. asiatica*, were regarded as the major active constituents responsible for neuroregenerative potential (Lokanathan *et al.*, 2016). However, it was believed that glycoside compounds tend to be hydrolyzed to aglycone products in the gastrointestinal tract after oral administration. In addition, the poor bioavailability of glycoside compounds were frequently reported (Gao *et al.*, 2012). Aglycones thus seem to be more promising therapeutic compounds than glycosides. However, recent pharmacokinetic studies revealed the presence of unchanged **MS** and **AS** in brain tissues after oral administration of *C. asiatic* extracts containing **MS** and **AS** (Anukunwithaya *et al.*, 2016), supporting the possibility of these triterpenoid glycosides to exert neurological effect. Despite that **MS, AS, MA** and **AA** were demonstrated to be neuroactive using various *in vitro* and *in vivo* models, they have not yet compared directly against each other in the same experimental setting. Therefore, it is the aim of the present study to revisit and compare the potency of each major *C. asiatic* triterpenoid in a controlled neurite outgrowth evaluation as well as to examine their mechanisms.

MS, AS, MA and **AA** were separately evaluated for their neurite outgrowth induction as well as their related signalings involved with neurite outgrowth. Our findings revealed that **MS** and **AS** exhibited more potent neurite outgrowth activities than **MA** and **AA**, suggesting the different potency between glycosides (**MS** and **AS**) and aglycones (**MA** and **AA**). Using neurite outgrowth assay performed in Neuro-2a cells, **MS** and **AS** exhibited higher potency in neurite outgrowth promotion determined by increasing %NBC and neurite length than **MA** and **AA**. Interestingly, **AS** exhibited higher potency in promoting neurite elongation than **MS**. This was consistent in

aglycones that **AA** was also better in neurite elongation promotion than **MA**. From the aspect of chemical structures, the only difference between **MS/MA** and **AS/AA** derivatives was hydroxylation at position 6. **AS** and **AA** are non-hydroxylated derivatives of **MS** and **MA**, respectively. This was interesting that this minor difference in the 6-hydroxyl group might result in different potency, as well as the sugar moiety between glycoside and aglycone derivatives. These led us to further investigate on effects of each compound on activation of intracellular signalings. From our mechanistic study also showed the different manner of activation on intracellular signalings between glycosides and aglycones. Our results suggested that **MS** and **AS** could induce neurite outgrowth through association with TrkA receptor signaling-induced ERK and Akt activation, while induction of neurite outgrowth by **MA** or **AA** was regulated by TrkA-independent signaling pathway.

Since activations of ERK are considered as one of major downstream signalings which regulated by Trk receptor signaling (Huang *et al.*, 2003), treatment with **MS** or **AS** was found to activate ERK1/2 phosphorylation in a sustained manner, while transient ERK1/2 activation occurred in **MA** or **AA** treatment. Previous studies reported the difference in duration of ERK phosphorylation may consequently result in different cellular responses (Ebisuya *et al.*, 2005; Ha *et al.*, 2008). Sustained ERK phosphorylation is one of the main transducing signals regulating neuronal differentiation, and can be induced by NGF through TrkA receptor in PC12 cells, while stimulating with other growth factor receptors such as epidermal growth factor (EGF) through its EGF receptor could trigger only transient ERK1/2 signal (von Kriegsheim *et al.*, 2009). Therefore, the role of ERK1/2 activation in neurite outgrowth was confirmed in this study. Inhibition on ERK1/2 phosphorylation resulted in suppression on neurite outgrowth induced by **MS** and **AS** but not **MA** and **AA**. These suggested that sustained ERK1/2 phosphorylation was involved in neurite outgrowth activity induced by **MS** and **AS**, while transient activation of ERK1/2 by **MA** and **AA** was not involved.

Phosphorylated CREB was reported to play role in regulating the gene transcription by forming a complex with the transcriptional activator CREB-binding protein (CBP) to stimulate the transcription of genes involved in neuronal

differentiation (Kida *et al.,* 2014). Our study on CREB activation also showed that **MS**- or **AS**-induced sustained ERK1/2 phosphorylation was found to further activate CREB phosphorylation, which was essential for neurite outgrowth activity. On the contrary, transient ERK1/2 activation was found to be not involved in neither CREB activation nor neurite outgrowth activity induced by **MA** and **AA**. Sustained ERK phosphorylation was reportedly required for CREB activation as evidenced from *in vitro* and *in vivo* investigations of neuroplasticity-related gene expression and cortical neuronal development (Papadeas *et al.,* 2004; Ha *et al.,* 2008). To confirm the essential role of CREB in the regulation of neurite outgrowth, inhibition on the binding between CREB and CBP by an inhibitor, **Naph**, resulted in suppression of CREB function. Our result clearly demonstrated that increasing level of βIII-tubulin expression as well as neurite outgrowth induced by **MS, AS, MA or AA** were suppressed by inhibition on the interaction of CREB and CBP, confirming the important role of CREB in neurite outgrowth regulation. Taken together, these results suggested that **MS** and **AS** could induce neurite outgrowth partly through activation of ERK1/2-CREB signaling pathway which possibly initiated by TrkA receptor signaling, while **MA** and **AA** also induced neurite outgrowth through CREB activation but was not originated from ERK1/2 or TrkA receptor signaling.

Not only ERK1/2 but also Akt phosphorylation could be activated through activation of Trk receptor. Activation of Akt has been well documented to modulate several neuronal processes including neurite outgrowth (Read and Gorman, 2009). From our study, **MS, AS, MA** and **AA** could induce Akt activation which was in accordance with previous reports (Soumyanath *et al.,* 2005; Wanakhachornkrai *et al.,* 2013; Jiang *et al.,* 2016). However, we found that only **MS**- and **AS**-induced Akt phosphorylation were regulated by TrkA receptor signaling, while Akt phosphorylation induced by **MA** or **AA** was found to be not involved. For the involvement of Akt signaling on neurite outgrowth, our results showed that inhibition on Akt suppressed the promotion of neurite length in either glycoside- or aglycone-treated cells. These results suggested that **MS, AS, MA,** and **AA** could promote neurite length through the association with Akt activation.

GSK3β is a key downstream signaling molecule of Akt and acts as an inhibitory molecule which stabilized the cytoskeleton reorganization during neuronal development (Ahn *et al.*, 2014). Several pieces of evidence also suggested that inactivation of GSK3β activity was required for neurite initiation and neurite elongation (Zhou *et al.*, 2004; Garrido *et al.*, 2007). GSK3β regulated cytoskeleton stabilization by controlling the activities of several microtubule-binding proteins which play roles in neurite establishment such as microtubule-associated protein (MAP), Tau and collapsin response mediator proteins (CRMP) (Garrido *et al.*, 2007). Moreover, GSK3β also regulated gene transcription by association with other transcription factors such as SMAD, c-Jun, and β-catenin which required for regulation of protein expression involving with phenotypic change (Xu *et al.*, 2009a; Saijilafu *et al.*, 2013). In this study, we found that **MS, AS, MA,** and **AA** could induce GSK3β phosphorylation at Ser9, resulting in possible suppression on GSK3β activity. These might allow the reorganization of cytoskeleton proteins, leading to neurite elongation. Moreover, our results also showed that inhibition on Akt signaling resulted in the reduction of GSK3β phosphorylation. These were in accordance with the previous study reported that inhibitory regulation of GSK3β by phosphorylation at Ser9 is mainly modulated by Akt phosphorylation (Cross *et al.*, 1995). These also correlated with our previous results which the suppression of neurite elongation occurred when Akt signaling was inhibited.

Another downstream effector of Akt signaling in the controlling of cytoskeleton dynamics is RhoA protein. Treatment with **MS**, **AS**, **MA** or **AA** was found to reduce the RhoA activity detected by measurement of the active RhoA-GTP level. RhoA is a small GTPase protein in the Rho family which plays an important role in cytoskeleton dynamics (Govek *et al.*, 2005). It functioned as molecular switches by converting between the inactive GDP-bound and the active GTP-bound state (RhoA-GTP). Activation of RhoA reportedly inhibited the neurite formation due to its function for stabilizing cytoskeleton rearrangement (Jeon *et al.*, 2012; Gu *et al.*, 2013; Nayak *et al.*, 2013). On the other hand, inhibition on RhoA activity resulted in the promotion of neurite elongation in neuronal cells (Lehmann *et al.*, 1999; Palazzolo *et al.*, 2012; Gu *et al.*, 2013). Our result revealed that treatment with all tested compounds could

reduce the RhoA activity detected by reduction of the active RhoA-GTP level. When compared between glycosides and aglycones, we found that **MS** and **AS** produced more inhibitory activity than **MA** and **AA**. These might be in accordance with our neurite outgrowth assay which revealed the potency in promoting neurite length of **MS** and **AS** was higher than **MA** and **AA**. We also confirmed that inhibitory activity on RhoA of **MS** and **AS** was originated from the activation of Akt signaling, while the inhibitory activity of **MA** or **AA** came from the Akt-independent signalings.

We also demonstrated that activation of Akt not only involved with inhibitions on GSK3β and RhoA activities but also induced Nrf2 translocation in **MS**-, **AS**-, **MA**- or **AA**-treated cells. Nrf2 is a transcription factor that modulated the oxidative stress homeostasis (Ma, 2013). Several studies revealed the additional role of Nrf2 in association with neuronal differentiation (Yang *et al.,* 2015; Zhao *et al.,* 2015). Treatment with **RA** was reportedly found to activate Nrf2 activity and up-regulation of its downstream genes such as NAD(P)H quinone oxidoreductase-1 and neurofilament in human neuroblastoma SY-SH5Y cells (Zhao *et al.,* 2009). Moreover, inhibition on Nrf2 expression was found to impair neurite outgrowth (Zhao *et al.,* 2009). From our result, **MS**, **AS**, **MA** and **AA** also induced Nrf2 activity which was regulated by Akt but not ERK1/2 phosphorylation. These suggested that induction of Nrf2 translocation by **MS**, **AS**, **MA** and **AA** might play a role in coordination with other pathways in the regulation of neuronal activity (Zhao *et al.,* 2015). Moreover, since the major role of Nrf2 is the modulation of cellular oxidative stress, *in vivo* studies of **MS** and **AS** containing standardized *C. asiatica* extract ECa233 reported the possible mechanism on memory improvement in β-amyloid and ischemia-induced memory impairment in mice by reducing of oxidative stress level in mouse brain (Tantisira *et al.,* 2010). Oral administration of **AA** also reportedly prevented quinolinic acid-induced the loss of spatial memory in rats by improving oxidative status (Loganathan *et al.,* 2018). Therefore, activation of Nrf2 translocation by **MS, AS, MA** or **AA** might be possibly accounted for regulation of neuronal oxidative stress homeostasis.

When considered between glycosides and aglycones, we could clearly conclude that neurite outgrowth activity of **MS** and **AS** was originated from TrkA

receptor signaling, resulting in activation of ERK1/2 and Akt, followed by their downstream signalings. On the other hand, neurite outgrowth activity and activations of ERK1/2 and Akt including their downstream signalings were not involved with TrkA receptor signaling. Although a study on the direct interaction of **MS** or **AS** on TrkA receptor is still lacking, there was a study suggested the ability of other saponins on activation of TrkA receptor as well as downstream signaling mediated by TrkA receptor (Hur *et al.*, 2009). Treatment of spicatoside A, a steroid glycoside, could activate TrkA receptor detected by phosphorylation of TrkA receptor, and phosphorylation of ERK1/2 and Akt were also induced (Hur *et al.*, 2009). Consideration on octanol-water partition coefficient value (Log P) of spicatoside A (Log P = 0.5), it implied that spicatoside A might not be able to freely diffuse across cell membrane due to its low lipophilicity, and might act on cell surface target to produce intracellular signalings. From this aspect, **MS** and **AS** also possessed the low lipophilicity by exhibiting relatively low Log P values at -1.2 and 0.1, respectively (Rafat *et al.*, 2008), suggesting that **MS** and **AS** might be hardly able to across cell membrane by passive diffusion. Another possibility of action on TrkA receptor was the possible ability of saponin on the interference of cell membrane dynamics, which is due to their structural similarity to cholesterol, a component in the cell membrane. TrkA and other receptors in its family are located on the specific region on cell membrane which called lipid raft that contained other components to facilitate receptor-mediated signalings (Korade *et al.*, 2008). Several lines of evidence suggested that disturbance on the dynamic of lipid raft containing TrkA receptor might affect signaling regulation on neurite outgrowth. Depletion on membrane cholesterol by treatment with cyclodextrin resulted in the impairment of neurite outgrowth in rat primary neurons (Ko *et al.*, 2005). On the other hand, induction of clustering of TrkA receptors and other components such as laminin-1 and β1-integrin by disturbing lipid raft dynamic might result in potentiation of signal transduction by promoting more effective interaction among signaling molecules, leading to neurite outgrowth induction (Ichikawa *et al.*, 2009). **MS** and **AS** are triterpenoid glycosides which contains lipophilic core triterpenoid structure and hydrophilic sugar moiety. They might be able to possess ability in membrane disturbance to facilitate receptor-signal transduction. Various pentacyclic triterpenoid glycosides exhibited potent hemolytic

activity by possible binding to cholesterol in the cell membranes of erythrocytes (Vo *et al.*, 2016). A study on triterpenoid glycoside from *Saponinum album* revealed its possible ability to penetrate into lipid bilayers and accumulate in lipid raft by binding to cholesterol, resulting in membrane dynamic changing (Smith *et al.*, 2017). However, not every triterpenoid glycoside is capable to penetrate the cell membrane. Structure-activity relationship in several triterpenoid glycosides revealed that the position of sugar moiety was also important for membrane insertion by tested triterpenoid glycosides which contained sugar moiety at *O*-28 position of ring D might possess membrane-affecting ability more than compounds that contained sugar moiety at ring A (Melzig *et al.*, 2001). Since **MS** and **AS** also contain sugar moiety at *O*-28 position of ring D, they might possess this possible capacity. This property of **MS** and **AS** on membrane dynamic alteration might need to be confirmed in the future study by some experiments such as observation on accumulation of TrkA receptor localization on the cell membrane.

In our study, we found that most activities of **MA** and **AA** were not initiated from TrkA receptor signalings. The question is raised on the target of action of **MA** and **AA**. We hypothesized that **MA** and **AA** might be able to diffuse across the cell membrane and trigger intracellular signalings to induce neurite outgrowth. Although the diffusion characteristic of **MA** and **AA** was still unproven, our hypothesis was supported by the comparative study on membrane permeability of glycyrrhetinic acid, an olean-type pentacyclic triterpenoid, and its glycoside forms suggested that aglycone form showed more membrane permeability than glycosides, and the greater number of sugar moiety resulted in lower membrane permeability in Caco-2 cells (Wang *et al.*, 2017). The Log P value of glycyrrhetinic acid was reported at 5.45, when compared to glycyrrhizin, a glycoside form with a di-sugar moiety of glycyrrhetinic acid, exhibited Log P value at 2.74 (Tanemoto *et al.*, 2015), suggesting the higher permeability of aglycone than glycoside form of glycyrrhetinic acid. According to physicochemical properties, the lipophilicity of **MA** (Log P = 3.0) and **AA** (Log P = 5.8) might allow them to freely diffuse across the cell membrane. Moreover, we found that the concentrations of **MA** and **AA** in culture medium were decreased when incubated with

the cells in our HPLC study. These results implied the possibility of cellular uptake of **MA** and **AA** because the concentrations of **MA** and **AA** were not changed when incubated in cell-free medium. Moreover, our cytotoxic study indicated that **MA** and **AA** exhibited higher cytotoxicity than **MS** and **AS**. These results were in accordance with the structure-cytotoxicity relationship study in rat hepatocytes that reported the high toxicity of **AA** (IC_{50} = 60.97 µM) and the cytotoxicity was greatly reduced when sugar moiety was attached to **AA** to become **AS** (IC_{50} > 2000 µM) (Dong *et al.*, 2004). Taken together, these shreds of evidence suggested the possibility that **MA** and **AA** might be uptaken into the Neuro-2a cells. After entering the cells, **MA** and **AA** might trigger intracellular signaling by direct binding to target proteins. A study on ganoderic acid DM, a triterpenoid found in mushroom, revealed that its derivative successfully diffused into the cytosol of human prostate cells, and interfered tubulin polymerization by binding to tubulin (Liu *et al.*, 2012). Another study on 18ß-glycyrrhetinic acid, a pentacyclic triterpenoid, also reported the involvement of its action on PI3K-Akt-mTOR which plays role in the regulation of cytoskeleton together with RhoA/ROCK pathway (Cai *et al.*, 2018). Interestingly, studies on Bardoxolone methyl (CDDO-Me), a synthetic pentacyclic triterpenoid derivative, revealed the direct interaction of this compound to several intracellular molecules such as IkB kinaseß (IKKß), Janus-activated kinase-1 (JAK1), receptor tyrosine-protein kinase (ErbB-2) and ubiquitin-specific enzymes 7 (USP7) (Ahmad *et al.*, 2006; Ahmad *et al.*, 2008; Kim *et al.*, 2012; Qin *et al.*, 2016). Results from these studies suggested the ability of pentacyclic triterpenoids on binding to intracellular protein targets. Therefore, additional experiments might be needed in order to clarify the targets of **MA** or **AA** in the future.

We also confirmed that the observed effects from all experiments came from the effects of intact molecules. Our stability study indicated that **MS** and **AS** were stable in both conditions of presence and absence of the cells analyzed by HPLC-UV. Although several studies reported that some mammalian cells could produce hydrolytic enzymes such as ß-glucosidase to convert glycoside compounds into deglycosylated forms (Day *et al.*, 1998; Srivastava *et al.*, 2009), but no peak of **MA** or

AA was observed in our analysis. For **MA** and **AA**, we also found that **MA** and **AA** were stable in the cell-free medium under cell culture condition, while incubation of **MA** or **AA** together with the cells resulted in significant decrease in the concentration of **MA** or **AA** in the medium. However, no additional peak of the degraded product was found in our HPLC analysis setting at any wavelength detection, suggesting that the degradation might not occur during incubation, or might need other techniques with high sensitivity to confirm. A study in glycyrrhetinic acid, an olean-type pentacyclic triterpenoid, reported that glycyrrhetinic acid was only degraded by acidic and photochemical hydrolysis, while exposure to base and heat did not affect the stability (Musharraf *et al.*, 2013). Together with our study in the cell-free system, these results suggested that **MA** and **AA** might not be degraded during incubation in cell culture condition. Therefore, another possibility to explain the reduction in the concentration of aglycones in the cellular medium was the diffusion of **MA** and **AA** across the cell membrane into cells as we mentioned earlier.

In conclusion, we revealed the action of **MS, AS, MA,** and **AA** on the possible pathways involved with neurite outgrowth in Neuro-2a cells. We firstly reported the differences in potency and mechanisms of triterpenoid glycosides (**MS** and **AS**) and aglycones (**MA** and **AA**) in exerting neuritogenic activity. Glycosides were found to exhibit greater potency than aglycones. Moreover, we observed some distinct phosphorylation and proposed preferentially different signaling pathways of glycosides and aglycones in stimulating neurite outgrowth. **MS** and **AS** clearly induced neurite outgrowth via activation of ERK1/2-CREB and promoted neurite elongation through Akt-mediated inhibition on GSK3β and RhoA activities, which were initiated from activation of TrkA receptor signaling. While **MA** and **AA** were found to activated intracellular signaling through TrkA receptor-independent signaling. Therefore, **MA** and **AA** might possibly enter the cells, and triggered intracellular such as ERK1/2-independent CREB activation, RhoA inhibitory as well as Akt-mediated GSK3β and Nrf2. Moreover, we also found the **AS** derivative could promote neurite length better than **MS** derivative. These effects might be correlated with the degree of inhibitory on GSK3β and RhoA activities. Therefore, our findings have clarified the different action of each triterpenoid found in

C. asiatica. This evaluation for neurite-promoting constituents could provide some information for the development of the *C. asiatica*-containing health products, which are currently diverse in amounts of their components.
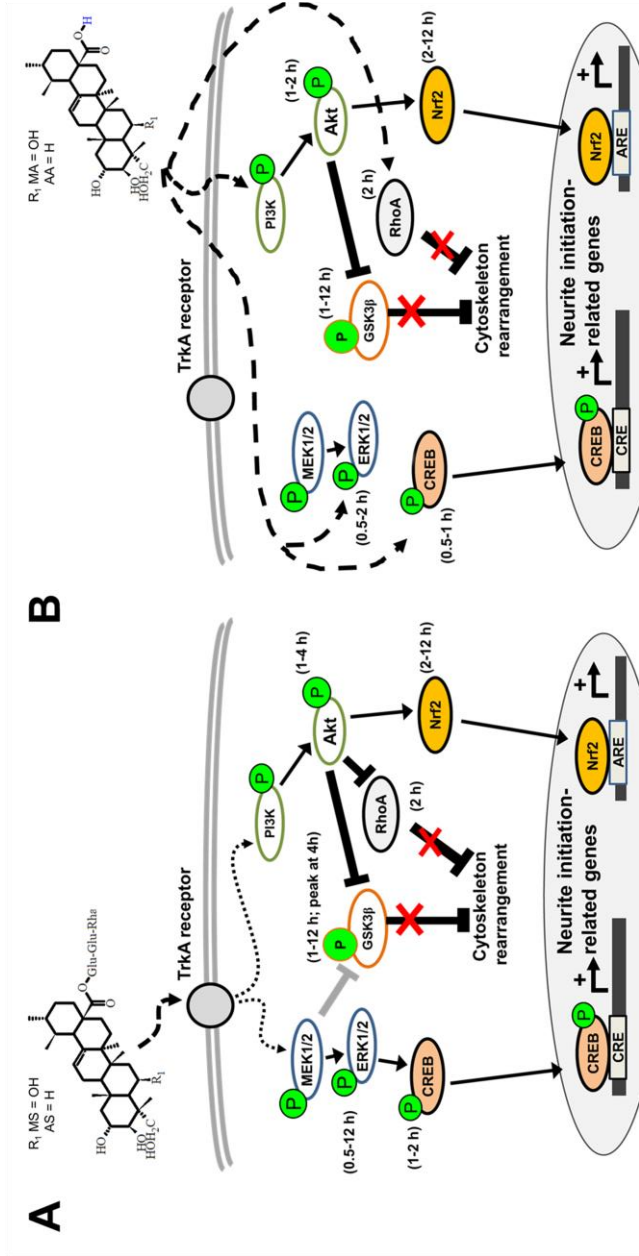
Figure 41 Schematic representation of possible signaling protein/pathways related to the proposed mechanisms of *C. asiatica* triterpenoids on inducing neurite outgrowth in Neuro-2a cells.

(**A**) Glycoside (**MS** and **AS**) activated TrkA receptor, resulted in signal transduction through ERK1/2-CREB, Akt-GSK3β, Akt-RhoA and Akt-Nrf2, while (**B**) aglycones (**MA** and **AA**) might possibly diffuse across cell membrane and triggered signaling molecules without activation of TrkA receptor. Labeled times indicate the onset and duration of each signaling activation.

APPENDICES

APPENDIX A SUPPLEMENTARY DATA

Table 1 Regression equation, LLOD and LLOQ parameters of **MS, AS, MA** and **AA** in extracted media

	Regression equation	LLOD (μg/mL)	LLOQ (μg/mL)
MS	y = 278093x - 429.92	46.34 ± 13.34	139.39 ± 40.58
	R² = 0.9993		
AS	y = 218099x + 25722	69.48 ± 15.19	210.38 ± 44.28
	R² = 0.9904		
MA	y = 454293x + 26254	130.85 ± 95.76	398.24 ± 158.15
	R² = 0.9936		
AA	y = 422423x - 78214	126.45 ± 70.85	382.26 ± 152.98
	R² = 0.9927		

LLOD = lower limit of detection; LLOQ = lower limit of quantitation

Table 2 Retention times of **MS, AS, MA** and **AA**

	Retention time (min)	
	methanol	extracted media
MS	14.43 ± 0.32	14.32 ± 0.66
AS	18.21 ± 0.23	18.69 ± 0.53
MA	28.64 ± 0.34	29.04 ± 0.32
AA	31.85 ± 0.41	32.17 ± 0.59
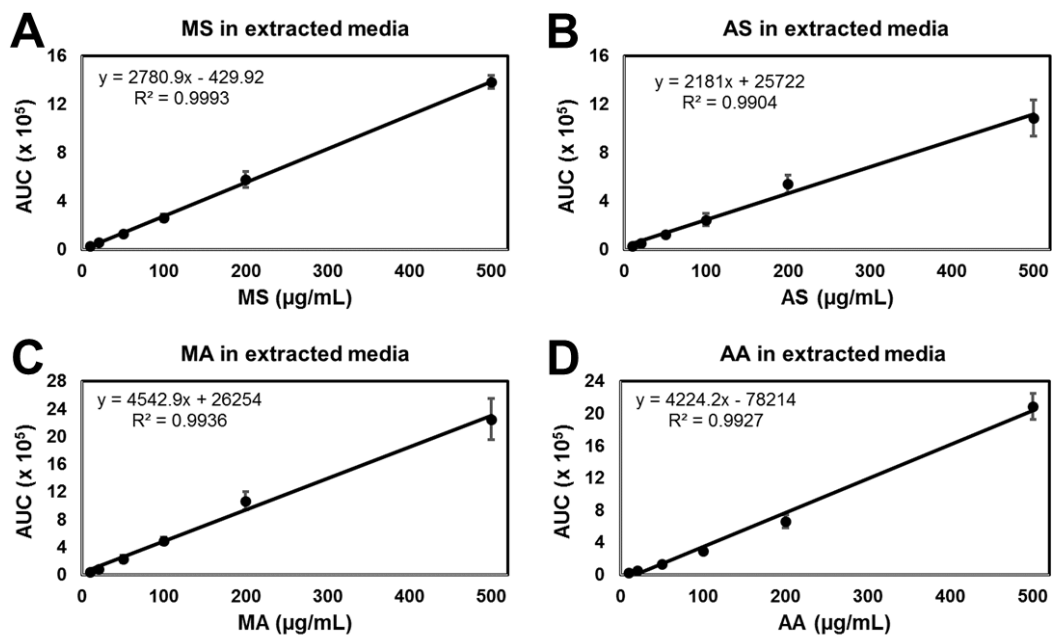
Figure 42 Standard curves of **MS, AS, MA** and **AA** in extracted media.

Standard curves of **(A) MS, (B) AS, (C) MA** and **(D) AA** were constructed from peak area detected at 206 nm.
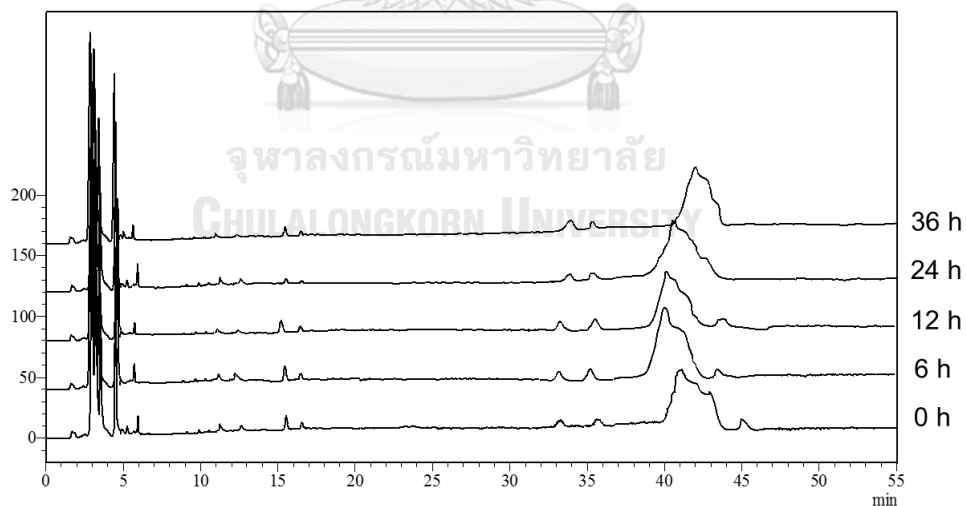
Figure 43 Representative overlay HPLC chromatograms of blank extracted media at various time points.

All chromatograms were detected at 206 nm.
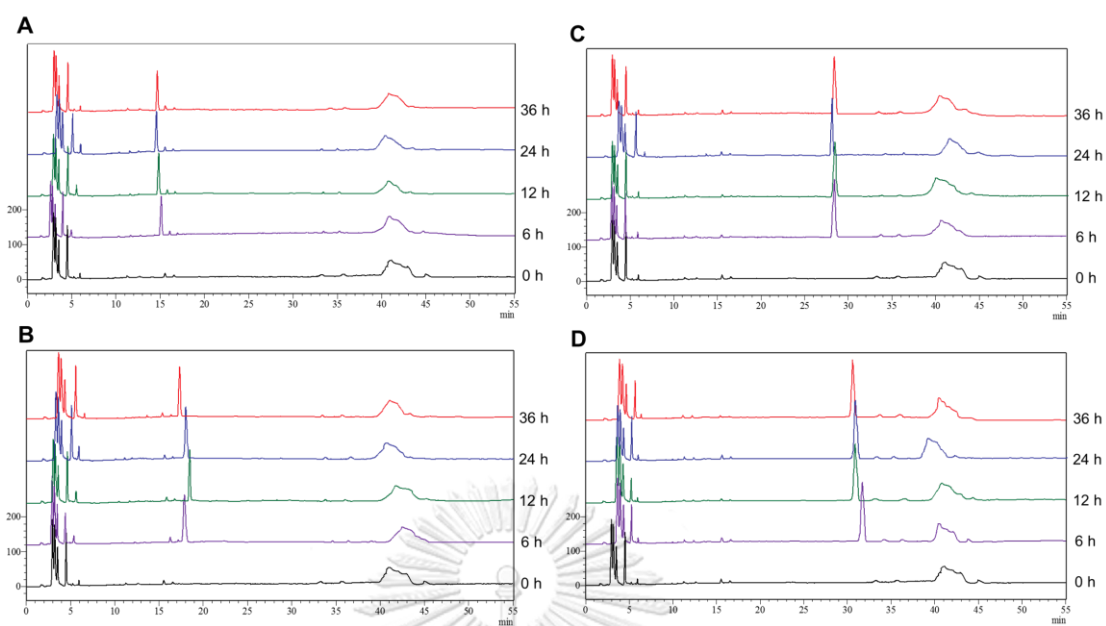
Figure 44 Representative overlay HPLC chromatograms of **(A) MS**, **(B) AS, (C) MA**
and (D) AA incubated in cell-free medium at indicated times.
All chromatograms were detected at 206 nm.
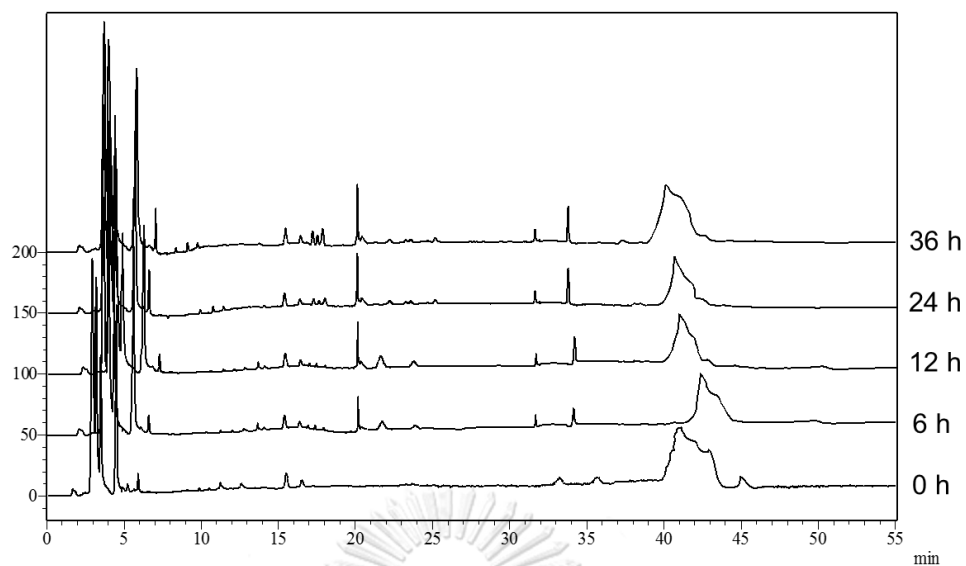
Figure 45 Representative overlay HPLC chromatograms of blank extracted media incubated with cells at various time points.

All chromatograms were detected at 206 nm.
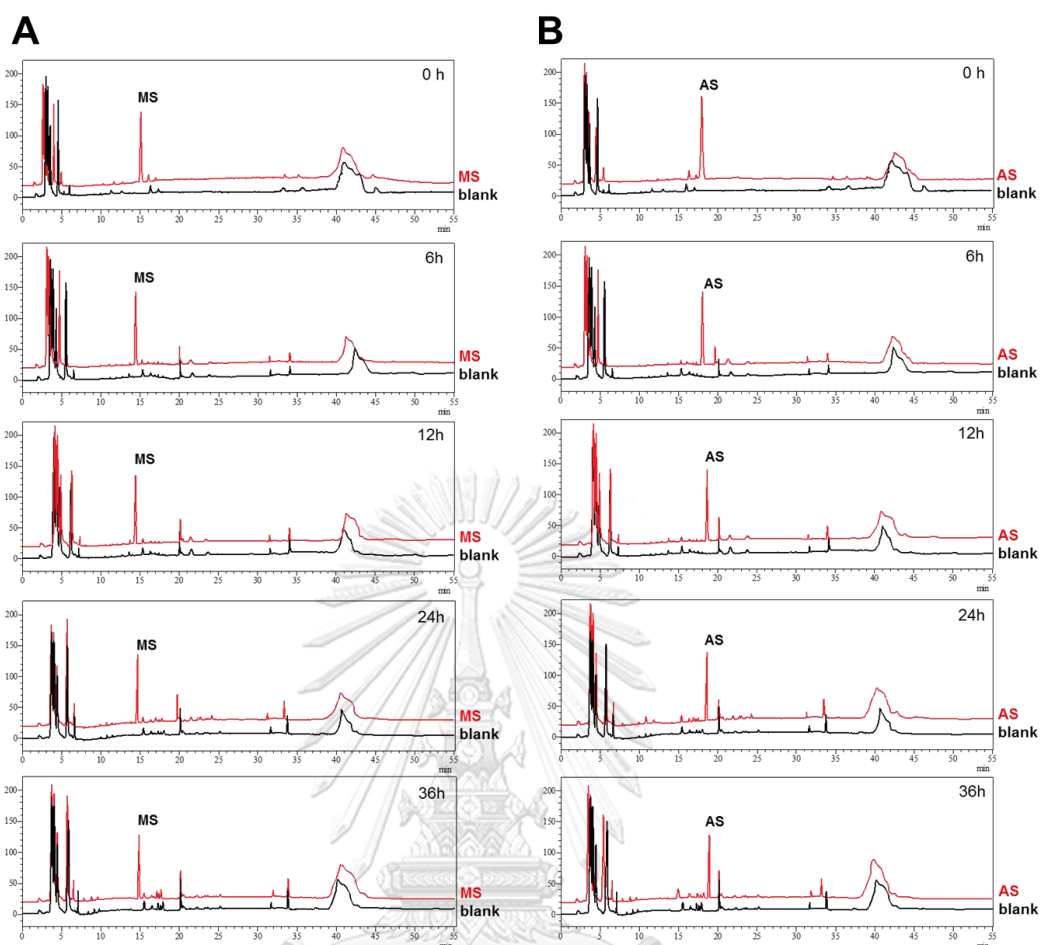
Figure 46 Representative chromatograms of (**A**) **MS** and (**B**) **AS** in cell-incubated media overlayered with blank extracted media at the same time points. All chromatograms were detected at 206 nm.
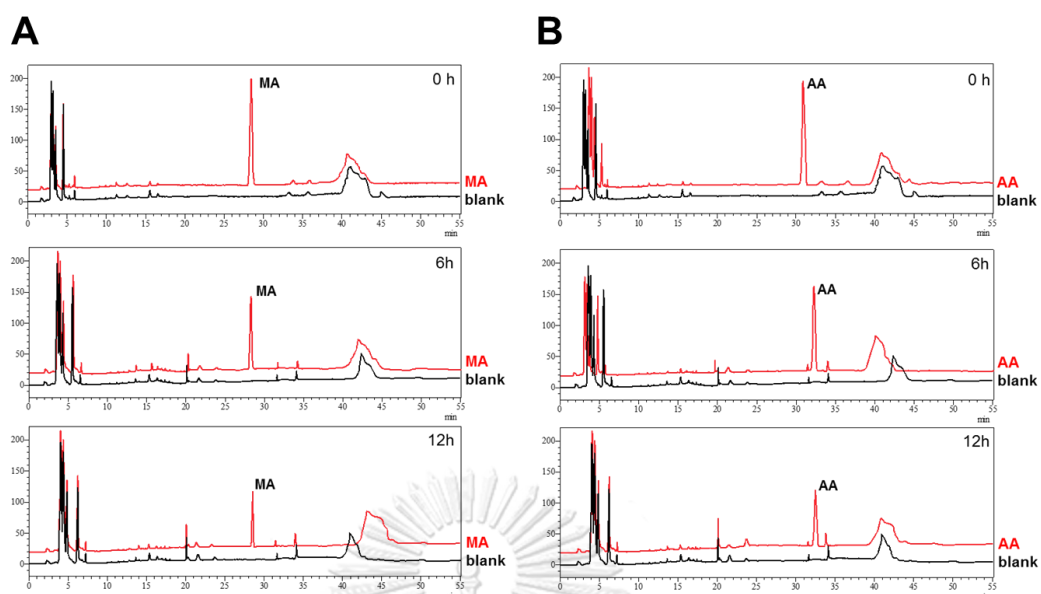
Figure 47 Representative chromatograms of (**A**) **MA** and (**B**) **AA** in cell-incubated media overlayered with blank extracted media at the same time points.

All chromatograms were detected at 206 nm.
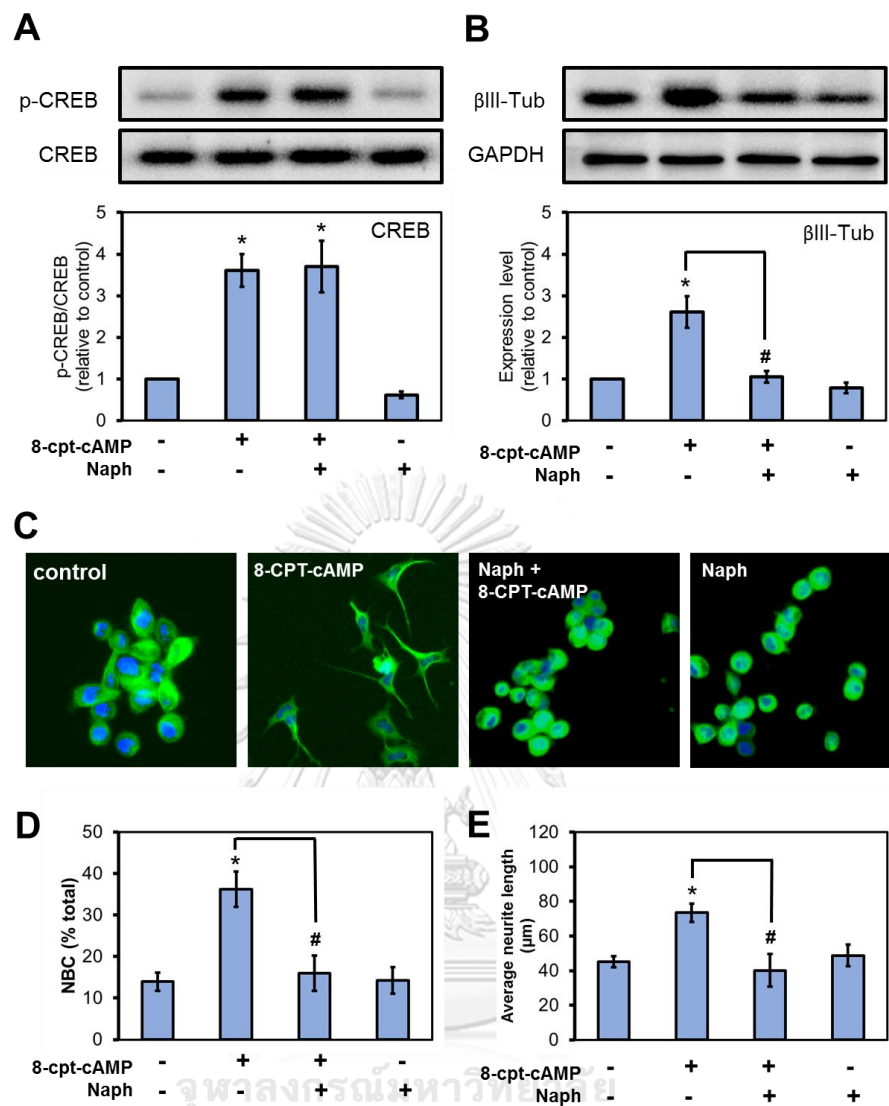
Figure 48 Effect of 8-cpt-cAMP on Neuro-2a cells.

Cells were treated with 8-cpt-cAMP (10 μM) with or without pre-treatment of 20 μM **Naph**. (**A**) Effect on 8-cpt-cAMP induced CREB phosphorylation detected at 2 h when compared to inhibited group. (**B**) Effect on βIII-tubulin expression detected at 6 h. (**C**) Representative images of βIII-tubulin-stained cells after 6 h treatment. Histograms showed neurite outgrowth parameters on (**D**) %NBC and (**E**) neurite length of 8-cpt-cAMP induced neurite outgrowth in the presence and absence of **Naph**. Data are presented as mean ± SD (n=3). * significant difference ($p < 0.05$) vs. control (DMSO). # significant difference between compared groups.
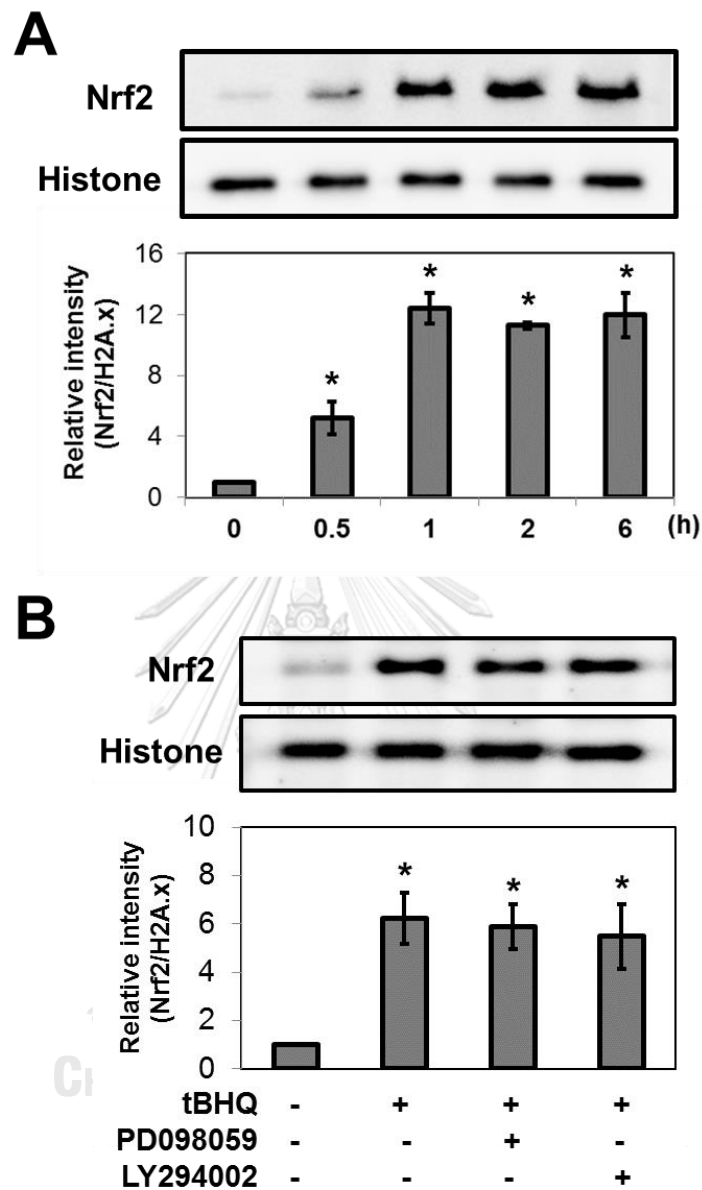
Figure 49 Effects of tBHQ, a Nrf2 activator on Nrf2 translocation.

(**A**) Neuro-2a cells were treated with 10 µM of tBHQ and nuclear level of Nrf2 was determined at 0.5, 1, 2 and 6 h. (**B**) Effects of ERK1/2 and Akt inhibition on tBHQ-induced Nrf2 translocation. Cells were pre-treated with PD098059 to inhibit ERK1/2 signaling or with LY294002 to inhibit Akt signaling prior to tBHQ treatment for 2 h. Data are presented as mean ± SD (n=3). * significant difference ($p < 0.05$) vs. control (DMSO).
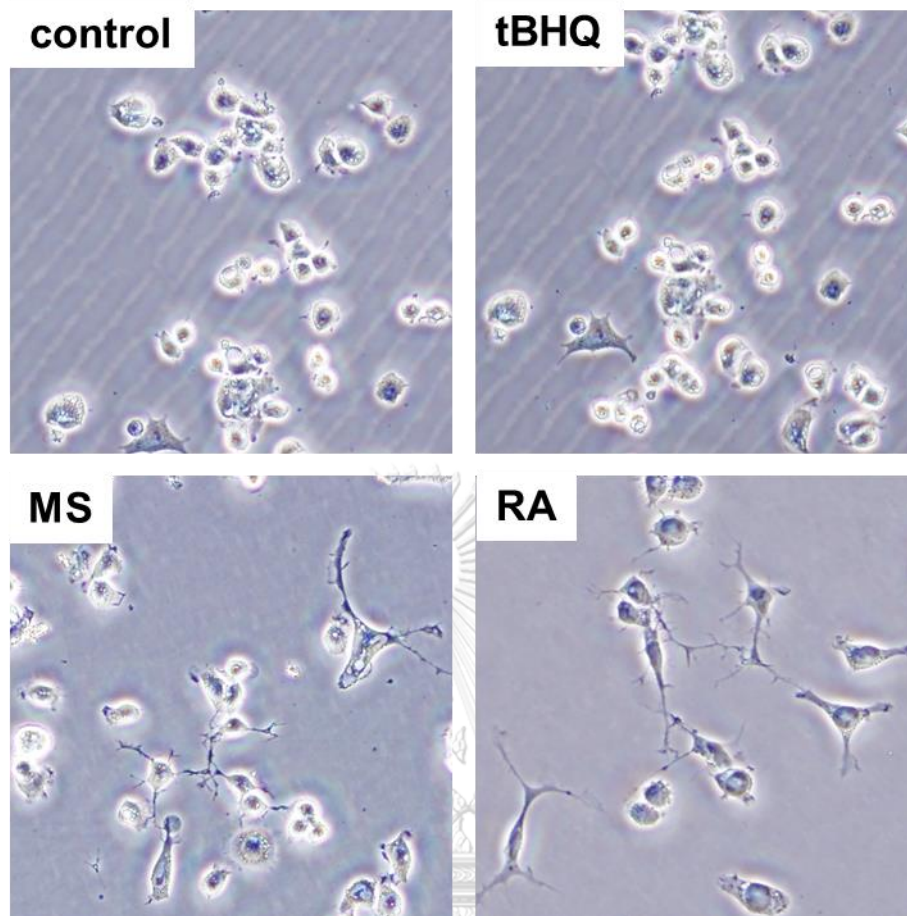
Figure 50 Effect of tBHQ on neurite outgrowth.

Representative phase-contrast images of Neuro-2a cells treated with tBHQ (25 µM) or positive inducers such as **MS** (10 µM) and **RA** (10 µM). Images were captured after 6 h of treatment.

APPENDIX B PREPARATION OF REAGENTS

Acrylamide solution

To make 100 mL of 30% acrylamide solution, 30.0 g of acrylamide and 0.8 g of N'N'-bis-methyleneacrylamide were dissolved in 30 mL of ultrapure water. The solution was stirred until completely solubilized, then adjusted volume to 100 mL. Store the solution in the dark at 4° C.

10% APS solution

To make 300 μL of 10% APS solution, 30 mg of APS was dissolved in 300 μL of ultrapure water. The solution was mixed until completely solubilized. Prepare freshly before use.

1× blotting buffer (25 mM Tris-base, 192 mM glycine, 20% MeOH)

To make 1 L of 1× blotting buffer, the ingredients were:

5X blotting buffer	200	mL
MeOH	200	mL
Adjust volume with ultrapure to	1	L

5× blotting buffer (125 mM Tris-base, 960 mM glycine)

To make 1 L of 5× blotting buffer, the ingredients were:

Tris-base	15.1	g
Glycine	72	g

All ingredients were dissolved in ultrapure water. The solution was stirred until completely solubilized. Finally, adjust the total volume to 1 L. Store the buffer at room temperature. Dilute to 1× before use.

Coomassie destaining solution

	10% MeOH		40% MeOH	
MeOH	200	mL	800	mL
Accetic acid	100	mL	200	mL
R.O. water	1700	mL	1000	mL

Coomassie staining solution

Coomassie Blue R250	1	g
MeOH	400	mL
Acetic acid	100	mL
R.O. water	500	mL

Growth medium DMEM

DMEM powder (1 package) was dissolved with 900 mL of ultrapure water and the g of sodium bicarbornate was added. The medium was mixed until completely dissolved and adjusted pH to 7.2 - 7.3 with 6N HCl. The medium was then adjusted volume to 1 L and further filtered through 0.22 μm Bottle-Top Vacuum Filters. Before use, medium was supplemented with 10% FBS and 1% penicillin-streptomycin under aseptic condition.

Immunofluorescent blocking solution

To make 10 mL, the ingredients were:

BSA	0.3	g
Triton-X100	30	μL
Adjust volume with ultrapure to	10	mL

Phosphate-buffer saline (PBS)

To make 1 L of PBS, the ingredients including 8.00 g of NaCl, 0.20 g of KCl, 1.15 g of Na_2HPO_4 and 0.20 g of KH_2PO_4 were dissolved in 800 mL of ultrapure water and adjusted the pH to 7.2 - 7.4 with 6N HCl. The solution was then adjusted volume to 1000 mL and sterilized by autoclave. Store the buffer at room temperature.

RIPA lysis buffer for immunoblotting

1 M Tris-HCl pH 8.0	50	μL
1 M NaCl	150	μL
10% SDS	10	μL
10% Na deoxycholate	50	μL
Triton-X100	10	μL
R.O. water	630	μL

Freshly add the 100× cocktail protease inhibitor in ratio of 1 μL per 100 μL of RIPA buffer before use.

10× Running buffer for SDS-PAGE (250 mM Tris-base, 1.92 M glycine, 1% SDS)

To make 1 L of 10× Tris-glycine running buffer, the ingredients were:

Tris-base	30.2	g
Glycine	144	g
SDS	10	g

All ingredients were dissolved in ultrapure water. The solution was stirred until completely solubilized. Finally, adjust the total volume to 1 L. Store the buffer at room temperature. Dilute to 1× before use.

1× Running buffer for SDS-PAGE (25 mM Tris-base, 192 mM glycine, 0.1% SDS)

To make 1 L of 1× Tris-glycine running buffer, the ingredients were:

10× running buffer	100	mL
Adjust volume with ultrapure to	1	L

10% SDS solution

To make 100 mL of 10% SDS solution, 10 g of SDS was dissolved in 80 mL of ultrapure water. The solution was stirred until completely solubilized. Carefully adjust the total volume to 100 mL. Store the solution at room temperature.

Separating gel

To prepare 2 separating gels, the ingredients of separating gel were:

	8%	12.5%	
Ultrapure water	10.2	14.464	mL
1.5 M Tris-HCl pH 8.8	5.5	11	mL
10% SDS	0.22	0.44	mL
30% acrylamide solution	5.86	17.856	mL
10% APS	220	220	µL
TEMED	13.2	22	µL

All ingredients were thoroughly mixed and immediately pour gel between the glass plates. Ultrapure water was immediately layered the top of the gel. The gels were leaved overnight for complete polymerization.

Stacking gel

Once the separating gel has completely polymerized, ultrapure was removed from the top of the polymerized gel. To prepare 2 stacking gels for Mighty small II SE250/SE260, the ingredients of stacking gel were:

Ultrapure water	3.06	mL
0.5 M Tris-HCl pH 6.8	1.26	mL
10% SDS	50	µL
30% acrylamide solution	0.66	mL
10% APS	31.2	µL
TEMED	5	µL

All ingredients were thoroughly mixed and immediately pour gel between the glass plates. Combs were inserted between the glass plates to make sample loading wells. The gels were leaved at least 40 min to polymerize.

Subcellular fractionation buffer

To make 10 mL, the ingredients were:

HEPES	47.7	mg
KCl	7.5	mg
$MgCl_2$	1.9	mg
EDTA	2.9	mg
EGTA	3.8	mg
Adjust volume with ultrapure to	10	mL

Freshly add DTT to final concentration 1 mM before use.

10× TBS

To make 1 L of 10× TBS buffer, the ingredients were:

Tris-base	24.23	g
NaCl	80.06	g

All ingredients were dissolved in ultrapure water. The solution was stirred until completely solubilized. Finally, adjust the total volume to 1 L. Store the buffer at room temperature. Dilute to 1× before use.

1× TBS-T

To make 1 L of 1× TBS-T buffer, the ingredients were:

10× TBS	100	mL
Tween 20	1	mL
Adjust volume with ultrapure to	1	L

0.5 M Tris-HCl pH 6.8

To make 100 mL of 0.5 M Tris-HCl pH 6.8 buffer, 6.1 g of Tris-base was dissolved in 80 mL of ultrapure water. The solution was stirred until completely solubilized. Adjust to pH 6.8 with 6N HCl. Finally, adjust the total volume to 100 mL. Store the buffer at 4°C.

1.5 M Tris-HCl pH 8.8

To make 100 mL of 1.5 M Tris-HCl pH 8.8 buffer, 18.15 g of Tris-base was dissolved in 80 mL of ultrapure water. The solution was stirred until completely solubilized. Adjust to pH 8.8 with 6N HCl. Finally, adjust the total volume to 100 mL. Store the buffer at 4°C.

0.25% Trypsin/0.038% EDTA solution

To prepare 100 mL of trypsin/EDTA solution, 0.25 g of trypsin and 0.038 g of EDTA were dissolved in PBS. Solution was filtered through 0.22 µm syring filter for sterilization.

REFERENCES

Abiko Y, Miura T, Phuc BH, Shinkai Y and Kumagai Y. 2011. Participation of covalent modification of Keap1 in the activation of Nrf2 by tert-butylbenzoquinone, an electrophilic metabolite of butylated hydroxyanisole. Toxicol Appl Pharmacol 255(1): 32-9.

Aguiar S and Borowski T. 2013. Neuropharmacological review of the nootropic herb Bacopa monnieri. Rejuvenation Res 16(4): 313-26.

Ahmad R, Raina D, Meyer C, Kharbanda S and Kufe D. 2006. Triterpenoid CDDO-Me blocks the NF-kappaB pathway by direct inhibition of IKKbeta on Cys-179. J Biol Chem 281(47): 35764-9.

Ahmad R, Raina D, Meyer C and Kufe D. 2008. Triterpenoid CDDO-methyl ester inhibits the Janus-activated kinase-1 (JAK1)-->signal transducer and activator of transcription-3 (STAT3) pathway by direct inhibition of JAK1 and STAT3. Cancer Res 68(8): 2920-6.

Ahn J, Jang J, Choi J, Lee J, Oh SH, Lee J, et al. 2014. GSK3beta, but not GSK3alpha, inhibits the neuronal differentiation of neural progenitor cells as a downstream target of mammalian target of rapamycin complex1. Stem Cells Dev 23(10): 1121-33.

Al-Ali H, Lee DH, Danzi MC, Nassif H, Gautam P, Wennerberg K, et al. 2015. Rational polypharmacology: systematically identifying and engaging multiple drug targets to promote axon growth. ACS Chem Biol:

Anukunwithaya T, Tantisira MH, Tantisira B and Khemawoot P. 2016. Pharmacokinetics of a standardized extract of Centella asiatica ECa 233 in Rats. Planta Med:

Barco A, Pittenger C and Kandel ER. 2003. CREB, memory enhancement and the treatment of memory disorders: promises, pitfalls and prospects. Expert Opin Ther Targets 7(1): 101-14.

Bibel M, Hoppe E and Barde YA. 1999. Biochemical and functional interactions between the neurotrophin receptors trk and p75NTR. EMBO J 18(3): 616-22.

Bito H, Furuyashiki T, Ishihara H, Shibasaki Y, Ohashi K, Mizuno K, et al. 2000. A critical role for a Rho-associated kinase, p160ROCK, in determining axon outgrowth in mammalian CNS neurons. Neuron 26(2): 431-41.

Brann AB, Scott R, Neuberger Y, Abulafia D, Boldin S, Fainzilber M, et al. 1999. Ceramide signaling downstream of the p75 neurotrophin receptor mediates the effects of nerve growth factor on outgrowth of cultured hippocampal neurons. J Neurosci 19(19): 8199-206.

Cai H, Chen X, Zhang J and Wang J. 2018. 18beta-glycyrrhetinic acid inhibits migration and invasion of human gastric cancer cells via the ROS/PKC-alpha/ERK pathway. J Nat Med 72(1): 252-9.

Carmichael J, DeGraff WG, Gazdar AF, Minna JD and Mitchell JB. 1987. Evaluation of a tetrazolium-based semiautomated colorimetric assay: assessment of chemosensitivity testing. Cancer Res 47(4): 936-42.

Chao MV. 2003. Neurotrophins and their receptors: A convergence point for many signalling pathways. Nat Rev Neurosci 4(4): 299-309.

Chen LW, Yung KK, Chan YS, Shum DK and Bolam JP. 2008. The proNGF-p75NTR-sortilin signalling complex as new target for the therapeutic treatment of Parkinson's disease. CNS Neurol Disord Drug Targets 7(6): 512-23.

Chen Z-a, Wang J-L, Liu R-T, Ren J-P, Wen L-Q, Chen X-J, et al. 2009. Liquiritin potentiate neurite outgrowth induced by nerve growth factor in PC12 cells. Cytotechnology 60(1-3): 125-32.

Chiang MC, Cheng YC, Chen HM, Liang YJ and Yen CH. 2014. Rosiglitazone promotes neurite outgrowth and mitochondrial function in N2A cells via PPARgamma pathway. Mitochondrion 14(1): 7-17.

Clagett-Dame M, McNeill EM and Muley PD. 2006. Role of all-trans retinoic acid in neurite outgrowth and axonal elongation. J Neurobiol 66(7): 739-56.

Conti AM, Fischer SJ and Windebank AJ. 1997. Inhibition of axonal growth from sensory neurons by excess nerve growth factor. Ann Neurol 42(6): 838-46.

Cosgaya JM, Garcia-Villalba P, Perona R and Aranda A. 1996. Comparison of the effects of retinoic acid and nerve growth factor on PC12 cell proliferation, differentiation, and gene expression. J Neurochem 66(1): 89-98.

Cross DA, Alessi DR, Cohen P, Andjelkovich M and Hemmings BA. 1995. Inhibition of glycogen synthase kinase-3 by insulin mediated by protein kinase B. Nature 378(6559): 785-9.

Day AJ, DuPont MS, Ridley S, Rhodes M, Rhodes MJ, Morgan MR, et al. 1998. Deglycosylation of flavonoid and isoflavonoid glycosides by human small intestine and liver beta-glucosidase activity. FEBS Lett 436(1): 71-5.

De Luca A and Giuditta A. 1997. Role of a transcription factor (CREB) in memory processes. Riv Biol 90(3): 371-84.

Dikshit P, Goswami A, Mishra A, Catterjee M and Jana NR. 2006. Curcumin induces stress response, neurite outgrowth and prevent NF-KB activation by inhibiting the proteasome function. Neurotox Res 9(1): 29-37.

Dong MS, Jung SH, Kim HJ, Kim JR, Zhao LX, Lee ES, et al. 2004. Structure-related cytotoxicity and anti-hepatofibric effect of asiatic acid derivatives in rat hepatic stellate cell-line, HSC-T6. Arch Pharm Res 27(5): 512-7.

Ebisuya M, Kondoh K and Nishida E. 2005. The duration, magnitude and compartmentalization of ERK MAP kinase activity: mechanisms for providing signaling specificity. J Cell Sci 118(Pt 14): 2997-3002.

Emery AC, Eiden MV and Eiden LE. 2014. Separate cyclic AMP sensors for neuritogenesis, growth arrest, and survival of neuroendocrine cells. J Biol Chem 289(14): 10126-39.

Evangelopoulos ME, Weis J and Krüttgen A. 2009. Mevastatin-induced neurite outgrowth of neuroblastoma cells via activation of EGFR. J Neurosci Res 87(9): 2138-44.

Fahnestock M, Yu G, Michalski B, Mathew S, Colquhoun A, Ross GM, et al. 2004. The nerve growth factor precursor proNGF exhibits neurotrophic activity but is less active than mature nerve growth factor. J Neurochem 89(3): 581-92.

Fang L, Wang YN, Cui XL, Fang SY, Ge JY, Sun Y, et al. 2012. The role and mechanism of action of activin A in neurite outgrowth of chicken embryonic dorsal root ganglia. J Cell Sci 125(Pt 6): 1500-7.

Gao S, Basu S, Yang Z, Deb A and Hu M. 2012. Bioavailability challenges associated with development of saponins as therapeutic and chemopreventive agents. Curr Drug Targets 13(14): 1885-99.

Gao XQ, Yang CX, Chen GJ, Wang GY, Chen B, Tan SK, et al. 2010. Ginsenoside Rb1 regulates the expressions of brain-derived neurotrophic factor and caspase-3 and induces neurogenesis in rats with experimental cerebral ischemia. J Ethnopharmacol 132(2): 393-9.

Garrido JJ, Simon D, Varea O and Wandosell F. 2007. GSK3 alpha and GSK3 beta are necessary for axon formation. FEBS Lett 581(8): 1579-86.

Gehler S, Gallo G, Veien E and Letourneau PC. 2004. p75 neurotrophin receptor signaling regulates growth cone filopodial dynamics through modulating RhoA activity. J Neurosci 24(18): 4363-72.

Gentry JJ, Barker PA and Carter BD. 2004. The p75 neurotrophin receptor: multiple interactors and numerous functions. Prog Brain Res 146(25-39.

Gohil KJ, Patel JA and Gajjar AK. 2010. Pharmacological review on Centella asiatica: A potential herbal cure-all. Indian J Pharm Sci 72(5): 546-56.

Govek EE, Newey SE and Van Aelst L. 2005. The role of the Rho GTPases in neuronal development. Genes Dev 19(1): 1-49.

Greene LA and Tischler AS. 1976. Establishment of a noradrenergic clonal line of rat adrenal pheochromocytoma cells which respond to nerve growth factor. Proc Natl Acad Sci U S A 73(7): 2424-8.

Gschwendtner A, Liu Z, Hucho T, Bohatschek M, Kalla R, Dechant G, et al. 2003. Regulation, cellular localization, and function of the p75 neurotrophin receptor (p75NTR) during the regeneration of facial motoneurons. Mol Cell Neurosci 24(2): 307-22.

Gu H, Yu SP, Gutekunst CA, Gross RE and Wei L. 2013. Inhibition of the Rho signaling pathway improves neurite outgrowth and neuronal differentiation of mouse neural stem cells. Int J Physiol Pathophysiol Pharmacol 5(1): 11-20.

Ha S and Redmond L. 2008. ERK mediates activity dependent neuronal complexity via sustained activity and CREB-mediated signaling. Dev Neurobiol 68(14): 1565-79.

Hallbook F. 1999. Evolution of the vertebrate neurotrophin and Trk receptor gene families. Curr Opin Neurobiol 9(5): 616-21.

Han WJ, Xia YF and Dai Y. 2012. Development and validation of high-performance liquid chromatography/electrospray ionization mass spectrometry for assay of madecassoside in rat plasma and its application to pharmacokinetic study. Biomed Chromatogr 26(1): 26-32.

Hannan MA, Kang JY, Mohibbullah M, Hong YK, Lee H, Choi JS, et al. 2014. Moringa oleifera with promising neuronal survival and neurite outgrowth promoting potentials. J Ethnopharmacol 152(1): 142-50.

Harrill JA and Mundy WR. 2011. Quantitative assessment of neurite outgrowth in PC12 cells. Methods Mol Biol 758(331-48.

Hashim P, Sidek H, Helan MH, Sabery A, Palanisamy UD and Ilham M. 2011. Triterpene composition and bioactivities of Centella asiatica. Molecules 16(2): 1310-22.

Hayakawa N, Shiozaki M, Shibata M, Koike M, Uchiyama Y, Matsuura N, et al. 2013. Resveratrol affects undifferentiated and differentiated PC12 cells differently, particularly with respect to possible differences in mitochondrial and autophagic functions. Eur J Cell Biol 92(1): 30-43.

Hirata K, Yamaguchi H, Takamura Y, Takagi A, Fukushima T, Iwakami N, et al. 2005. A novel neurotrophic agent, T-817MA [1-{3-[2-(1-benzothiophen-5-yl) ethoxy] propyl}-3-azetidinol maleate], attenuates amyloid-β-induced neurotoxicity and promotes neurite outgrowth in rat cultured central nervous system neurons. J Pharmacol Exp Ther 314(1): 252-9.

Hu X, Wang S, Xu J, Wang DB, Chen Y and Yang GZ. 2014. Triterpenoid saponins from Stauntonia chinensis ameliorate insulin resistance via the AMP-activated protein kinase and IR/IRS-1/PI3K/Akt pathways in insulin-resistant HepG2 cells. Int J Mol Sci 15(6): 10446-58.

Huang EJ and Reichardt LF. 2001. Neurotrophins: roles in neuronal development and function. Annu Rev Neurosci 24(677-736.

Huang EJ and Reichardt LF. 2003. Trk receptors: roles in neuronal signal transduction. Annu Rev Biochem 72(609-42.

Hur J, Lee P, Moon E, Kang I, Kim S-H, Oh MS, et al. 2009. Neurite outgrowth induced by spicatoside A, a steroidal saponin, via the tyrosine kinase A receptor pathway. Eur J Pharmacol 620(1–3): 9-15.

Ichikawa N, Iwabuchi K, Kurihara H, Ishii K, Kobayashi T, Sasaki T, et al. 2009. Binding of laminin-1 to monosialoganglioside GM1 in lipid rafts is crucial for neurite outgrowth. J Cell Sci 122(Pt 2): 289-99.

Ina A and Kamei Y. 2006. Vitamin B12, a chlorophyll-related analog to pheophytin a from marine brown algae, promotes neurite outgrowth and stimulates differentiation in PC12 cells. Cytotechnology 52(3): 181-7.

Ishima T, Nishimura T, Iyo M and Hashimoto K. 2008. Potentiation of nerve growth factor-induced neurite outgrowth in PC12 cells by donepezil: Role of sigma-1 receptors and IP3 receptors. Prog Neuropsychopharmacol Biol Psychiatry 32(7): 1656-9.

James JT and Dubery IA. 2009. Pentacyclic triterpenoids from the medicinal herb, Centella asiatica (L.) Urban. Molecules 14(10): 3922-41.

Jeon CY, Moon MY, Kim JH, Kim HJ, Kim JG, Li Y, et al. 2012. Control of neurite outgrowth by RhoA inactivation. J Neurochem 120(5): 684-98.

Jeong D, Kim D and Sohn D. 2014. Pharmacokinetics and disposition of madecassoside and asiaticoside after the administration of a titrated extract of Centella asiatica in rats. J Appl Biopharm Pharmacokinet 2(1-9.

Jew SS, Yoo CH, Lim DY, Kim H, Mook-Jung I, Jung MW, et al. 2000. Structure-activity relationship study of asiatic acid derivatives against beta amyloid (A beta)-induced neurotoxicity. Bioorg Med Chem Lett 10(2): 119-21.

Jiang H, Zheng G, Lv J, Chen H, Lin J, Li Y, et al. 2016. Identification of Centella asiatica's Effective Ingredients for Inducing the Neuronal Differentiation. Evid Based Complement Alternat Med 2016(9634750.

Jin Y, Sui H-j, Dong Y, Ding Q, Qu W-h, Yu S-x, et al. 2012. Atorvastatin enhances neurite outgrowth in cortical neurons in vitro via up-regulating the Akt/mTOR and Akt/GSK-3[beta] signaling pathways. Acta Pharmacol Sin 33(7): 861-72.

Jonides J, Lewis RL, Nee DE, Lustig CA, Berman MG and Moore KS. 2008. The mind and brain of short-term memory. Annu Rev Psychol 59(193-224.

Jun W and Jun L. 2006. Characterization of absorption and metabolism of asiaticoside and its analogs. PLA Mili Acad Med Sci R285(

Kam-eg A, Tantisira B and Tantisira MH. 2009. Preliminary study on effects of standardized extract of Centella asiatica, Eca 233, on deficit of learning and memory induced by an intracerebroventricular injection of ß-amyloid peptide in mice. Thai J Pharmacol 31(79-82.

Kandhare A, Basliyal A, Mohan V, Thakurdesai P and Bodhankar L. 2013. Pharmacokinetics study of asiaticoside after oral administration in rats. Nat Con Adv Bioanal techn OR-14(

Kano Y, Horie N, Doi S, Aramaki F, Maeda H, Hiragami F, et al. 2008. Artepillin C derived from propolis induces neurite outgrowth in PC12m3 cells via ERK and p38 MAPK pathways. Neurochem Res 33(9): 1795-803.

Kaplan DR and Miller FD. 1997. Signal transduction by the neurotrophin receptors. Curr Opin Cell Biol 9(2): 213-21.

Kida S and Serita T. 2014. Functional roles of CREB as a positive regulator in the formation and enhancement of memory. Brain Res Bull 105(17-24.

Kim EH, Deng C, Sporn MB, Royce DB, Risingsong R, Williams CR, et al. 2012. CDDO-methyl ester delays breast cancer development in BRCA1-mutated mice. Cancer Prev Res (Phila) 5(1): 89-97.

Kimhi Y, Palfrey C, Spector I, Barak Y and Littauer UZ. 1976. Maturation of neuroblastoma cells in the presence of dimethylsulfoxide. Proc Natl Acad Sci U S A 73(2): 462-6.

Ko M, Zou K, Minagawa H, Yu W, Gong JS, Yanagisawa K, et al. 2005. Cholesterol-mediated neurite outgrowth is differently regulated between cortical and hippocampal neurons. J Biol Chem 280(52): 42759-65.

Korade Z and Kenworthy AK. 2008. Lipid rafts, cholesterol, and the brain. Neuropharmacology 55(8): 1265-73.

Kozma R, Sarner S, Ahmed S and Lim L. 1997. Rho family GTPases and neuronal growth cone remodelling: relationship between increased complexity induced by Cdc42Hs, Rac1, and acetylcholine and collapse induced by RhoA and lysophosphatidic acid. Mol Cell Biol 17(3): 1201-11.

Kubo T, Yamaguchi A, Iwata N and Yamashita T. 2008. The therapeutic effects of Rho-ROCK inhibitors on CNS disorders. Ther Clin Risk Manag 4(3): 605-15.

Kuhn TB, Meberg PJ, Brown MD, Bernstein BW, Minamide LS, Jensen JR, et al. 2000. Regulating actin dynamics in neuronal growth cones by ADF/cofilin and rho family GTPases. J Neurobiol 44(2): 126-44.

Lee B, Park J, Park J, Shin H-J, Kwon S, Yeom M, et al. 2011. Cordyceps Militaris improves neurite outgrowth in Neuro2A cells and reverses memory impairment in rats. Food Sci Biotechnol 20(6): 1599-608.

Leggio MG, Mandolesi L, Federico F, Spirito F, Ricci B, Gelfo F, et al. 2005. Environmental enrichment promotes improved spatial abilities and enhanced dendritic growth in the rat. Behav Brain Res 163(1): 78-90.

Lehmann M, Fournier A, Selles-Navarro I, Dergham P, Sebok A, Leclerc N, et al. 1999. Inactivation of Rho signaling pathway promotes CNS axon regeneration. J Neurosci 19(17): 7537-47.

Leng DD, Han WJ, Rui Y, Dai Y and Xia YF. 2013. In vivo disposition and metabolism of madecassoside, a major bioactive constituent in Centella asiatica (L.) Urb. J Ethnopharmacol 150(2): 601-8.

LePage KT, Dickey RW, Gerwick WH, Jester EL and Murray TF. 2005. On the use of neuro-2a neuroblastoma cells versus intact neurons in primary culture for neurotoxicity studies. Crit Rev Neurobiol 17(1): 27-50.

Lesburgueres E, Gobbo OL, Alaux-Cantin S, Hambucken A, Trifilieff P and Bontempi B. 2011. Early tagging of cortical networks is required for the formation of enduring associative memory. Science 331(6019): 924-8.

Li BX, Yamanaka K and Xiao X. 2012. Structure-activity relationship studies of naphthol AS-E and its derivatives as anticancer agents by inhibiting CREB-mediated gene transcription. Bioorg Med Chem 20(23): 6811-20.

Li M, Li S and Li Y. 2015. Liraglutide promotes cortical neurite outgrowth via the MEK–ERK pathway. Cell Mol Neurobiol: 1-7.

Liao KK, Wu MJ, Chen PY, Huang SW, Chiu SJ, Ho CT, et al. 2012. Curcuminoids promote neurite outgrowth in PC12 cells through MAPK/ERK- and PKC-dependent pathways. J Agric Food Chem 60(1): 433-43.

Liffert R, Hoecker J, Jana CK, Woods TM, Burch P, Jessen HJ, et al. 2013. Withanolide A: synthesis and structural requirements for neurite outgrowth. Chem Sci 4(7): 2851-7.

Lin LF, Chiu SP, Wu MJ, Chen PY and Yen JH. 2012. Luteolin induces microRNA-132 expression and modulates neurite outgrowth in PC12 cells. PLoS One 7(8): e43304.

Lin X, Huang R, Zhang S, Wei L, Zhuo L, Wu X, et al. 2013. Beneficial effects of asiaticoside on cognitive deficits in senescence-accelerated mice. Fitoterapia 87(69-77.

Lin X, Zhang S, Huang R, Wei L, Tan S, Liang C, et al. 2014. Protective effect of madecassoside against cognitive impairment induced by D-galactose in mice. Pharmacol Biochem Behav 124(434-42.

Liu J, He J, Huang L, Dou L, Wu S and Yuan QL. 2014. Neuroprotective effects of ginsenoside Rb1 on hippocampal neuronal injury and neurite outgrowth. Neural Regen Res 9(9): 943-50.

Liu J, Shimizu K, Tanaka A, Shinobu W, Ohnuki K, Nakamura T, et al. 2012. Target proteins of ganoderic acid DM provides clues to various pharmacological mechanisms. Sci Rep 2(905.

Liu L, Hoang-Gia T, Wu H, Lee MR, Gu L, Wang C, et al. 2011. Ginsenoside Rb1 improves spatial learning and memory by regulation of cell genesis in the hippocampal subregions of rats. Brain Res 1382(147-54.

Loganathan C and Thayumanavan P. 2018. Asiatic acid prevents the quinolinic acid-induced oxidative stress and cognitive impairment. Metab Brain Dis 33(1): 151-9.

Lokanathan Y, Omar N, Ahmad Puzi NN, Saim A and Hj Idrus R. 2016. Recent updates in neuroprotective and neuroregenerative potential of Centella asiatica. Malays J Med Sci 23(1): 4-14.

Longo FM and Massa SM. 2013. Small-molecule modulation of neurotrophin receptors: a strategy for the treatment of neurological disease. Nat Rev Drug Discov 12(7): 507-25.

Ma Q. 2013. Role of nrf2 in oxidative stress and toxity. Annu Rev Pharmacol Toxicol 53(401-26.

Malouf R and Birks J. 2004. Donepezil for vascular cognitive impairment. Cochrane Database Syst Rev 1): CD004395.

Mao AJ, Bechberger J, Lidington D, Galipeau J, Laird DW and Naus CC. 2000. Neuronal differentiation and growth control of neuro-2a cells after retroviral gene delivery of connexin43. J Biol Chem 275(44): 34407-14.

Marder K. 2008. Donepezil in patients with subcortical vascular cognitive impairment. Curr Neurol Neurosci Rep 8(5): 361-2.

Martin SJ, Grimwood PD and Morris RG. 2000. Synaptic plasticity and memory: an evaluation of the hypothesis. Annu Rev Neurosci 23(649-711.

Meakin SO, MacDonald JI, Gryz EA, Kubu CJ and Verdi JM. 1999. The signaling adapter FRS-2 competes with Shc for binding to the nerve growth factor receptor TrkA. A model for discriminating proliferation and differentiation. J Biol Chem 274(14): 9861-70.

Melzig MF, Bader G and Loose R. 2001. Investigations of the mechanism of membrane activity of selected triterpenoid saponins. Planta Med 67(1): 43-8.

Moser MB, Trommald M and Andersen P. 1994. An increase in dendritic spine density on hippocampal CA1 pyramidal cells following spatial learning in adult rats suggests the formation of new synapses. Proc Natl Acad Sci U S A 91(26): 12673-5.

Mu LH, Huang CL, Zhou WB, Guo DH and Liu P. 2013. Methanolysis of triterpenoid saponin from Ardisia gigantifolia stapf. and structure-activity relationship study against cancer cells. Bioorg Med Chem Lett 23(22): 6073-8.

Musharraf SG, Kanwal N and Arfeen QU. 2013. Stress degradation studies and stability-indicating TLC-densitometric method of glycyrrhetic acid. Chem Cent J 7(1): 9.

Nair SN, Menon S and Shailajan S. 2012. A liquid chromatography/electrospray ionization tandem mass spectrometric method for quantification of asiatic acid from plasma: application to pharmacokinetic study in rats. Rapid Commun Mass Spectrom 26(17): 1899-908.

Nakajima K-i, Niisato N and Marunaka Y. 2011. Genistein enhances the NGF-induced neurite outgrowth. Biomed Res 32(5): 351-6.

Nam KN, Jung W-S, Park J-H and Lee EH. 2013. Ginsenoside Rb1 increases synaptophysin and microtubule-associated protein 2 mRNA expression in primary cultures of rat hippocampal neurons. Orient Pharm Exp Med 13(3): 231-4.

Nayak RC, Chang KH, Vaitinadin NS and Cancelas JA. 2013. Rho GTPases control specific cytoskeleton-dependent functions of hematopoietic stem cells. Immunol Rev 256(1): 255-68.

Nishina A, Kimura H, Tsukagoshi H, Kozawa K, Koketsu M, Ninomiya M, *et al.* 2013. Neurite outgrowth in PC12 cells stimulated by components from *Dendranthema x grandiflorum* cv.

"Mottenohoka" is enhanced by suppressing phosphorylation of p38MAPK. Evid Based Complement Alternat Med 2013(403503.

Nusser N, Gosmanova E, Zheng Y and Tigyi G. 2002. Nerve growth factor signals through TrkA, phosphatidylinositol 3-kinase, and Rac1 to inactivate RhoA during the initiation of neuronal differentiation of PC12 cells. J Biol Chem 277(39): 35840-6.

Obara Y, Aoki T, Kusano M and Ohizumi Y. 2002. β-eudesmol induces neurite outgrowth in rat pheochromocytoma cells accompanied by an activation of mitogen-activated protein kinase. J Pharmacol Exp Ther 301(3): 803-11.

Oberdoerster J and Rabin RA. 1999. NGF-differentiated and undifferentiated PC12 cells vary in induction of apoptosis by ethanol. Life Sci 64(23): PL 267-72.

Oda T, Kume T, Katsuki H, Niidome T, Sugimoto H and Akaike A. 2007. Donepezil potentiates nerve growth factor-induced neurite outgrowth in PC12 cells. J Pharmacol Sci 104(4): 349-54.

Orhan IE. 2012. Centella asiatica (L.) Urban: From Traditional Medicine to Modern Medicine with Neuroprotective Potential. Evid Based Complement Alternat Med 2012(946259.

Page M, Pacico N, Ourtioualous S, Deprez T and Koshibu K. 2015. Procognitive compounds promote neurite outgrowth. Pharmacology 96(3-4): 131-6.

Palazzolo G, Horvath P and Zenobi-Wong M. 2012. The flavonoid isoquercitrin promotes neurite elongation by reducing RhoA activity. PLoS One 7(11): e49979.

Papadeas ST, Blake BL, Knapp DJ and Breese GR. 2004. Sustained extracellular signal-regulated kinase 1/2 phosphorylation in neonate 6-hydroxydopamine-lesioned rats after repeated D1-dopamine receptor agonist administration: implications for NMDA receptor involvement. J Neurosci 24(26): 5863-76.

Park SJ, Jin ML, An HK, Kim KS, Ko MJ, Kim CM, et al. 2015. Emodin induces neurite outgrowth through PI3K/Akt/GSK-3β-mediated signaling pathways in Neuro2a cells. Neuroscience Letters 588(101-7.

Pera M, Camps P, Munoz-Torrero D, Perez B, Badia A and Clos Guillen MV. 2013. Undifferentiated and differentiated PC12 cells protected by huprines against injury induced by hydrogen peroxide. PLoS One 8(9): e74344.

Poldrack RA and Gabrieli JD. 1997. Functional anatomy of long-term memory. J Clin Neurophysiol 14(4): 294-310.

Price RD, Yamaji T and Matsuoka N. 2003. FK506 potentiates NGF-induced neurite outgrowth via the Ras/Raf/MAP kinase pathway. Br J Pharmacol 140(5): 825-9.

Puttagunta R, Schmandke A, Floriddia E, Gaub P, Fomin N, Ghyselinck NB, et al. 2011. RA-RAR-beta counteracts myelin-dependent inhibition of neurite outgrowth via Lingo-1 repression. J Cell Biol 193(7): 1147-56.

Qin D, Wang W, Lei H, Luo H, Cai H, Tang C, *et al*. 2016. CDDO-Me reveals USP7 as a novel target in ovarian cancer cells. Oncotarget 7(47): 77096-109.

Radad K, Gille G, Moldzio R, Saito H, Ishige K and Rausch WD. 2004. Ginsenosides Rb1 and Rg1 effects on survival and neurite growth of MPP+-affected mesencephalic dopaminergic cells. J Neural Transm 111(1): 37-45.

Radio NM and Mundy WR. 2008. Developmental neurotoxicity testing in vitro: models for assessing chemical effects on neurite outgrowth. Neurotoxicology 29(3): 361-76.

Rafamantanana MH, Rozet E, Raoelison GE, Cheuk K, Ratsimamanga SU, Hubert P, *et al*. 2009. An improved HPLC-UV method for the simultaneous quantification of triterpenic glycosides and aglycones in leaves of *Centella asiatica* (L.) Urb (APIACEAE). J Chromatogr B Analyt Technol Biomed Life Sci 877(23): 2396-402.

Rafat M, Fong KW, Goldsipe A, Stephenson BC, Coradetti ST, Sambandan TG, *et al*. 2008. Association (micellization) and partitioning of aglycon triterpenoids. J Colloid Interface Sci 325(2): 324-30.

Raina V, Gupta S, Yadav S and Surolia A. 2013. Simvastatin induced neurite outgrowth unveils role of cell surface cholesterol and acetyl CoA carboxylase in SH-SY5Y cells. PLoS One 8(9): e74547.

Ramm P, Alexandrov Y, Cholewinski A, Cybuch Y, Nadon R and Soltys BJ. 2003. Automated screening of neurite outgrowth. J Biomol Screen 8(1): 7-18.

Restivo L, Vetere G, Bontempi B and Ammassari-Teule M. 2009. The formation of recent and remote memory is associated with time-dependent formation of dendritic spines in the hippocampus and anterior cingulate cortex. J Neurosci 29(25): 8206-14.

Roloff F, Scheiblich H, Dewitz C, Dempewolf S, Stern M and Bicker G. 2015. Enhanced neurite outgrowth of human model (NT2) neurons by small-molecule inhibitors of Rho/ROCK signaling. PLoS ONE 10(2):

Rumalla CS, Ali Z, Weerasooriya AD, Smillie TJ and Khan IA. 2010. Two new triterpene glycosides from Centella asiatica. Planta Med 76(10): 1018-21.

Saijilafu, Hur EM, Liu CM, Jiao Z, Xu WL and Zhou FQ. 2013. PI3K-GSK3 signalling regulates mammalian axon regeneration by inducing the expression of Smad1. Nat Commun 4(2690.

Sarina, Yagi Y, Nakano O, Hashimoto T, Kimura K, Asakawa Y, *et al*. 2013. Induction of neurite outgrowth in PC12 cells by artemisinin through activation of ERK and p38 MAPK signaling pathways. Brain Res 1490(0): 61-71.

Seira O and Del Rio JA. 2014. Glycogen synthase kinase 3 beta (GSK3beta) at the tip of neuronal development and regeneration. Mol Neurobiol 49(2): 931-44.

Silva AJ. 2003. Molecular and cellular cognitive studies of the role of synaptic plasticity in memory. J Neurobiol 54(1): 224-37.

Silva AJ, Kogan JH, Frankland PW and Kida S. 1998. CREB and memory. Annu Rev Neurosci 21(127-48.

Skaper SD. 2008. The biology of neurotrophins, signalling pathways, and functional peptide mimetics of neurotrophins and their receptors. CNS Neurol Disord Drug Targets 7(1): 46-62.

Smith WS, Baker EJ, Holmes SE, Koster G, Hunt AN, Johnston DA, *et al.* 2017. Membrane cholesterol is essential for triterpenoid saponin augmentation of a saporin-based immunotoxin directed against CD19 on human lymphoma cells. Biochim Biophys Acta Biomembr 1859(5): 993-1007.

Soumyanath A, Zhong YP, Gold SA, Yu X, Koop DR, Bourdette D, *et al.* 2005. *Centella asiatica* accelerates nerve regeneration upon oral administration and contains multiple active fractions increasing neurite elongation in-vitro. J Pharm Pharmacol 57(9): 1221-9.

Soumyanath A, Zhong YP, Henson E, Wadsworth T, Bishop J, Gold BG, *et al.* 2012. *Centella asiatica* extract improves behavioral deficits in a mouse model of Alzheimer's disease: investigation of a possible mechanism of action. Int J Alzheimers Dis 2012(381974.

Srivastava JK and Gupta S. 2009. Extraction, characterization, stability and biological activity of flavonoids isolated from Chamomile flowers. Mol Cell Pharmacol 1(3): 138.

Stuchlik A. 2014. Dynamic learning and memory, synaptic plasticity and neurogenesis: an update. Front Behav Neurosci 8(106.

Sun A, Xu X, Lin J, Cui X and Xu R. 2015a. Neuroprotection by saponins. Phytother Res 29(2): 187-200.

Sun BF, Wang QQ, Yu ZJ, Yu Y, Xiao CL, Kang CS, *et al.* 2015b. Exercise prevents memory impairment induced by arsenic exposure in mice: implication of hippocampal BDNF and CREB. PLoS One 10(9): e0137810.

Sun Y, Lim Y, Li F, Liu S, Lu JJ, Haberberger R, *et al.* 2012. ProBDNF collapses neurite outgrowth of primary neurons by activating RhoA. PLoS One 7(4): e35883.

Takashima A, Nieuwenhuis IL, Jensen O, Talamini LM, Rijpkema M and Fernandez G. 2009. Shift from hippocampal to neocortical centered retrieval network with consolidation. J Neurosci 29(32): 10087-93.

Takechi M, Uno C and Tanaka Y. 1996. Structure-activity relationships of synthetic saponins. Phytochemistry 41(1): 121-3.

Tanemoto R, Okuyama T, Matsuo H, Okumura T, Ikeya Y and Nishizawa M. 2015. The constituents of licorice (Glycyrrhiza uralensis) differentially suppress nitric oxide production in interleukin-1beta-treated hepatocytes. Biochem Biophys Rep 2(153-9.

Tantisira M, Tantisira B, Patarapanich C, Suttisri R, Luangcholatan S, Mingmalailak S, *et al.* 2010. Effects of standardized extract of *Centella asiatica* ECa 233 on learning and memory impairment induced by transient bilateral common carotid artery occlusion in mice. Thai J Pharmacol 32(22-33.

Thomas MT, Kurup R, Johnson AJ, Chandrika SP, Mathew PJ, Dan M, *et al.* 2010. Elite genotypes/chemotypes, with high contents of madecassoside and asiaticoside, from sixty

accessions of *Centella asiatica* of south India and the Andaman Islands: For cultivation and utility in cosmetic and herbal drug applications. Ind Crops Prod 32(3): 545-50.

Tohda C and Joyashiki E. 2009. Sominone enhances neurite outgrowth and spatial memory mediated by the neurotrophic factor receptor, RET. Br J Pharmacol 157(8): 1427-40.

Tronel S, Fabre A, Charrier V, Oliet SH, Gage FH and Abrous DN. 2010. Spatial learning sculpts the dendritic arbor of adult-born hippocampal neurons. Proc Natl Acad Sci U S A 107(17): 7963-8.

Tsang CK and Kamei Y. 2002. Novel effect of vitamin K1 (phylloquinone) and vitamin K2 (menaquinone) on promoting nerve growth factor-mediated neurite outgrowth from PC12D cells. Neurosci Lett 323(1): 9-12.

Vo NN, Fukushima EO and Muranaka T. 2016. Structure and hemolytic activity relationships of triterpenoid saponins and sapogenins. J Nat Med:

von Kriegsheim A, Baiocchi D, Birtwistle M, Sumpton D, Bienvenut W, Morrice N, *et al.* 2009. Cell fate decisions are specified by the dynamic ERK interactome. Nat Cell Biol 11(12): 1458-64.

Vyas S, Juin P, Hancock D, Suzuki Y, Takahashi R, Triller A, *et al.* 2004. Differentiation-dependent sensitivity to apoptogenic factors in PC12 cells. J Biol Chem 279(30): 30983-93.

Wan JY, Liu P, Wang HY, Qi LW, Wang CZ, Li P, *et al.* 2013. Biotransformation and metabolic profile of American ginseng saponins with human intestinal microflora by liquid chromatography quadrupole time-of-flight mass spectrometry. J Chromatogr A 1286(83-92.

Wanakhachornkrai O, Pongrakhananon V, Chunhacha P, Wanasuntronwong A, Vattanajun A, Tantisira B, *et al.* 2013. Neuritogenic effect of standardized extract of *Centella asiatica* ECa233 on human neuroblastoma cells. BMC Complement Altern Med 13(204.

Wanasuntronwong A, Tantisira MH, Tantisira B and Watanabe H. 2012. Anxiolytic effects of standardized extract of *Centella asiatica* (ECa 233) after chronic immobilization stress in mice. J Ethnopharmacol 143(2): 579-85.

Wang Q, Sun LH, Jia W, Liu XM, Dang HX, Mai WL, *et al.* 2010. Comparison of ginsenosides Rg1 and Rb1 for their effects on improving scopolamine-induced learning and memory impairment in mice. Phytother Res 24(12): 1748-54.

Wang X, Wang Z, Yao Y, Li J, Zhang X, Li C, *et al.* 2011a. Essential role of ERK activation in neurite outgrowth induced by α-lipoic acid. Biochim Biophys Acta Mol Cell Res 1813(5): 827-38.

Wang X, Zhang S, Sun C, Yuan ZG, Wu X, Wang D, *et al.* 2011b. Proteomic profiles of mouse neuro N2a cells infected with variant virulence of rabies viruses. J Microbiol Biotechnol 21(4): 366-73.

Wang XX, Liu GY, Yang YF, Wu XW, Xu W and Yang XW. 2017. Intestinal absorption of triterpenoids and flavonoids from *Glycyrrhizae radix* et rhizoma in the human Caco-2 monolayer cell model. Molecules 22(10):

Wartman BC and Holahan MR. 2014. The impact of multiple memory formation on dendritic complexity in the hippocampus and anterior cingulate cortex assessed at recent and remote time points. Front Behav Neurosci 8(128.

Wattanathorn J, Mator L, Muchimapura S, Tongun T, Pasuriwong O, Piyawatkul N, *et al.* 2008. Positive modulation of cognition and mood in the healthy elderly volunteer following the administration of *Centella asiatica.* J Ethnopharmacol 116(2): 325-32.

Wheeler AP and Ridley AJ. 2004. Why three Rho proteins? RhoA, RhoB, RhoC, and cell motility. Exp Cell Res 301(1): 43-9.

Wijeweera P, Arnason JT, Koszycki D and Merali Z. 2006. Evaluation of anxiolytic properties of Gotukola--(*Centella asiatica*) extracts and asiaticoside in rat behavioral models. Phytomedicine 13(9-10): 668-76.

Xiao J and Hogger P. 2015. Stability of dietary polyphenols under the cell culture conditions: avoiding erroneous conclusions. J Agric Food Chem 63(5): 1547-57.

Xu C, Kim NG and Gumbiner BM. 2009a. Regulation of protein stability by GSK3 mediated phosphorylation. Cell Cycle 8(24): 4032-9.

Xu CL, Qu R, Zhang J, Li LF and Ma SP. 2013. Neuroprotective effects of madecassoside in early stage of Parkinson's disease induced by MPTP in rats. Fitoterapia 90(112-8.

Xu CL, Wang QZ, Sun LM, Li XM, Deng JM, Li LF, *et al.* 2012a. Asiaticoside: Attenuation of neurotoxicity induced by MPTP in a rat model of Parkinsonism via maintaining redox balance and up-regulating the ratio of Bcl-2/Bax. Pharmacol Biochem Behav 100(3): 413-8.

Xu MF, Xiong YY, Liu JK, Qian JJ, Zhu L and Gao J. 2012b. Asiatic acid, a pentacyclic triterpene in *Centella asiatica*, attenuates glutamate-induced cognitive deficits in mice and apoptosis in SH-SY5Y cells. Acta Pharmacol Sin 33(5): 578-87.

Xu N, Engbers J, Khaja S, Xu L, Clark JJ and Hansen MR. 2012c. Influence of cAMP and protein kinase A on neurite length from spiral ganglion neurons. Hear Res 283(1-2): 33-44.

Xu X-H, Zhou J-F, Li T-Z, Zhang Z-H, Shan L, Xiang Z-h, *et al.* 2009b. Polygalasaponin G promotes neurite outgrowth of cultured neuron on myelin. Neurosci Lett 460(1): 41-6.

Xu Y, Cao Z, Khan I and Luo Y. 2008. Gotu Kola (*Centella Asiatica*) extract enhances phosphorylation of cyclic AMP response element binding protein in neuroblastoma cells expressing amyloid beta peptide. J Alzheimers Dis 13(3): 341-9.

Yamashita T, Tucker KL and Barde YA. 1999. Neurotrophin binding to the p75 receptor modulates Rho activity and axonal outgrowth. Neuron 24(3): 585-93.

Yang C, Cheng Y, Zhao J and Rong J. 2015. Releasing Nrf2 to promote neurite outgrowth. Neural Regen Res 10(12): 1934-5.

Yang D, Kim KH, Phimister A, Bachstetter AD, Ward TR, Stackman RW, *et al.* 2009. Developmental exposure to polychlorinated biphenyls interferes with experience-dependent dendritic plasticity and ryanodine receptor expression in weanling rats. Environ Health Perspect 117(3): 426-35.

Yoshikawa K, Matsumoto Y, Hama H, Tanaka M, Zhai H, Fukuyama Y, *et al.* 2009. Russujaponols g-L, Illudoid sesquiterpenes, and their neurite outgrowth promoting activity from the fruit body of russula japonica. Chem Pharm Bull 57(3): 311-4.

Yu K, Chen F and Li C. 2012. Absorption, disposition, and pharmacokinetics of saponins from Chinese medicinal herbs: what do we know and what do we need to know more? Curr Drug Metab 13(5): 577-98.

Yuan Y, Zhang H, Sun F, Sun S, Zhu Z and Chai Y. 2015. Biopharmaceutical and pharmacokinetic characterization of asiatic acid in *Centella asiatica* as determined by a sensitive and robust HPLC-MS method. J Ethnopharmacol 163(31-8.

Zhang WD, Zhang C, Liu RH, Li HL, Zhang JT, Mao C, *et al.* 2006. Preclinical pharmacokinetics and tissue distribution of a natural cardioprotective agent astragaloside IV in rats and dogs. Life Sci 79(8): 808-15.

Zhang X, Wu J, Dou Y, Xia B, Rong W, Rimbach G, *et al.* 2012. Asiatic acid protects primary neurons against C2-ceramide-induced apoptosis. Eur J Pharmacol 679(1-3): 51-9.

Zhang Z, Cai L, Zhou X, Su C, Xiao F, Gao Q, *et al.* 2015. Methyl 3,4-dihydroxybenzoate promote rat cortical neurons survival and neurite outgrowth through the adenosine A2a receptor/PI3K/Akt signaling pathway. Neuroreport 26(6): 367-73.

Zhao F, Wu T, Lau A, Jiang T, Huang Z, Wang XJ, *et al.* 2009. Nrf2 promotes neuronal cell differentiation. Free Radic Biol Med 47(6): 867-79.

Zhao J, Cheng YY, Fan W, Yang CB, Ye SF, Cui W, *et al.* 2015. Botanical drug puerarin coordinates with nerve growth factor in the regulation of neuronal survival and neuritogenesis via activating ERK1/2 and PI3K/Akt signaling pathways in the neurite extension process. CNS Neurosci Ther 21(1): 61-70.

Zhou BP, Deng J, Xia W, Xu J, Li YM, Gunduz M, *et al.* 2004. Dual regulation of Snail by GSK-3beta-mediated phosphorylation in control of epithelial-mesenchymal transition. Nat Cell Biol 6(10): 931-40.

Zhou FQ and Snider WD. 2005. Cell biology. GSK-3beta and microtubule assembly in axons. Science 308(5719): 211-4.

Zou K, Zhu S, Meselhy MR, Tohda C, Cai S and Komatsu K. 2002. Dammarane-type saponins from *Panax japonicus* and their neurite outgrowth activity in SK-N-SH cells. J Nat Prod 65(9): 1288-92.

VITA

NAME	Nonthaneth Nalinratana
DATE OF BIRTH	18 April 1986
PLACE OF BIRTH	Bangkok, Thailand
INSTITUTIONS ATTENDED	B.Sc. in Pharm., Chulalongkorn University
	M.Sc. (Biomedicinal Chemistry), Chulalongkorn University
HOME ADDRESS	61 Ekkachai 130 Bangbon Bangkok 10150

PUBLICATION

1. Nalinratana N, Meksuriyen D, Ongpipattanakul B. Differences in Neuritogenic Activity and Signaling Activation of Madecassoside, Asiaticoside, and Their Aglycones in Neuro-2a cells. Planta Med 84(16):1165-1173, 2018.

2. Chansriniyom C, Bunwatcharaphansakun P, Eaknai W, Nalinratana N, Ratanawong A, Khongkow M, Luechapudiporn R. A synergistic combination of Phyllanthus emblica and Alpinia galanga against H_2O_2-induced oxidative stress and lipid peroxidation in human ECV304 cells. J Funct Foods 43(4):44-54, 2018.

3. Nusuetrong P, Boonmalert M, Koobkokkruad T, Chantong B, Nalinratana N, Meksuriyen D. Cytotoxic and genotoxic potential of Trigonostemon reidioides extract on human Caco-2 cells. J Med Assoc Thai 100:61, 2017.

4. Nakchat O, Nalinratana N, Meksuriyen D, Pongsamart S. Tamarind seed coat extract restores reactive oxygen species through attenuation of glutathione level and antioxidant enzyme expression in human skin fibroblasts in response to oxidative stress. Asian Pac J Trop Biomed 4(5):379-385, 2014.

5. Nalinratana N, Kaewprem W, Tongumpai S, Luechapudiporn R, Sotanaphun U, Meksuriyen D. Synergistic antioxidant action of Phikud Navakot ameliorates hydrogen peroxide-induced stress in human endothelial cells. Integr Med Res 3(2):74-82, 2014.